JOURNAL OF NUCLEAR CARDIOLOGY

UPDATED IMAGING GUIDELINES FOR NUCLEAR CARDIOLOGY PROCEDURES

Part 1

Editor
E. Gordon DePuey, MD

Assistant Editor
Ernest V. Garcia, PhD

PUBLICATION SUPPORTED BY EDUCATIONAL GRANTS FROM

ADAC Laboratories
DuPont Pharmaceuticals, Inc
Mallinckrodt, Inc
Nycomed Amersham Imaging
Siemens Medical Systems

JOURNAL OF NUCLEAR CARDIOLOGY

UPDATED IMAGING GUIDELINES FOR NUCLEAR CARDIOLOGY PROCEDURES

Part 1

Editor
E. Gordon DePuey, MD

Assistant Editor
Ernest V. Garcia, PhD

COMMITTEE CHAIRMEN

Salvador Borges-Neto, MD
Edward P. Fiacro, PhD
Mark Groch, PhD
Diwakar Jain, MD
Kenneth J. Nichols, MD
Frans J. Th. Wackers, MD, PhD
I. George Zubal, PhD

COMMITTEE MEMBERS

Stephen L. Bacharach, PhD
Daniel S. Berman, MD
Salvador Borges-Neto, MD
Ignasi Carrio, MD
S. James Cullom, PhD
John Friedman, MD
L. Steve Graham, PhD
Rory Hachamovitch, MD
Hosen Kiat, MD
Scott M. Leonard, BS, CNMT
John Mahmarian, MD
Kenneth J. Nichols, PhD
Robert Pagnanelli, BSRT(R)(N), CNMT
Dudley J. Pennell, MD
Pierluigi Pieri, MD
Steven Port, MD
Janet Saffer, PhD
Douglas Schulman, MD
Albert J. Sinusas, MD
H. William Strauss, MD
Kenneth Van Train, MS
Kim A. Williams, MD
Michael Yester, PhD
Robert Zimmerman, MS

We acknowledge the following individuals who wrote the original, previously published Imaging Guidelines for Nuclear Cardiology Procedures, Part 1 (J Nucl Cardiol 1996;3:G1-G46), which is updated here: *Editor:* Ernest V. Garcia; *Committee Chairmen*: Stephen L. Bacharach, PhD, John J. Mahmarian, MD, Steven C. Port, MD, Kenneth Van Train, MS, and Denny D. Watson, PhD; *Committee Members:* Daniel S. Berman, MD, Jeffrey S. Borer, MD, S. James Cullom, PhD, E. Gordon DePuey, MD, John D. Friedman, MD, James R. Galt, PhD, Guido Germano, PhD, L. Stephen Graham, PhD, Hosen S. Kiat, MD, Kenneth J. Nichols, PhD, Albert J. Sinusas, MD, Wendy R. Smeltzer, CNMT, Patricia Stewart-Henney, RT, and Kenneth J. Tillman, CNMT.

JOURNAL OF NUCLEAR CARDIOLOGY

Volume 8 • Number 1 January/February 2001

UPDATED IMAGING GUIDELINES FOR NUCLEAR CARDIOLOGY PROCEDURES, Part 1

Contents continued

INTRODUCTION

This manual has been developed by the Quality Assurance Committee of the American Society of Nuclear Cardiology (ASNC). It serves as an update of the Imaging Guidelines published previously in the Journal of Nuclear Cardiology in 1996 (Garcia EV, editor. Imaging guidelines for nuclear cardiology procedures. Part 1. J Nucl Cardiol 1996;3:G1-46). Since that publication, there have been significant advancements in instrumentation, computer software methodology, and radiopharmaceuticals which warrant this update.

The task of the Committee has been to document state-of-the-art applications and protocols approved by experts in the field and distribute these protocols to the nuclear cardiology community. Subcommittees were formed to document guidelines for the particular applications addressed in this manual. The final document was reviewed and approved by the American Society of Nuclear Cardiology Board of Directors.

Within the document protocol items judged to be required are indicated as such. Standard means that the parameter value listed represents methodology judged to be standard by the consensus of the committee; its utilization is recommended, but other techniques may also be valid. Preferred means that the parameter value listed is expected to provide the best results and its selection is strongly recommended. Techniques termed optional indicate that the parameter value listed may be employed or another acceptable parameter may be substituted.

This manual is designed to provide imaging guidelines for those physicians and technologists who are qualified in the practice of nuclear cardiology. Although care has been taken to ensure that information supplied is accurate, representing the consensus of experts, it should not be considered as medical advice or a professional service. The imaging guidelines described in this manual should not be utilized in clinical studies at any institution until they have been reviewed and approved by qualified physicians from that institution.

The experts who worked on the revision of these guidelines are listed below by the protocol they contributed.

Instrumentation quality assurance and performance: George Zubal, PhD (chairman), L. Steve Graham, PhD, Michael Yester, PhD, Robert Zimmerman, MS, Janet Saffer, PhD

Stress myocardial perfusion imaging protocols: Diwakar Jain, MD (chairman), Salvador Borges-Neto, MD, Ignasi Carrio, MD, Rory Hachamovich, MD, John Mahamarian, MD, Dudley J. Pennell, MD, Pierluigi Pieri, MD, Douglas Schulman, MD

First pass radionuclide angiography imaging: Salvador Borges-Neto, MD (chairman), Steven Port, MD, John Friedman, MD, Kenneth Nichols, PhD, Kim A. Williams, MD, Robert Pagnanelli, BSRT (R)(N), CNMT

Equilibrium radionuclide angiocardiography protocols: Mark W. Groch, PhD (chairman), H. William Strauss, MD, Stephen L. Bacharach, PhD, Scott M. Leonard, BS, CNMT

Myocardial perfusion planar protocols: Frans J. Th. Wackers, MD (chairman), Albert J. Sinusas, MD

Myocardial perfusion and function SPECT protocols: Kenneth Nichols, PhD (chairman), Kenneth Van Train, MS, Hosen Kiat, MD, S. James Cullom, PhD, Daniel S. Berman, MD

Transmission-emission tomographic systems to be used for attenuation correction: Edward P. Ficaro, PhD (chairman), S. James Cullom, PhD, L. Stephen Graham, PhD, E. Gordon DePuey, MD, Ernest V. Garcia, PhD

INSTRUMENTATION QUALITY ASSURANCE AND PERFORMANCE

Equipment

Planar Imaging. The small field of view (FOV) scintillation camera is ideal for cardiac imaging. The 10-inch FOV covers the heart and shows enough surrounding area to evaluate lung uptake and to sample extra-cardiac background activity. A computer image matrix of 128 pixels over this FOV results in pixel spacing of about 2 mm, which is adequate for the highest obtainable resolution. A camera with 15-inch FOV should be zoomed using a magnification factor of 1.2 to 1.5, so that the pixel size is less than 3 mm and approximately equal to 2.5 or 2.0 mm.

Energy windows should be symmetric about the photopeak. A window of 20% is standard for technetium-99m (Tc-99m). With the improved energy resolution of many modern cameras, a 15% window can be used with very little loss of

Reprint requests: American Society of Nuclear Cardiology,
9111 Old Georgetown Rd, Bethesda, MD 20814-1699.
J Nucl Cardiol 2001;8:G1-58.

1071-3581/2001/$35.00 + 0 **43/1/112538**
doi:10.1067/mnc.2001.112538

"good" counts and some improvement in contrast. The low energy and greater width of the thallium-201 (Tl-201) photopeak require a wider window. Window settings of 30% or 35% may be appropriate. The absolute energy calibration is unreliable at the low energy of Tl-201 falling at slightly different energy positions in the spectrum of different cameras. Thus the peak and window width settings should be set for each individual camera based on the energy spectrum display.

Parallel hole collimation is standard. The low-energy, high-resolution collimator is usually best for Tc-99m, although some "all-purpose" collimators give excellent results. Imaging with Tl-201 is usually best with the low-energy, medium-resolution (all-purpose) collimators because count statistics become limiting when using high-resolution collimators. The difference in medium- and high-resolution collimators is usually that the collimator depth (length of the collimator hole) is greater in high-resolution collimators. They have similar near-field resolution. The "high-resolution" collimator maintains good resolution at a greater distance from the collimator face. The difference is more important in single photon emission computed tomography (SPECT) imaging where the distance from patient to collimator is greater.

A quality control (QC) program capable of determining camera performance parameters should be in place. The quality and consistency of images should be tested as well as the performance of the camera. The frequency of testing is suggested in the QC Procedures section. An effective QC program should recognize inconsistent equipment performance. The inconsistencies associated with equipment malfunction should be corrected promptly. Suggested parameters of camera performance are tabulated below.

Performance parameters for low energy (<150 keV collimators)

Collimator type	Resolution (FWHM at 10 cm)	Relative sensitivity
Ultra-high resolution	6 mm	0.3
High resolution	7.8 mm	0.6
All/general purpose	9.3 mm	1*
High sensitivity	13.2 mm	2.1

*A relative sensitivity of 1 corresponds approximately to a collimator efficiency of 2.7×10^{-4}, whereas efficiency is defined as the fraction of gamma- and x-rays passing through the collimator per gamma- and x-ray emitted by the source.

Collimators. The selection of which collimator to use is one of the most important pieces of information supplied by these guidelines. A confounding aspect of this selection is that collimators with the same name (eg, general purpose) tend to vary in performance between manufacturers. The table above gives approximate values for what is expected for a type of collimator when that collimator is suggested. It is essential that collimator performance be the guiding factor in selecting which collimator to use rather than the collimator name given by the manufacturer. Refer to specific imaging protocols for collimator selection.

SPECT Imaging. SPECT detectors are basically sophisticated scintillation cameras mounted on a gantry. Many variables dictate the performance of a SPECT imaging system. The number of detectors is perhaps the most important variable. Single-head cameras have been used widely for cardiac imaging. Adding more detectors is an obvious benefit since doubling the number of detectors should double the number of counts acquired if all other variables remain fixed. For cardiac SPECT studies in which a 180° orbit is recommended, the preferred configuration is to have two detectors separated by 90° as they rotate around the heart. For studies in which a 360° orbit is preferred, three detectors separated by 120° from each other seem optimal.

The trend is to trade off some of the additional counts that would be obtained with multiple detectors equipped with general purpose collimators for higher resolution imaging by using higher resolution collimators. Fan beam collimators are now commonly available. These collimators allow more of the crystal area to be imaging the heart, magnifying the image and increasing sensitivity. In large patients or when using a converging geometry with a steep angle there is a potential for cutting-off or truncating portions of the heart and/or chest. This truncation could generate artifacts.

Another variable in modern SPECT systems is the shape of the detector's orbit. The traditional orbit used for SPECT acquisition has been circular, with a rotational range of 180° or 360° and with step-and-shoot motion. Most systems today allow for detector motion which is elliptical or follow the body contour of the patient, minimizing the distance from the camera to the body and thus increasing spatial resolution. This increase is sometimes accompanied by imaging artifacts due to variable resolution of cardiac structures across the angular range. If elliptical orbits are used the detector should be "backed-off" the heart's apex by approximately 2 cm to prevent apical artifacts.

For single-head cameras the 180° angular range from the 45° right anterior oblique (RAO) to left posterior oblique (LPO) orientation (or vice versa) has been the orbit of choice because the detector is closer to the heart in these views, resulting in higher spatial and contrast resolution. There is also less scatter and attenuation over this angular range. The 360° orbit usually results in better uniformity of normal myocardium due to more consistent spatial resolution (which is a function of the distance to the collimator). Some double and triple multiple-head systems acquire the entire 360° orbit because of the fixed separation of the detectors. In these systems the entire 360° orbit could be used since otherwise acquired counts could be wasted. One concern in using 360° acquisitions is that the reconstructed images will have a different "normal distribution" as compared to those from 180° orbits. This could cause a misdiagnosis if interpreted as a 180° acquired study.

Most SPECT systems have used the step-and-shoot mode of acquisition in which the detector is dead (does not count) as it moves from one angle to the next. Newer devices offer either continuous and/or continuous step-and-shoot acquisition modes in which the detector is live as it moves thus not wasting any acquisition time. Although there is some minimal spatial resolution loss due to the continuous motion, the added sensitivity results in better images.

QC Procedures

Planar Imaging. Appropriate QC procedures are necessary to ensure images of the highest possible technical quality for the equipment used and thus allow the best possible diagnostic service to the patient population.

Planar QC procedures

Test	Frequency	For info see paragraph
Energy peaking	Daily	1
Intrinsic uniformity test	Daily	2
Intrinsic sensitivity test	Weekly or daily	3
Resolution and linearity	Weekly	4

Performance parameters for detectors

Parameter	Standard	Preferred	For info see paragraph
Integral uniformity	<5%	<3%	2
Differential uniformity	<5%	<3%	2
Intrinsic resolution FWHM	<6 mm	<4 mm	4

1. **Energy peaking.** Energy peaking is performed to verify that the camera is counting photons having the correct energy. This test consists of either manually or automatically placing the correct pulse height analyzer's energy window over the photopeak energy to be used. Care must be taken that the technologist verifies the correct placement of the window and that a radioactive point source is used at a distance away (1.5+ meters) from the uncollimated camera; a sheet source is typically used in front of a collimated camera. In either case, the full FOV of the camera should be illuminated by the source. Window verification should be done even on automated systems where there are single buttons or computer protocols to select for each energy; even in these automated systems the energy windows tend to drift. These systems allow for window offsets to correct for these drifts. This peaking test should indicate whether the camera's automatic peaking circuitry is working properly, whether the peak appears at the correct energy, and whether the shape of the spectrum is correct. If cost, time, and the equipment permit, photographs of the spectra with the superimposed energy window should be taken and stored.
2. **Intrinsic uniformity test.** Intrinsic uniformity testing is performed to verify that the camera's sensitivity response is uniform across the detector's face. This test consists of exposing (flooding) the camera with a radioactive source. The scientifically preferred method is that this test be performed intrinsically (ie, acquired without a collimator) using a radioactive point source located at a distance at least five times the crystal's useful FOV (UFOV) from the center of the detector. The point source should consist of a small volume (0.5 mL) of fluid and low activity such as 200 to 300 μCi. For large rectangular cameras (where the point should be approximately 8 feet away), 600 μCi is

appropriate. In many cameras, obtaining intrinsic flood-fields is difficult. Because of these difficulties many institutions prefer performing this test extrinsically (ie, acquired with a collimator) using extended radioactive sheet flood sources. To ensure a true response during acquisition, count rates should be kept between 20 and 30 kcps depending on the age of the detector. If available, a lead ring should be used to shield the outermost tubes from the radiation to prevent edge packing. Flood images that will be inspected visually should be acquired as 256 × 256 matrices for 1.25M counts for a small FOV camera and 2.5M for a large, circular FOV camera (4M for large rectangular detectors). Photographs of the flood-field should be taken and stored; it is most desirable (and convenient) to store these flood images on the computer.

Flood images to be used for a mathematical calculation of uniformity require two to three times more counts to reduce statistical noise. The recommended number of counts is at least 4500 counts/cm^2. For example, for a 400 mm circular FOV the total counts needed would be 5.7M. The National Electrical Manufacturers Association (NEMA) has recommended acquiring a minimum of 10,000 counts for the center (6.4 mm) pixel of the flood image.

Two kinds of parameters are computed to measure and document flood uniformity. These are called integral and differential uniformity. Integral uniformity is a global parameter that measures uniformity over an extended area of the detector, and is expressed as:

$$\text{Integral uniformity} = 100\% \times (\text{Max} - \text{Min}) / (\text{Max} + \text{Min})$$

where "Max" is the maximum count and "Min" is the minimum count found in any pixel within the specified area. Differential uniformity is a regional parameter that measures contrast over a small neighborhood. This measurement is performed using all possible 5 × 1 pixel areas in both the X and Y directions and is expressed as:

$$\text{Differential uniformity} = 100\% \times \text{Largest deviation } (\text{Max} - \text{Min}) / (\text{Max} + \text{Min})$$

3. **Resolution and linearity test.** This test is performed to document spatial resolution and its change over time as well as the detector's ability to reproduce straight lines. The test consists of imaging a flood source intrinsically through a spatial resolution test phantom. The flood source should be acquired as described in the intrinsic flood section. Most commercially available bar phantoms are suitable for this test. These include the parallel-line-equal-space (PLES) bar phantoms and orthogonal hole or 4-quadrant phantoms. If the 4-quadrant phantom is used, each time the test is conducted, it should be rotated 90° so that every fifth time the test is done, the pattern position repeats. Images of these phantoms should be photographed and recorded. These images should be assessed for how straight the lines are imaged and for intrinsic spatial resolution. Change in resolution is assessed by documenting the smallest bars that are discerned. Spatial resolution as measured by the full-width-at-half-maximum (FWHM) may be approximated by multiplying 1.7 times the smallest bar size seen.
4. **Intrinsic sensitivity test.** This test is performed to document the sensitivity of the detector and more importantly the change of sensitivity over time. The test consists of calculating detector sensitivity (expressed in terms of counts per minute per μCi) of a known source, calibrating with a dose calibrator. The point source should always be located at the same exact distance in front of the camera for repeat measurements. A convenient means of measuring sensitivity changes is by recording the time that it takes to acquire the preset counts for an intrinsic (or extrinsic) flood source.

SPECT Imaging. All of the QC procedures required of planar imaging instruments are also required for SPECT imaging since tomography depends on acquiring accurate planar projections. In addition, procedures specific to SPECT imaging systems are discussed below.

SPECT QC procedures

Test	Requirement	For info see paragraph
COR	Mandatory	2
Uniformity correction	Mandatory	2
Motion correction	Optional	3

1. **Center-of-rotation (COR).** An alignment error between the electronic matrix of the detector and the mechanical COR can potentially result in a characteristic "doughnut" (if a 360° orbit and a point source are used) or "tuning fork" artifact (if a 180° orbit is used) in the transverse images. The effects are most significant when the error is

greater than approximately two pixels in a 64 × 64 matrix. Errors less than this can reduce spatial resolution and image contrast through blurring of the image and cause artifacts. The accuracy of COR alignment should be checked weekly. Many manufacturers require that a specific protocol be followed for the determination and recalibration of the COR. When no specific COR acquisition protocol is recommended by the manufacturer, the COR may be determined through the acquisition of a point source of activity (500 to 1000 μCi) on the patient table 4 to 8 inches away from the COR. A rapid SPECT acquisition over 360° with equally spaced projections is then acquired. The same angular orientation, collimation, zoom, matrix size, and energy window employed for the patient study should be employed for the COR acquisition. Five to ten seconds per frame for 16 or 32 views is usually sufficient. COR correction values for each orbit are then computed and stored in the computer and used to realign the projection data before reconstruction. It is essential that the COR errors be checked for each collimator that is to be used clinically. For an active SPECT program, it is recommended that these measurements be performed weekly (or bi-monthly). Although most systems' COR variation does not warrant this daily check, this procedure will assure the technologist that the detector is rotating and acquiring adequately. Always recalculate the COR values after servicing of the camera or computer and especially after significant software upgrades.

2. **Flood-field uniformity correction.** In SPECT, it is implicitly assumed that the efficiency of photon detection is constant across the surface of the collimated detector. Flood-field uniformity errors result when the variation in efficiency is significant as compared to the performance parameters in the above table. Anger cameras utilize stored flood-field correction maps to correct for variations in sensitivity across the FOV before reconstruction. Deficiencies can lead to characteristic "ring" artifacts if the region is discrete and is either lighter or darker than surrounding regions in the transverse images. More subtle variations can lead to perfusion artifacts. Daily checks of flood-field extrinsic (with collimator) uniformity are performed with a 3 million count flood for a typical FOV 128 × 128 or 256 × 256 matrix. To correct for sensitivity variations due to the collimator typically up to a 100 million count image is acquired for each detector (128 × 128 or 256 × 256 matrix) and stored for uniformity correction. It is essential to perform uniformity measurements for each collimator and that the same collimator that was used to acquire the flood and generate the correction matrix be used to acquire the patient study. It is important that energy values similar to those being used for clinical studies also be used for the flood source. 57Co solid sheet sources (122 keV) and Tc-99m fillable sources are commonly used for Tl-201 and Tc-99m imaging. A solid sheet source is less problematic for daily use, and it is preferred for QC of Tc-99m and Tl-201 studies. Unfortunately, this approach requires a large initial and periodic financial investment. Using the lower energy correction floods for higher energy radionuclides can result in incorrect compensation and therefore is not recommended.
3. **Motion correction.** Critical to the accurate reconstruction of the tracer distribution is the fixed alignment of the detector coordinates and the organ being imaged. The most common source of misalignment is the motion of the patient or heart relative to the detector coordinates during acquisition. This motion is separate from the motion over the cardiac cycle, which is unavoidable and accepted as a known source of image degradation. Heart motion can occur either by the patient moving or as a result of diaphragmatic movement that can occur with heavy or erratic breathing patterns. With patient or heart motion, count values are erroneously placed back into the tomographic image, resulting in potential artifacts that can corrupt the accuracy of tracer representation. It is critically important that the rotating projection views be played in a cine format and evaluated for potential motion. If significant motion is detected, a repeat study is required. When repeating stress perfusion studies it should be taken into account that if the Tl-201 myocardial distribution might have redistributed significantly the study might have to be repeated on a different day. This is not usually a problem with sestamibi studies since there is little redistribution that takes place. Translational motion along the patient axis ("up" and "down" motion) is the most frequently detected type of motion as it is perpendicular to the movement of the heart in the rotating cine views. The influence of motion depends on: in which frame the motion occurs. For instance with a single-detector camera if there is motion in the first frames and then no motion for the rest of the study, this will produce a very small effect. However, with multidetector systems the single episode of motion will be propagated throughout other frames of the 189-degree arc. On the other hand, a 1-pixel shift (vertical translation) over as few as 4 frames in the middle of the projection set can produce an inferior or basal defect. Rotational angular motion is less frequently detected since it appears parallel to the motion of the heart in the cines. Motion toward or away from a detector cannot be detected. A horizontal line of reference drawn on the screen or in one's mind can be used as the reference point for evaluation of the magnitude of motion. If motion is detected, a determination of its severity must be made. A rule of thumb is that translational motion (eg, the patient moves and remains there throughout the study) on the order of 1 pixel in a 64 × 64 matrix represents an approximate limit before significant structural artifacts can result. Motion of one-half

pixel can often be detected but generally does not result in clinically significant artifacts and represents the upper limit of motion detectable with automated methods. Once motion is detected, manual methods (if available) can be used to shift the frames back to the expected correct position or a manufacturer specific automated method can be executed that tracks the myocardium across the FOV and performs an approximate realignment. Translational motion along the patient axis in dual and multidetector systems yields unique "jumps" in the position of the myocardium where the detector views are joined. The criteria for significance of motion for multiple-detector systems should be applied the same as that described above for single-detector systems.

Clinical QC for Each Patient Procedure

- The imaging procedure should be explained to the patient before acquisition, who should be aware of exactly what is expected of him/her during the acquisition.
- When using 180° orbits the patient's left arm must be positioned away from his/her side. This is usually accomplished by placing the arm above the head using an arm support device to maximize comfort. With some arm support systems it is more comfortable to raise both arms into the support system. When using 360° orbits both arms need to be positioned away from the patient's side.
- The patient should be observed throughout the acquisition to ensure that patient motion does not occur. Talking, irregular breathing, and sleeping are not allowed during the acquisition.
- Review cine of raw projection data: Reviewed by a technologist immediately after acquisition and by a physician at the time of image interpretation. Projections with motion should be corrected or reacquired before reconstruction.
- Count rates for individual projection images: Results presented in the table represent ranges of counts from acceptable SPECT studies. Note: Heart average = Counts × 1000. These represent the average counts in the mid-left anterior oblique (LAO) planar projection over the myocardium.

Expected ranges of counts per projection

	Heart avg (×1000)	Max counts
Tl-201 (3 mCi/HR/64 stops)	10-28	85-134
Tc-99m (22 mCi/HR/64 stops)	21-77	190-298
Tl-201 (3 mCi/LEAP/32 stops) STRESS	53-134	91-235
Tl-201 (3 mCi/LEAP/32 stops) REST	33-100	66-185

HR, High resolution collimator.

Bibliography

1. Bushberg JT, Seibert JA, Leidholt EM, Boone JM. The essential physics of medical imaging. Baltimore: Williams and Wilkins; 1994.
2. Galt JR, Germano G. Advances in instrumentation for cardiac SPECT. In: DePuey EG, Berman DS, Garcia EV, editors. Cardiac SPECT imaging. New York: Raven Press; 1995. p. 91-102.
3. Klingensmith WC, Eshima D, Goddard J, editors. Nuclear medicine procedure manual. Englewood (CO): Wick Publishing; 1995.
4. Nichols KI, Galt JR. Quality control for SPECT imaging. In: DePuey EG, Berman DS, Garcia EV, editors. Cardiac SPECT imaging. New York: Raven Press; 1995. p. 21-47.
5. Sorenson JA, Phelps ME. Physics in nuclear medicine. Philadelphia: WB Saunders; 1987.
6. NEMA standards publication NU 1-1994. Performance measurements of scintillation cameras. National Electrical Manufacturers Association; 1994.
7. Rosenthal MS, Cullom J, Hawkins W, Moore SC, Tsui BM, Yester M. Quantitative SPECT Imaging: a review and recommendations by the Focus Committee of the Society of Nuclear Medicine and Instrumentation Council. J Nucl Med 1995;36:1489-513.
8. Rotating scintillator camera SPECT acceptance testing and quality control. Report No. 22. AAPM; June 1987.
9. ANZSNM guidelines for minimum quality control requirements for nuclear medicine practices. Available at: http://xray.anu.edu.au/anzsnm/physics/qc/qc0.htm and IAEA Tec-doc.
10. Hines H, Kayayan R, Colsher J, Hashimoto D, Shubert R, Fernando J, et al. National Electrical Manufacturers Association recommendation for implementing SPECT instrumentation quality control. J Nucl Med 2000;41:383-9.

STRESS MYOCARDIAL PERFUSION IMAGING PROTOCOLS

Exercise Stress

Exercise is the preferred stress modality in patients who can exercise to an adequate workload.

1. **Indications**
   - For the detection of coronary artery disease (CAD) and assessing prognosis in patients with symptoms suggestive of CAD or in those with risk factors for CAD.
   - For risk stratification of post myocardial infarction patients and in patients with unstable angina or chronic CAD into low risk category who can be managed medically, or into high risk category who should be considered for revascularization procedure.
   - For cardiac risk stratification prior to non-cardiac surgery in patients with known CAD or those with risk factors for CAD.
   - For the evaluation of the efficacy of therapeutic interventions (anti-ischemic drug therapy/revascularization) in patients with known CAD.
2. **Absolute contraindications**
   - Patients with uncontrolled unstable angina should not be stressed. However, patients with suspected unstable angina at presentation, who are otherwise stable and pain free can undergo stress testing.
   - Patients with decompensated or inadequately controlled congestive heart failure.
   - Uncontrolled hypertension (blood pressure ≥200/115 mm of Hg).
   - Acute myocardial infarction within last 2 to 3 days.
   - Severe pulmonary hypertension.
3. **Relative contraindications**
   - Severe aortic stenosis.
   - Hypertrophic obstructive cardiomyopathy.
4. **Limitations.** Exercise test has a limited value in patients who cannot achieve an adequate heart rate and blood pressure response due to a noncardiac physical limitation such as pulmonary, peripheral vascular, musculoskeletal abnormalities or due to a lack of motivation. These patients should undergo pharmacological stress perfusion imaging.
5. **Exercise modalities.** Treadmill is the most widely used exercise modality. Several treadmill exercise protocols are available which differ in speed and inclination of the treadmill. Bruce protocol and modified Bruce protocol are the most widely used exercise protocols.

   Upright bicycle exercise is commonly used in Europe. This is preferable if dynamic first pass imaging is planned during exercise. Supine or semi-supine exercise is relatively suboptimal and should only be used while performing exercise radionuclide angiocardiography.
6. **Test procedure**
   - A large-bore (18-20 gauge) intravenous (IV) cannula should be inserted for radiopharmaceutical injection during exercise.
   - The electrocardiogram should be monitored continuously during the exercise test and for at least 3 to 5 minutes of recovery. A 12-lead electrocardiogram should be obtained at every stage of exercise, at peak exercise, and during recovery.
   - The blood pressure should be checked every 3 minutes during exercise.
   - Exercise should be symptom limited with patients achieving ≥85% of their age predicted maximum heart rate.
   - The radiopharmaceutical should be injected close to the peak exercise. The patients should be encouraged to continue the exercise for another 2 minutes after the radiotracer injection.
7. **Indications for early termination of exercise.** The exercise should be terminated early under the following circumstances:
   - The appearance of cardiac symptoms: chest pain, marked dyspnea, dizziness or fatigue
   - Marked ST segment depression (≥3 mm)
   - Ischemic ST segment elevation of >1 mm in leads without pathological Q waves
   - Appearance of ventricular or supraventricular tachycardia
   - A decrease in systolic blood pressure of ≥20 mm Hg below the starting blood pressure

- Markedly abnormal elevation of blood pressure (systolic blood pressure ≥250 mm or diastolic blood pressure ≥130 mm Hg)

Pharmacological Vasodilator Stress

Adenosine

1. **Mechanism of action.** Adenosine is a direct coronary arteriolar vasodilator and results in a 3.5- to 4-fold increase in myocardial blood flow. Myocardial regions supplied by diseased coronary arteries have an attenuated hyperemic response. Depending upon the severity of coronary stenosis and coronary flow reserve limitation, a relative flow heterogeneity is induced. In patients with severe CAD, true ischemia may also be induced because of a coronary steal phenomenon. Since the myocardial tracer uptake is proportional to the regional myocardial blood flow, an unequal distribution of radiotracer occurs in the myocardium.
2. **Adenosine dose.** Adenosine should be given as continuous infusion at a rate of 140 μg/kg/min over a 6 minute period. Recently, a shorter duration of adenosine infusion, lasting 4.5 minutes, has been found to be equally effective compared to the standard 6 minute infusion, for the detection of CAD.
3. **Indications.** The indications for adenosine stress perfusion imaging are the same as for exercise myocardial perfusion imaging in the presence of the following conditions:
   - Inability to perform adequate exercise due to any extracardiac factors (pulmonary, peripheral vascular, musculoskeletal conditions).
   - Left bundle branch block (LBBB).
   - Concomitant treatment with medications which blunt the heart rate response (beta blockers, calcium channel blockers).
   - Evaluation of patients very early after acute myocardial infarction (<3 days) or very early after angioplasty/stenting (<2 weeks).
4. **Hemodynamic effects.** Adenosine results in a modest increase in heart rate and a modest decrease in both systolic and diastolic blood pressures.
5. **Absolute contraindications**
   - Asthmatic patients with ongoing wheezing should not undergo adenosine stress testing. However, patients with adequately controlled asthma can undergo adenosine stress test.
   - Greater than first degree heart block without a pacemaker or sick sinus syndrome.
   - Systolic blood pressure less than 90 mm of Hg.
   - Use of dipyridamole in last 24 hours or use of xanthines (aminophylline, caffeine) in the last 12 hours. Pentoxifylline (Trental) need not be stopped prior to adenosine stress perfusion imaging.
6. **Relative contraindications**
   - Severe sinus bradycardia (heart rate <40/min).
7. **Procedure**
   - An infusion pump is necessary for adenosine administration at a constant infusion rate.
   - An IV line with dual-port Y-connector is required for the injection of radiotracer during adenosine infusion.
   - Electrocardiographic (ECG) monitoring should be carried out as with exercise stress testing.
   - Blood pressure should be monitored every minute during infusion and 3 to 5 minutes of recovery.
   - Adenosine infusion should be given at a rate of 140 μg/kg/min for 1.5 minutes (3 minutes with 6 minute injection protocol), followed by the injection of the radiotracer. The infusion should be continued for another 3 minutes. For patients deemed to be at a higher risk for complications (recent ischemic event, borderline hypotension, inadequately controlled asthma), adenosine infusion may be started at a lower dose (70 μg/kg/min). If this dose is tolerated well for 1 minute, the infusion rate should be increased to 140 μg/kg/min and should be continued for 4 minutes. The radiotracer should be injected 1 minute after starting the 140 μg/kg/min dose.
8. **Early termination of adenosine infusion.** Adenosine infusion should be stopped early under any of the following circumstances:
   - Severe hypotension (systolic blood pressure <80 mm of Hg).
   - Development of symptomatic, persistent second degree or complete heart block.
   - Wheezing.
   - Severe chest pain associated with ≥2 mm ST depression.

9. **Side effects of adenosine**
   - Minor side effects are common and occur in approximately 80% of patients. The common side effects are flushing (35%-40%), chest pain (25%-30%), dyspnea (20%), dizziness (7%), nausea (5%), and symptomatic hypotension (5%). Chest pain is non-specific and is not necessarily indicative of the presence of CAD.
   - High degree atrioventricular (AV) block occurs in approximately 7% of cases.
   - ≥1 mm ST segment depression occurs in 15% to 20% of cases. However, unlike chest pain, this is indicative of significant CAD.
   - Fatal or non-fatal myocardial infarction is extremely rare and the reported incidence is less than 1 in 1000 cases.
   - Due to an exceedingly short half life of adenosine (<10 seconds), most side effects resolve in a few seconds after discontinuation of the adenosine infusion and aminophylline infusion is only very rarely required.
10. **Combination of low level exercise with adenosine infusion.** Recently combination of low-level upright treadmill exercise with adenosine infusion has been found to be safe. This results in a significant reduction in the side effects of adenosine (flushing, dizziness, nausea, and headache). This attenuates the adenosine induced drop in the blood pressure. This also improves the image quality by decreasing the artifacts due to high hepatic radiotracer uptake, which is common with pharmacological stress perfusion imaging. Therefore, low level exercise may be performed in combination with pharmacology stress. However, since it is desirable *not* to increase the heart rate of patients with LBBB undergoing pharmacologic stress, low level exercise supplementation should not be used in patients with LBBB.

Dipyridamole

1. **Mechanism of action.** Dipyridamole is an indirect coronary artery vasodilator that increases the tissue levels of adenosine by preventing the intracellular reuptake and deamination of adenosine. However, coronary hyperemia induced with dipyridamole is somewhat less predictable than that induced by adenosine infusion. Moreover, dipyridamole induced hyperemia lasts for more than 15 minutes.
2. **Dipyridamole dose**
   - 0.56 mg/kg intravenously over a 4-minute period.
3. **Indications.** Same as for exercise myocardial perfusion imaging in the presence of the following conditions:
   - Inability to perform adequate exercise due to any extracardiac factors (peripheral vascular, musculoskeletal conditions).
   - LBBB.
   - Concomitant treatment with medications which blunt the heart rate response (beta blockers, calcium channel blockers).
   - Evaluation of patients very early after acute myocardial infarction (<3 days) or very early after angioplasty/stenting (<2 weeks).
   - In patients taking oral dipyridamole, IV dipyridamole may be administered safely and efficaciously.
4. **Hemodynamic effects.** Dipyridamole results in a modest increase in heart rate and a modest decrease in both systolic and diastolic blood pressures.
5. **Contraindications.** Contraindications for dipyridamole stress testing are the same as with adenosine.
6. **Procedure.** The drug is infused intravenously over 4 minutes. Although an infusion pump is desirable, dipyridamole can also be administered by hand injection. The radiotracer is injected 3 to 5 minutes after the completion of dipyridamole infusion. This obviates the need for a Yconnector.
7. **Side effects.** Over 50% of patients develop side effects (flushing, chest pain, headache, dizziness, or hypotension). The frequency of these side effects is less than that seen with adenosine, but they last for a longer period of time (15-25 minutes) and aminophylline (125-250 mg IV) is often required to reverse these side effects. Incidence of high degree AV block with dipyridamole is less than that observed with adenosine (2%).
8. **Combination of low level exercise with dipyridamole infusion.** This is performed routinely in many laboratories. Patients who are ambulatory are given a low level treadmill exercise for 4 to 6 minutes soon after the completion of dipyridamole infusion. Radiotracer is injected during this low-level exercise. This significantly reduces the side effects and improves image quality. As stated above with regard to adenosine stress, low level exercise supplementation is not recommended for patients with LBBB.

Dobutamine

1. **Mechanism of action.** Dobutamine infusion results in direct β_1 and β_2 stimulation with a dose-related increase in heart rate, blood pressure, and myocardial contractility. Dobutamine increases regional myocardial blood flow based

on physiologic principles of coronary flow reserve. A similar dose-related increase in subepicardial and subendocardial blood flow occurs within vascular beds supplied by normal coronary arteries. However, blood flow increases minimally within vascular beds supplied by significantly stenosed arteries with most of the increase occurring within the subepicardium rather than the subendocardium. However, at a dose of 20 μg/kg/min, dobutamine induced coronary flow heterogeneity is significantly less than that induced by adenosine or dipyridamole.

2. **Dobutamine dose.** Dobutamine is infused incrementally starting at a dose of 5 to 10 μg/kg/min, which is increased at 3-minute intervals to 20, 30, and 40 μg/kg/min. It is customary to use atropine in patients where heart rate does not increase beyond 120 beats/min with the maximum dose of dobutamine while performing stress echocardiogram. However, the necessity of this approach with dobutamine stress myocardial perfusion imaging is not well proven.
3. **Indications**
   - Dobutamine is a secondary pharmacologic stressor that is used in patients who cannot undergo exercise stress and have contraindications to pharmacologic vasodilator stressors.
   - Dobutamine perfusion imaging has not been studied as extensively as adenosine or dipyridamole in the evaluation and prognostication of patients with CAD.
4. **Contraindications.** Dobutamine stress testing should not be used under the following circumstances:
   - Recent (<1 week) myocardial infarction.
   - Unstable angina.
   - Hemodynamically significant left ventricular (LV) outflow tract obstruction.
   - Critical aortic stenosis.
   - Atrial tachyarrhythmias with uncontrolled ventricular response.
   - Prior history of ventricular tachycardia.
   - Uncontrolled hypertension.
   - Patients with aortic dissection or large aortic aneurysm.
   - Patients who are on beta blockers may not show adequate heart rate response to dobutamine. It is preferable to use adenosine or dipyridamole in these patients.
5. **Procedure**
   - An infusion pump is necessary for dobutamine administration.
   - An IV line with a Y-connector is required for injecting radioisotope during dobutamine infusion.
   - ECG monitoring and blood pressure monitoring should be performed as with other pharmacologic stressors.
   - Dobutamine infusion should start at a dose of 10 μg/kg/min. The dobutamine dose should then be increased at 3-minute intervals up to a maximum of 40 μg/kg/min. The radiotracer should be injected at 1 minute into the highest dobutamine dose and dobutamine infusion should be continued for 2 minutes after the radiotracer injection.
6. **Early termination of dobutamine.** The indications for early termination of dobutamine are similar to those for exercise stress. Termination for ventricular tachycardia or ST segment elevation is more likely with dobutamine than with other stressors.
7. **Side effects.** Side effects occur in about 75% of patients. The common side effects are palpitation (29%), chest pain (31%), headache (14%), flushing (14%), dyspnea (14%), and significant supraventricular or ventricular arrhythmias (8%-10%). Ischemic ST segment depression occurs in approximately one third of patients undergoing dobutamine infusion. Severe side effects may require IV administration of a short acting β-blocker (Esmolol).

Radiotracers

The currently available myocardial perfusion tracers with SPECT are divided into two groups: Tl-201 and Tc-99m agents (Tc-99m sestamibi and Tc-99m tetrofosmin). Tl-201 is used in a dose of 2.5 to 3.0 mCi and the Tc-99m tracers can be used in a dose of 15 to 30 mCi.

Imaging Protocols

- A single dose of Tl-201 is used for stress and redistribution imaging, done 2.5 to 4.0 hours apart. Additional rest imaging using an additional dose of Tl-201 is only required in cases where standard stress-redistribution imaging shows a fixed or minimally reversible perfusion abnormality.
- Tc-99m–labeled tracers require two separate injections for stress and rest imaging: 15 to 30 mCi for each injection.
- Ideally stress and rest imaging with Tc-99m agents should be performed on two separate days (2-day imaging protocol). However, because of logistical reasons, both stress and rest studies are often performed on the same day

(1-day imaging protocol). This requires use of unequal radiotracer doses: smaller dose (8-10 mCi) for the first injection and larger dose (24-30 mCi) for the second injection. (These are the commonly used doses in the United States. The allowable upper limits of radiotracers may differ in different countries.) Issues regarding the imaging sequence (stress vs rest first) and the minimum time interval between the two radiotracer injections are not fully settled. For exercise myocardial perfusion imaging in patients with known CAD or with high likelihood of CAD, both rest-stress and stress-rest imaging sequence are equally acceptable. However, in patients with a relatively low likelihood of CAD, it is preferable to start with exercise imaging first. If the exercise study is completely normal with regard to both perfusion and function, rest imaging is not required. A delay of 2 to 3 hours is required between the two injections to allow time for hepatobiliary and gastrointestinal clearance of the radiotracer from the first injection. In overweight patients (above 200 lbs) low dose of Tc-99m radiotracer may result in suboptimal images, therefore, 2-day imaging protocol is preferable. Since pharmacological stress perfusion imaging results in higher hepatic and gastrointestinal tracer uptake with slower clearance compared to exercise studies, a rest-stress imaging sequence may offer an advantage. Use of Tl-201 for initial rest imaging and a Tc-99m–labeled tracer for stress perfusion imaging allows a shorter duration of the entire imaging protocol. However, this may not be an ideal approach for patient population with low likelihood of CAD, who may not require rest perfusion imaging.

Interval between the radiotracer injection and imaging. Unlike Tl-201, where stress perfusion imaging should start within 5 to 10 minutes after the tracer injection, Tc-99m agents require a longer delay in order to allow adequate hepatobiliary clearance of the radiotracer. For Tc-99m sestamibi, a minimum delay of 15 to 20 minutes for exercise, 45 to 60 minutes for rest, and 60 minutes for pharmacological stress are optimal. For Tc-99m tetrofosmin, a minimum delay of 10 to 15 minutes for exercise, 30 to 45 minutes for rest, and 45 minutes for pharmacological stress are optimal. Since there is minimal redistribution with these agents, longer delays up to two hours between the radiotracer injection and imaging can be given for logistical reasons.

Bibliography

1. Zaret BL, Wackers FJTh. Nuclear cardiology. N Engl J Med 1993;329:775-83, 855-63.
2. Miller DD, Labovitz AJ. Dipyridamole and adenosine vasodilator stress for myocardial imaging: vive la difference [editorial]. J Am Coll Cardiol 1994;23:390-2.
3. Lette J, Tatum JL, Fraser S, Miller DD, et al. Safety of dipyridamole testing in 73,806 patients: the Multicenter Dipyridamole Safety Study. J Nucl Cardiol 1995;2:3-17.
4. Chua T, Kiat H, Germano G, et al. Gated technetium-99m sestamibi for simultaneous assessment of stress myocardial perfusion, post exercise regional ventricular function and myocardial viability: correlation with echocardiography, and rest thallium-201 scintigraphy. J Am Coll Cardiol 1994;35:1185-92.
5. Wackers FJTh, Berman DS, Maddahi J, et al. Technetium-99m hexakis 2-methoxyisobutyl isonitrile: human biodistribution, dosimetry, safety and preliminary comparison to thallium-201 for myocardial perfusion imaging. J Nucl Med 1989;30:301-11.
6. Taillefer R, Laflamme L, Dupras G, Picard M, Phaneuf DC, Leveille J. Myocardial perfusion imaging with ^{99m}Tc-methoxy-isobutyl-isonitrile (MIBI): comparison of short and long time intervals between rest and stress injections. Preliminary results. Eur J Nucl Med 1988;13:515-22.
7. Berman DS, Hachamovitch R, Kiat H, Cohen I, Cabico JA, Wang FP, et al. Incremental value of prognostic testing in patients with known or suspected ischemic heart disease: a basis for optimal utilization of exercise technetium-99m sestamibi myocardial perfusion single-photon emission computed tomography. J Am Coll Cardiol 1995;26:639-47.
8. Kelley JD, Forster AM, Higley B, Archer CM, et al. Technetium-99m-tetrofosmin a new radiopharmaceutical for myocardial perfusion imaging. J Nucl Med 1993;34:222-7.
9. Higley B, Smith FW, Smith T, et al. Technetium-99m-1,2 bis[bis(2-ethoxyethyl)phosphino]ethane: human biodistribution, dosimetry and safety of a new myocardial perfusion imaging agent. J Nucl Med 1993;34:30-8.
10. Iskandrian AS, Verani MS, Heo J. Pharmacologic stress testing: mechanism of action, hemodynamic responses, and results in detection of coronary artery disease. J Nucl Cardiol 1994;1:94-111.
11. Jain D, Wackers FJTh, Mattera J, McMahon M, Sinusas AJ, Zaret BL. Biokinetics of technetium-99m-tetrofosmin: myocardial perfusion imaging agent: implications for a one day imaging protocol. J Nucl Med 1993;34:1254-9.
12. Jain D, Zaret BL. Technetium 99m tetrofosmin. In: Iskandrian AE, Verani MS, editors. New developments in cardiac nuclear imaging. 1st ed. Armonk (NY): Futura Publishing; 1998. p. 29-58.
13. Jain D. Technetium labeled myocardial perfusion imaging agents. Semin Nucl Med 1999;29:221-36.
14. Glover DK, Okada RD. Myocardial kinetics of Tc-MIBI in canine myocardium after dipyridamole. Circulation 1990;81:628-37.
15. Braat SH, Leclercq B, Itti R, Lahiri A, Sridhara B, Rigo P. Myocardial imaging with technetium-99m-tetrofosmin: comparison of one-day and two-day protocols. J Nucl Med 1994;35:1581-5.
16. Zaret BL, Rigo P, Wackers FJTh, Hendel RC, Braat SH, Iskandrian AS, et al, and the Tetrofosmin International Trial Group. Myocardial perfusion imaging with technetium-99m tetrofosmin: comparison to thallium-201 imaging and coronary angiography in a phase III multicenter trial. Circulation 1995;91:313-9.

17. Leppo JA, DePuey EG, Johnson LL. A review of cardiac imaging with sestamibi and teboroxime. J Nucl Med 1991;32:2012-22.
18. Samady H, Wackers F, Deman P, Natale D, Marlett K, Zaret BL, et al. Low level exercise combined with adenosine myocardial perfusion imaging improve image quality, diagnostic accuracy and side effect profile [abstract]. Circulation 1997;96(Suppl):I-735.
19. Candell-Riera J, Santana-Boado C, Castell-Conesa J, et al. Simultaneous dipyridamole/maximal subjective exercise with Tc-99m-MIBI SPECT: improved diagnostic yield in coronary artery disease. J Am Coll Cardiol 1997;29:531-6.
20. Berman DS, Kiat H, Friedman JD, et al. Separate acquisition rest thallium-201/stress technetium-99m sestamibi dual-isotope myocardial perfusion single-photon emission computed tomography: a clinical validation study. J Am Coll Cardiol 1993;22:1455-64.
21. Mahmood S, Gunning M, Bomanji JB, et al. Combined rest thallium-201/stress technetium-99m-tetrofosmin SPECT: feasibility and diagnostic accuracy of a 90-minute protocol. J Nucl Med 1995;36:932-5.
22. Samady H, Lee J, Natale D, Pestalozzi J, Jain D, Wackers F. Fast ninety minute Tc-99m tetrofosmin stress-rest imaging protocol: value and limitations [abstract]. J Am Coll Cardiol 1998;31(Suppl A):175A.
23. Stratmann HG, Mark AL, Amato M, et al. Risk stratification with pre-hospital discharge exercise technetium-99m sestamibi myocardial tomography in men after acute myocardial infarction. Am Heart J 1998;136:87-93.
24. Desideri A, Candelpergher G, Zanco P, et al. Exercise technetium 99m sestamibi single-photon emission computed tomography late after coronary artery bypass surgery: long-term follow-up. Clin Cardiol 1997;20:779-84.
25. Boyne TS, Koplan BA, Parsons WJ, et al. Predicting adverse outcome with exercise SPECT technetium-99m sestamibi imaging in patients with suspected or known coronary artery disease. Am J Cardiol 1997;79:270-4.
26. Iskander S, Iskandrian AE. Risk assessment using single-photon emission computed tomographic technetium-99m sestamibi imaging. J Am Coll Cardiol 1998;32:57-62.
27. Amanullah AM, Berman DS, Erel J, et al. Incremental prognostic value of adenosine myocardial perfusion single-photon emission computed tomography in women with suspected coronary artery disease. Am J Cardiol 1998;82:725-30.
28. Taillefer R, DePuey EG, Udelson JE, et al. Comparative diagnostic accuracy of Tl-201 and Tc-99m sestamibi SPECT imaging (perfusion and ECG-gated SPECT) in detecting coronary artery disease in women. J Am Coll Cardiol 1997;29:69-77.
29. Travin MI, Duca MD, Kline GM, et al. Relation of gender to physician use of test results and to the prognostic value of stress technetium 99m sestamibi myocardial single-photon emission computed tomography scintigraphy. Am Heart J 1997;134:73-82.
30. Amanullah AM, Berman DS, Hachamovitch R, et al. Identification of severe or extensive coronary artery disease in women by adenosine technetium-99m sestamibi SPECT. Am J Cardiol 1997;80:132-7.
31. Pennell DJ, Underwood SR, Swanton RH, Walker JM, Ell PJ. Dobutamine thallium myocardial perfusion tomography. J Am Coll Cardiol 1991;18:1471-9.
32. Pennell DJ, Underwood SR, Ell PJ. Safety of dobutamine stress for thallium myocardial perfusion tomography in patients with asthma. Am J Cardiol 1993;71:1346-50.
33. Pennell DJ, Mavrogeni S, Forbat SM, Karwatowski SP, Underwood SR. Adenosine combined with dynamic exercise for myocardial perfusion imaging. J Am Coll Cardiol 1995;25:1300-9.

FIRST-PASS RADIONUCLIDE ANGIOGRAPHY (FPRNA)

Purpose. To assess LV and right ventricular (RV) function at rest or during stress (evaluation of wall motion, ejection fraction [EF], and other systolic and diastolic parameters). To assess and measure left-to-right shunts.

Acquisition Protocols

Acquisition parameters

	Rest	Exercise		For info see paragraph
Radiopharmaceutical	Tc-99m	Tc-99m	Standard	1
Dose				2,13,19
Multicrystal (LV & RV)	10-25 mCi	25 mCi	Standard	
Single crystal (LV & RV)	20-25 mCi/0.3-0.5 mL	20-25 mCi/0.3-0.5 mL	Standard	
Shunt	10-15 mCi/0.3-0.5 mL		Standard	
Injection site				3,14
RV function	Antecubital vein	Antecubital vein	Standard	
	External jugular	External jugular	Optional	
LV function	Antecubital vein	Antecubital vein	Standard	
	External jugular	External jugular	Optional	
Shunt	Antecubital vein		Preferred	
	External jugular		Optional	
IV cannula	18 gauge-arm	18 gauge-arm	Standard	4
	20 gauge-neck	20 gauge-neck	Optional	
Injection rate				5,15,16,20
RV function	Slow (FWHM 2-3 s)	Slow (FWHM 2-3 s)	Preferred	
LV function	Rapid (FWHM <1 s)	Rapid (FWHM <1 s)	Standard	
Shunt	Rapid (FWHM <1 s)		Standard	
Position				6, 17, 21
RV function	Upright	Upright	Standard	
	Supine	Supine	Optional	
	20˚-30˚ RAO	20˚-30˚ RAO	Preferred	
	Anterior	Anterior	Optional	
LV function	Upright	Upright	Preferred	
	Supine	Supine	Optional	
	Anterior	Anterior	Standard	
	RAO	RAO	Optional	
Shunt	Anterior		Standard	
ECG signal				7, 22
RV & LV function	Multicrystal no	Multicrystal no	Standard	
	Single crystal yes	Single crystal yes	Standard	
Shunt	No		Standard	
Energy window	120-160 keV	120-160 keV	Standard	8
Frame time				9, 23
LV & RV function	25 ms	25 ms	Standard	
	50 ms	50 ms	Optional	
Shunt	50 ms		Standard	
	100 ms		Optional	
Total frames				10, 24
LV & RV function	2000	1500-2000	Standard	
Shunt	2000		Standard	
Matrix-multicrystal				11, 25

Continued on next page

Acquisition parameters—cont'd

	Rest	Exercise		For info see paragraph
RV & LV function	20 × 20	20 × 20	Standard	
	14 × 20	14 × 20	Optional	
Shunt	20 × 20 or 14 × 20		Standard	
Matrix-single crystal				11, 25
RV function	64 × 64	64 × 64	Preferred	
	32 × 32	32 × 32	Optional	
LV function	32 × 32	32 × 32	Preferred	
	64 × 64	64 × 64	Optional	
Shunt	32 × 32 or 64 × 64		Standard	
Collimator-single crystal				12, 18, 26
LV & RV function & shunt	High sensitivity	High sensitivity	Standard	
LV function	Ultra-high sensitivity	Ultra-high sensitivity	Preferred	
RV function	Ultra-high sensitivity	Ultra-high sensitivity	Optional	
Shunt	Diverging		Optional	
Collimator multicrystal				12, 18, 26
(SIM 400) (RV, LV & shunt)	18 mm	18 mm	Standard	
	13 mm-10 mCi	13 mm-10 mCi	Optional	
	27 mm-25 mCi	27 mm-25 mCi	Optional	
System 77	1 inch	1 inch	Standard	

FPRNA—LV Function

1. Tc-99m, typically as Tc-99m diethylamine triamine pentaacetic acid (DTPA), is the radionuclide of choice for standard FPRNA because it enhances renal excretion. Tc-99m pertechnetate may also be used. Other technetium-based compounds, such as the technetium perfusion agents sestamibi and tetrofosmin are suitable. The short-lived radionuclides, gold-195m and iridium-191m, have been used for FPRNA but are not currently approved by the Food and Drug Administration (FDA).
2. The standard dose given is 25 mCi for both rest and exercise studies. A dose as low as 10 mCi may be used as an option in rest studies for multicrystal cameras. Since the study is count dependent and the single crystal cameras have limited count rate capabilities, doses of 20 to 25 mCi are typically recommended. When predicated by dosimetry considerations, lower doses may have to be used. Doses as low as 10 mCi may be used with reasonable clinical success but run the risk of inadequate count rates especially for wall motion analysis. A rule that should be applied to test if enough counts have been acquired for a diagnostic clinical study is that the end diastolic frame of the representative cycle should have more than 2500 counts in the LV region of interest (ROI).
3. No peripheral sites other than the antecubital (preferably medial) and external jugular veins are suitable for FPRNA. The study should not be attempted if those sites are not available.
4. Some users prefer larger bore cannulae in the 14 to 16 gauge range, but they are optional and not highly recommended because of the increased trauma. The cannula should be directly connected to a suitable length of IV tubing, preferably 12 to 20 inches. The free end of the tubing should be attached to a three-way stopcock with a sufficiently large bore to accommodate rapid injections. All IV connections should be lock-type rather than slip, to avoid contamination. A 10 to 20 mL saline bolus is used to flush the radionuclide bolus into the venous system. The saline bolus should be injected at a continuous, uninterrupted rate so that the entire 10 to 20 mL is injected in 2 to 3 seconds.
5. The injection for LV studies must be rapid. The FWHM of the bolus transit in the superior vena cava should be <1 second and, if possible, <0.5 second. That will virtually guarantee a technically adequate study, all other variables being equal.
6. The most common position used is the upright, straight anterior view. Its advantages are the ease with which the chest may be stabilized against the detector and the straightforward approach to positioning the patient so that the left ventricle will be in the FOV. A transmission source or a 1 mCi tracer dose is recommended to ensure proper

positioning. The chief disadvantage of the anterior view is the anatomic overlap that may occur with the descending aorta and the basal portion of the inferoseptal wall and with the left atrium and the basal portion of the left ventricle. The shallow RAO view helps eliminate both of those sources of overlap but is more difficult to standardize. A foam cushion cut at a 30° angle may be used for such positioning. The choice of upright versus supine positioning depends, to some degree, on the clinical situation. The upright position is, in general, preferred. Pulmonary background is reduced in the upright position, which enhances study quality. Position of the patient during treadmill exercise is a critical issue since the FOV of the detectors is small. It is suggested that a person should be behind the patient during peak stress for proper positioning of the chest in relation to the detector. This is of crucial importance, so that the heart will be within the FOV during acquisition. A point source should also be placed in such a manner (left border of the sternum) that counts from the point source will be acquired during injection of the Tc-99m tracer. It is important to emphasize that for accurate studies of first pass during treadmill exercise, the heart, lung, and point source should all be in the FOV throughout the entire acquisition.

7. In high count rate studies, as are typically acquired with the multicrystal camera, there are enough counts at end diastole (ED) and end systole (ES) to reliably identify the end diastolic and end systolic frames without the aid of an ECG signal. However, for single crystal gamma cameras, count rates during the LV phase may occasionally be inadequate for reliable identification of the end diastolic frames. Acquisition of an ECG signal is therefore highly recommended to facilitate data processing. Single crystal cameras vary widely in their count-rate capabilities and thus in how appropriate they are for imaging a first-pass cardiac study. Several state-of-the-art gamma cameras can count at least 150,000 counts per second at a 20% loss of total counts. Use of cameras with lower count rate capabilities could lead to clinically significant inaccuracies in the determination of LVEF and particularly in the assessment of wall motion.
8. The 140 keV photopeak of Tc-99m ± 15% (140 ± 21 keV) is fairly standard and results in adequate count rates. This corresponds very closely to the 120 to 160 keV window used. The window may be widened to ± 30% for low-dose injections.
9. Theoretically the frame time should be varied to suit the heart rate at the time of acquisition. The relationship is fairly linear with 50 milliseconds being quite adequate at heart rates < 80 beats per minute and 25 milliseconds for heart rates of 125 to 175 beats per minute. At very high heart rates, 10 to 20 millisecond frame times should be considered especially if diastolic function is of interest. In practice, to avoid the potential errors that might occur if the frame time was constantly being manipulated, a standard of 25 milliseconds per frame is recommended for all acquisitions.
10. Fifteen hundred to 2000 frames are sufficient to document the entire study: beginning with the fact that the system is providing count rate followed by documentation bolus injection, and finally that there will be enough frames to capture the entire LV phase.
11. The matrix size of the multicrystal camera is a given due to the inherent design of the systems. It cannot be altered. However, for single crystal cameras the matrix size will largely depend on the computer system being used since most vendors do not offer many, if any, choices for dynamic studies. Most systems that have first-pass software support 64×64 acquisitions. Some systems also support 32×32 matrices. The latter is preferable because count density per pixel is maximized. The 64×64 matrix works reasonably well when count rates are high, but when counts are suboptimal or when the LVEF is high, there is a tendency for the endosystolic frame to have insufficient counts per pixel for assessment of regional wall motion. The actual minimum number of counts per frame needed varies depending on the number of frames per cardiac cycle, the actual LVEF, the amount of background radiation, and whether the study is performed to measure LVEF alone or in conjunction with an assessment of wall motion.
12. The choice of collimators depends on the objectives of the study and the dose to be injected. For standard rest and exercise studies using 20 to 25 mCi doses, the 18 mm thick collimator provides a good compromise between sensitivity and spatial resolution for multicrystal cameras. A thinner collimator sacrifices spatial resolution but may be necessary for lower dose injections. For single crystal cameras, most vendors offer high sensitivity collimators and some offer ultra-high sensitivity collimators. It is helpful to categorize the collimators quantitatively in counts per millicurie per minute because one vendor's high sensitivity collimator may be equivalent to another vendor's ultra-high sensitivity collimator. For the purposes of first-pass studies, a high sensitivity collimator should provide approximately 12,000 to 24,000 counts/s/mCi or as an alternative criteria. This number may vary significantly depending on crystal thickness and dead time of the system. For LFOV systems, it may be desirable to shield part of the peripheral FOV to reduce unwanted pulse pileup which increases the dead time of the system.

FPRNA—RV Function

13. Since the injection bolus reaches the RV without significant dispersion, lower doses may be adequate; 10 to 25 mCi doses are acceptable.
14. The use of the antecubital vein is appropriate for RV studies. The external jugular vein may be used but, unlike the LV study, it may result in too rapid an appearance and disappearance of the radionuclide from the chamber.
15. A 10 to 20 mL saline bolus is generally used to flush the radionuclide bolus into the venous system. The saline bolus should be injected at a continuous, uninterrupted rate so that the entire 10 to 20 mL is injected in 3 to 4 seconds.
16. To optimize assessment of RV function the FWHM of the bolus in the superior vena cava should be 2 to 3 seconds, much slower than that of an LV study. The slower bolus increases the number of beats available for analysis. For assessment of biventricular function a bolus with an FWHM of 1 to 2 seconds in the superior vena cava may be used as a compromise realizing that assessment of neither ventricle is optimized.
17. A shallow (20° to 30°) RAO view is recommended to enhance right atrial-RV separation, which is the chief advantage of first-pass RNA over gated equilibrium RNA for the measurement of RVEF.
18. As for LV function studies, the choice of collimators depends on the objectives of the study and the dose to be injected. For standard rest and exercise studies using 10 to 25 mCi doses, the 18 mm collimator from multicrystal cameras provides a good compromise between sensitivity and spatial resolution. A thinner collimator sacrifices spatial resolution but may be necessary for lower dose injections. For single crystal cameras, the high sensitivity collimator is the standard.

FPRNA—Shunt Study

19. A 10 to 15 mCi dose of the Tc-99m radiopharmaceutical is typically used.
20. The injection should be rapid for shunt studies. The premise of the shunt study is that the appearance in and clearance of the radionuclide bolus from the pulmonary circulation is monoexponential in character. A delayed bolus may result in a pulmonary curve that deviates enough from a monoexponential curve as to make the data uninterpretable. A 10 to 20 mL saline bolus is generally used to flush the radionuclide bolus into the venous system. The saline bolus should be injected at a continuous, uninterrupted rate so that the entire 10 to 20 mL is injected in 2 to 3 seconds.
21. Acquisition in the anterior view is best for imaging the lung fields, which are the areas of interest for the shunt study. If both lung fields cannot be visualized due to the detector size, the lung field of interest should be the right lung for suspected intracardiac shunts and the left lung for a suspected PDA.
22. Since only pulmonary data will be quantified, an ECG signal is unnecessary.
23. Frame time is not crucial in a shunt study since the data will ultimately be analyzed using curves whose data points do not require more than 100 millisecond temporal resolution. Shorter frame times may be used since they may be added together during the analysis.
24. Total frames acquired should be 2000.
25. For multicrystal systems, the matrix is not an option. For single crystal systems, a 64×64 matrix is appropriate. The 32×32 matrix may also be used.
26. Spatial resolution is much less important in the shunt study. Standard high sensitivity collimators are adequate. If available, a diverging collimator may be used.

Processing Protocols

Measurement of Ventricular Function. Processing first-pass data has become increasingly automated and considerably faster than in previous years. However, it is unlikely that processing of first-pass data can ever be reliably, totally automated. There are too many variations in tracer transit due to technical and/or pathophysiological reasons for automated processing to be successful in all cases. The operator must be observant and careful at a few crucial steps in the processing to ensure consistently accurate results.

Preprocessing. Preprocessing of first-pass data is frequently performed, although it is not mandatory. Time-smoothing, uniformity correction, and dead-time correction are options that are typically applied when supported by the software.

Processing. First-pass data processing can be divided into four major routines: creation of the initial time-activity curve (TAC); beat selection and creation of the initial representative cycle; background correction; and creation of the final representative cycle. A fifth optional routine is that of motion correction.

The Initial TAC

Grouping or Reformatting. The raw or preprocessed data should be grouped into 0.5 to 1.0 second images to facilitate drawing an ROI around the ventricle. If an ECG signal has been acquired, the raw or preprocessed data may be cyclically added using the R wave to identify end diastolic frames, thus creating a preliminary representative cycle. The end diastolic frame of that preliminary representative cycle may then be used to draw an initial ventricular ROI.

Ventricular ROI. The operator or the computer should draw an initial ventricular ROI. This ROI need not be highly accurate since it is only used for generating the initial TAC. A TAC of the raw or preprocessed data using the initial ROI should be displayed using the acquisition frame time.

Beat Selection. Most first-pass software allows the operator to identify the first and last beats to be included in the representative cycle. End diastolic and end systolic frames may be identified automatically by the computer, but the operator must have the opportunity to override the computer to select only appropriate beats. Because of variable mixing in the chamber, it is advisable to select beats both before and after the beat with the maximum counts. Beats whose end diastolic counts are below 50% of the maximum end diastolic count should be excluded as long as this editing does not preclude a statistically adequate representative cycle. Premature ventricular beats and post-PVC beats should be excluded. If there are few sinus beats, it may be difficult to generate a statistically adequate representative cycle.

Beat editing is an optional routine in which individual beats of varying duration may be time corrected so that the final beat lengths are all identical. That approach typically involves an interpolation of the data, but actual end systolic counts should always be preserved so that the EF is not altered by the time correction.

Background Correction. Several approaches to background correction have been proposed. They include the lung frame method, the count threshold method, and the periventricular method. The lung method has been shown to give better results than the other two and is thus the preferred method. The periventricular background region is used as a standard in many single-crystal camera systems.

Lung Frame Method. In this approach, a frame of data just before the appearance of activity in the LV ROI is chosen as representative of the distribution of the background (nonventricular activity). This is a crucial step since variation in the background frame can substantially alter the calculated EF, volumes, and the apparent wall motion. The selected frame should be visualized. That background "mask," after appropriate normalization, is subtracted from the LV representative cycle. A washout factor must be applied to the background since the counts in the background are decreasing throughout the LV phase. This approach has been shown to produce results that compare favorably with contrast angiographic data and is somewhat better than either of the other two approaches.

Count Threshold Method. A frame of data just before the appearance of the radionuclide in the left ventricle is identified and the counts in that frame become the new zero level for each subsequent frame of the LV phase.

Periventricular Method. This method is quite analogous to the periventricular background method in gated equilibrium imaging. A horseshoe-shaped background ROI is drawn around the ventricle, usually 2 to 3 pixels wide and 1 to 2 pixels away from the LV border.

The Final ROI. Once the background correction has been applied to the initial representative cycle, the end diastolic and end systolic frames should be displayed again and any necessary modifications of the initial ROI then performed.

Dual ROI Method. For first-pass studies acquired in the anterior view, separate ROI for the end diastolic and end systolic frames is recommended. The operator must manually draw the final ROI on both frames. In drawing the end systolic ROI, left atrial (LA) activity must be excluded from the end systolic counts. The LVEF calculated with the dual ROI approach tends to be higher than that calculated with a single ROI because the valve plane is placed lower during systole compared to diastole.

Single ROI Method. With the single ROI method, only an end diastolic ROI is used. This approach works fairly well with studies acquired in the RAO projection, where there is better LA-LV separation. In the anterior view, the single ROI method may result in spuriously low EFs because it can potentially include extra ventricular counts in the end systolic ROI.

Motion Correction. Motion correction of first-pass data is occasionally necessary for studies acquired during bicycle exercise and almost always necessary for studies acquired during treadmill exercise. Motion correction may be performed using either or both of two methods, the "single isotope" (internal correction method) or the "dual isotope" (external marker correction). The dual isotope method is preferred for treadmill exercise while the single isotope method is usually adequate for bicycle exercise.

Single Isotope Correction. The position of the ventricle is determined in each frame of the representative cycle by applying a center-of-mass algorithm within an operator-defined ROI. The latter should greatly exceed the actual size of the ventricle. By calculating the average x,y location of the center-of-mass, the location of the ventricle $^{x}n^{y}n$ in any frame, may be reregistered to x,y.

Dual Isotope Correction. An external point source (Am-241, I-125) is applied to the chest, usually midsternally or just to the right of the sternum. A dual-energy acquisition is performed at peak exercise such that two first-pass studies are acquired, one using the external marker's photopeak and the other the standard Tc-99m photopeak. After acquisition, the position of the marker is determined in each frame using a center-of-mass algorithm. The average x,y location of the marker is taken to represent the correct position of the marker had there been no motion. All data frames are then reregistered by the direction and magnitude of the displacement of the marker in that frame.

The Final Representative Cycle. The finalized ROIs are then used to regenerate the TAC and the final representative cycle is created from that curve using the previously determined beat selection. It is this representative cycle that will be used to generate all the quantitative results describing ventricular function.

FPRNA: Quantitation of Results

LVEF. The LVEF is calculated from the final background corrected representative cycle (see Data Processing) as (End diastolic counts – End systolic counts) / End diastolic counts. On occasion, it is impossible to correct accurately for background activity (very delayed bolus, markedly prolonged RV tracer transit, etc). In that case, it is appropriate to report an estimated LVEF or LVEF range based on the uncorrected data.

Systolic Emptying Rates. Systolic emptying rates such as the peak ejection rate may be calculated by applying a Fourier filter (third to fifth order harmonic) to the LV representative cycle curve and then taking the first derivative of that filtered curve. The peak ejection rate should be expressed in end diastolic volumes per second (EDV/s).

Diastolic Filling Rates. Diastolic filling rates such as the peak filling rate may be calculated by applying a Fourier filter (third to fifth order harmonic) to the LV representative cycle curve and then taking the first derivative of that filtered curve. The peak filling rate should be expressed in EDV/s. The time-to-peak-filling rate may be calculated and expressed in milliseconds.

Ventricular Volumes. LV end diastolic volume may be measured using either a geometric or count-proportional technique. In the geometric approach, the end diastolic frame of the representative cycle is displayed using a threshold for edge detection. The area of the left ventricle is measured using the pixel area and the known size of a pixel. The longest length of the left ventricle is identified by the operator and end diastolic volume calculated using the modified Sandler Dodge equation. In the count proportional approach the required data are the total counts in the left ventricle, the counts in the hottest pixel in the left ventricle, and the area of a pixel (m) in cm. The end diastolic volume is then calculated as $1.38\ m^{3/2}R^{3/2}$ where R = Total LV counts / Counts in the hottest pixel.

Left-to-right Shunt Study. The input function for the first-pass shunt study is a high count density, TAC obtained from a pulmonary ROI. In practice, either the left lung, the right lung, or both may be used. In most cases, the right lung is preferred because it is easier to create a pulmonary ROI that is free of contamination from the cyclic changes in counts in the left heart and great vessels. Regardless of the acquisition frame time, the pulmonary curve should be displayed at a frame time of approximately 100 to 300 milliseconds. That allows the operator to easily visualize the entire curve for qualitative assessment of the presence or absence of a shunt. Not infrequently, the raw curve requires time-smoothing to eliminate high-frequency contamination of the curve from cardiac chamber or great vessel counts or from random noise.

The first frame of the curve should unequivocally represent pulmonary activity rather than any SVC, RA, or RV activity because the shape of the early part of the curve will determine the shape of the subsequent mathematical fit. It may be helpful to mask out the SVC and right heart from the image before drawing the pulmonary ROI. Careful attention to the statistical content of the pulmonary curve and its freedom from contamination are crucial. The operator may then apply either a gamma variate or an exponential fit to the raw data. Qualitative assessment of the closeness of the fitted curve to the raw curve is important. Varying the initial frame of the fit and the final frame of the fit may be necessary to produce the best fitted curve possible. The fitted curve may then be subtracted from the raw data to leave the shunt component behind, which can, itself be fitted with another curve that represents the shunt component. The shunt ratio Qp:Qs is then calculated as A1 + A2 / A1 where A1 = the area under the primary fitted curve and A2 = the area under the secondary (shunt) fitted curve.

Bibliography

1. Aroney CN, Ruddy TD, Dighero H, et al. Differentiation of restrictive cardiomyopathy from pericardial constriction: assessment of diastolic function by radionuclide angiography. J Am Coll Cardiol 1989;13:1007-14.
2. Berger HJ, Matthay RA, Loke J, et al. Assessment of cardiac performance with quantitative radionuclide angiocardiography: RV ejection fraction with reference to findings in chronic obstructive pulmonary disease. Am J Cardiol 1978;41:897-905.
3. Berger H, Reduto L, Johnstone D, et al. Global and regional left ventricular response to bicycle exercise in coronary artery disease: assessment by quantitative radionuclide angiocardiography. Am J Med 1979:66:13-21.
4. Borges-Neto S, Coleman RE, Jones RH. Perfusion and function at rest and treadmill exercise using technetium-99m sestamibi: comparison of one and two day protocols in normal volunteers. J Nucl Med 1990;31:1128-32.
5. Borges-Neto S, Coleman RE, Potts JM, Jones RH. Combined exercise radionuclide angiocardiography and single photon emission computed tomography perfusion studies for assessment of coronary disease. Semin Nucl Med 1991;21:223-9.
6. Borges-Neto S, Shaw L. The added value of simultaneous myocardial perfusion and left ventricular function. Curr Opin Cardiol 1999;14:460-3.
7. Borges-Neto S. Perfusion and function assessment by nuclear cardiology techniques. Curr Opin Cardiol 1997;12:581-6.
8. Campos CT, Chu HW, D'Agostino HJ Jr, Jones RH. Comparison of rest and exercise radionuclide angiocardiography and exercise treadmill testing for diagnosis of anatomically extensive coronary artery disease. Circulation 1983;67:1204-10.
9. DePace NL, Iskandrian AS, Hakki A, et al. Value of left ventricular ejection fraction during exercise in predicting the extent of coronary artery disease. J Am Coll Cardiol 1983;1:1002-10.
10. Foster C, Dymond DS, Anholm JD, et al. Effect of exercise protocol on the left ventricular response to exercise. Am J Cardiol 1983;51:859-64.
11. Friedman JD, Bennan DS, Kiat H, et al. Rest and treadmill exercise first-pass radionuclide ventriculography: validation of left ventricular ejection fraction measurements. J Nucl Cardiol 1994;4:382-8.
12. Gal R, Grenier RP, Carpenter J, et al. High count rate first-pass radionuclide angiography using a digital gamma camera. J Nucl Med 1986;27:198-206.
13. Gal R, Grenier RP, Schmidt DH, Port SC. Background correction in first-pass radionuclide angiography: comparison of several approaches. J Nucl Med 1986;27:1480-6.
14. Gal R, Grenier RP, Port SC, Dymond DS. Left ventricular volume calculation using a count-based ratio method applied to firstpass radionuclide angiography. J Nucl Med 1992;33:2124-32.
15. Johnson LL, Rodney RA, Vaccarino RA, et al. Left ventricular perfusion and performance from a single radiopharmaceutical and one camera. J Nucl Med 1992;33:1411-6.
16. Jones RH, McEwen P, Newman GE, et al. Accuracy of diagnosis of coronary artery disease by radionuclide measurement of left ventricular function during rest and exercise. Circulation 1981;64:586-601.
17. Lee KL, Pryor DB, Pieper KS, Hasell FE Jr. Prognostic value of radionuclide angiography in medically treated patients with coronary artery disease. Circulation 1990;82:1705-17.
18. Maltz DL, Treves S. Quantitative radionuclide angiocardiography: determination of Qp:Qs in children. Circulation 1973;47:1048-56.
19. Morrison DA, Turgeon J, Quitt T. Right ventricular ejection fraction measurements: contrast ventriculography versus gated blood pool and gated first-pass method. Am J Cardiol 1984;54:651-3.
20. Nichols K, DePuey EG, Gooneratne N, et al. First-pass ventricular ejection fraction using a single crystal nuclear camera. J Nucl Med 1994;35:1292-1300.
21. Nichols K, DePuey EG, Rozanski A. First-pass radionuclide angiocardiography using single crystal gamma cameras. J Nucl Cardiol 1997;4:61-73.
22. Nickel O, Schad N, Andrews EJ, et al. Scintigraphic measurement of left ventricular volumes from the count-density distribution. J Nucl Med 1982;23:404-10.
23. Philippe L, Mena I, Darcourt J, French WJ. Evaluation of valvular regurgitation by factor analysis of first-pass angiography. J Nucl Med 1988;29:159-67.
24. Potts JM, Borges-Neto S, Smith LR, Jones RH. Comparison of bicycle and treadmill radionuclide angiocardiography. J Nucl Med 1991;32:1918-22.
25. Reduto LA, Wickemeyer W J, Young JB, et al. Left ventricular diastolic performance at rest and during exercise in patients with coronary artery disease. Circulation 1981;63:1228-37.
26. Upton MT, Rerych SK, Newman GE, et al. The reproducibility of radionuclide angiographic measurements of LV function in normal subjects at rest and during exercise. Circulation 1980;62:126-32.
27. Verani MS, Lacy JL, Guidry GW, et al. Quantification of left ventricular performance during transient coronary occlusion at various anatomic sites in humans: a study using tantalum-178 and a multiwire gamma camera. J Am Coll Cardiol 1992;19:297-306.
28. Williams KA, Bryant TA, Taillon LA. First-pass radionuclide angiographic analysis with two regions of interest to improve left ventricular ejection fraction accuracy. J Nucl Med 1998;39:1857-61.

EQUILIBRIUM RADIONUCLIDE ANGIOCARDIOGRAPHY (ERNA) IMAGING PROTOCOLS

Purpose. To measure LV function at rest or during stress. Evaluation of ventricular wall motion, EF, and other systolic and diastolic functional parameters.

Acquisition Protocols: Planar Imaging

Acquisition parameters

	Rest	Exercise		For info see paragraph
Radiopharmaceutical	Tc-99m–labeled RBCs	Tc-99m–labeled RBCs	Preferred	1
Dose	20-25 mCi/70 kg	25-35 mCi/70 kg	Preferred	1
Labeling method	In vitro or modified in vivo (2-3 mg SN-PYP)	In vitro or modified in vivo (2-3 mg SN-PYP)	Preferred (either)	2
	Ultra-tag kit	Ultra-tag kit	Optional	2
Collimator (rest/exercise)	Parallel-LEAP	Parallel-LEAP	Preferred	3
	Parallel-high SENS	Parallel-high SENS	Optional	3
Collimator (rest only)	Parallel-high Res		Preferred	3
	Parallel-LEAP		Optional	3
	Slant hole	Slant hole	Optional	3
Pixel size	<4 mm/pixel	<4 mm/pixel	Standard	4, 5
	2-3 mm/pixel	2-3 mm/pixel	Preferred	4, 5
Energy window	140 KeV ± 10%	140 KeV ± 10%	Standard	6
Bad beat	Buffered beat	Buffered beat	Preferred	7
	On-the-fly:	On-the-fly:	Standard	7
	Reject beat and next beat	Reject beat and next beat		7
Beat length window	± 10%-15%	± 10%-15%	Standard	7
	Check trigger	Check trigger	Preferred	7
Acquisition method	Frame mode	Frame mode	Standard	8
	List mode	List mode	Optional	8
Frame rate (EF)	>16 Fr/cycle	16-32 Fr/cycle	Standard	9
	24-32 Fr/cycle	24-32 Fr/cycle	Preferred	9
Count density	>1800/pixel (3 mm) or 20,000/cm^2 (high RES collimator)	NA	Standard	10
	>3600/pixel (3 mm) or 40,000/cm^2 (high SENS collimator)	>2 min acquisition	Standard	10
Positioning	LAO (best right/ left separation)	LAO (best right/ left separation)	Standard	11
	LAO (caudal tilt),	LAO (caudal tilt)	Optional	11
	Plus ANT, LAT		Standard	11
QC	View cine-loop	View cine-loop	Preferred	12
	R-R histogram	R-R histogram	Preferred	12

ERNA is used to determine the global and regional function of, primarily, the left ventricle. The following sections provide a technical description of the techniques to acquire and process the data necessary to assess parameters of ventricular performance.

Radiopharmaceutical

1. Inject the patient with Tc-99m–labeled red blood cells, with activity of approximately 20 to 25 mCi/70 kg-body weight (11 to 13 MBq/kg) to provide the radioisotope tag for resting studies. For exercise studies the activity can be increased to 25 to 35 mCi/70 kg patient.

2. **Labeling methods**
   - In vitro or modified in vivo/in vitro methods (eg, using 2 to 3 mg stannous pyrophosphate 15 minutes before injection of the radiopharmaceutical).
   - Ultra-tag kit.

Camera/computer Set Up

3. **Collimator.** For resting studies, use of a parallel hole, high resolution, collimator with spatial resolution of approximately 8 to 10 mm FWHM (of a line spread function) or better at 10 cm distance from the collimator, and a sensitivity (for Tc) of approximately 4000 to 5000 counts/s/mCi (108 to 135 counts/s/MBq) is preferred. If a time-limited stress study (eg, bicycle exercise) is to be performed, a higher sensitivity (and therefore poorer spatial resolution) collimator may be considered, such as a low-energy all-purpose (LEAP) collimator (typically 12 mm FWHM at 10 cm and sensitivity of approximately 10,000 counts/s/mCi, or approximately 280 counts/s/MBq), or optionally a high sensitivity collimator. In this case, it is especially important to keep collimator-chest wall distance minimized. It is recommended that the same collimator be used for both the rest and stress study, with parallel hole LEAP collimator preferred. If caudal tilt is used (see paragraph 11), a slant hole collimator may be considered instead of a parallel hole collimator to provide 10˚ to 15˚ of caudal tilt, while maintaining minimal collimator-chest wall distance.
4. **Pixel size.** Any matrix size that results in a pixel size ~<4 mm/pixel (approximately 2 to 3 mm/pixel preferred) can be used. These acquisitions are usually performed using a zoomed 64×64 matrix of 16-bit (word) pixels. The zoom required to meet the <4 mm/pixel criteria will depend on the FOV of the camera used. Minimal to no zoom is recommended for small FOV cameras (circular - 10 inch diameter, or square - 8 inch) to zoom factors of 1.5 to 2.2 for large FOV (rectangular - 21 inch) cameras. Smaller FOV cameras, if available, are preferred. In any case, pixel size should not exceed 5 mm. See paragraph 5.
5. **FOV.** The effective FOV is dependent on the camera size and acquisition zoom utilized. Typically an 18 cm $\times$ 18 cm square FOV will be sufficient, but any FOV size sufficient to encompass all four cardiac chambers and at least 2 cm beyond the cardiac blood pool (for positioning of a background ROI) is acceptable. Larger FOVs are acceptable, provided they (1) do not inhibit minimizing collimator-chest distance and (2) are not so large as to cause increased gamma camera dead time. If large FOVs are used, care must be taken to prevent acquisitions terminated on liver or spleen overflow, and to ensure that data are displayed with cardiac structures at maximum intensity. Use of a lead apron as a shield for the liver/spleen may be appropriate, positioned with the aid of a persistence scope.
6. **Energy window.** 140 KeV, ± 10% window.
7. **Bad beat/beat length window (arrhythmia rejection).** If systolic function only (EF) is to be assessed, accepting <10% to 15% arrhythmic beats is acceptable. If the examination is performed to determine diastolic function, beat length windowing (arrhythmia rejection) is necessary. The preferred arrhythmia rejection mode is buffered beat, where each beat is temporarily stored in memory to assess whether its beat length is within the (typical) ± 10% to 15% R-R beat length window. If the beat is outside the window it is rejected without contaminating the gated data acquired. Standard arrhythmia rejection methods typically terminate data acquisition if a premature beat is seen outside of the (± 10% to 15%) beat length window (a portion of the bad beat will be acquired). Rejection of the short or long beat, along with rejection of the subsequent (compensatory) beat is preferred. The typical beat length window is ± 10% to 15%, but will vary depending on heart rate and rhythm. If the study is acquired with significant arrhythmias, poor statistics may result, and accurate computation of EF may be compromised. The beat length window may require lengthening to improve statistics, but will compromise measurement of diastolic function, and may adversely affect cine loop displays, if end frames are not corrected or deleted. See paragraph 8.

   Triggers: It is recommended that the ECG trigger point be checked to ensure that the ECG gating circuitry is synchronized to the peak of the ECG R wave. Checks can be performed either visually, with a dual trace oscilloscope, or checked with a commercially available dynamic phantom. Poor quality or delayed triggers can adversely affect the ventricular volume curve.
8. **Acquisition method.** Frame mode gating is standard (forward framing), although forward/backward, and forward/backward by thirds, methods are optional. If arrhythmias are present, the frames at the end of the cardiac cycle (containing data acquired over shorter total acquisition time) should be either corrected or deleted (preferred). List mode data acquisition is optional, and offers increased beat length windowing flexibility, particularly for analysis of diastolic function.
9. **Frame rate.** A frame rate of less than 50 ms/frame is preferred for resting EF. A frame rate of less than 30 ms/frame is preferred if ejection and filling rates are to be computed. For rest studies, a minimum of 16 to 19 frames per car-

diac cycle is recommended, with 24 or 32 preferred for EF calculation and for calculation of ejection and filling parameters. For stress studies (R-R < 600 ms), 32 frame/cycle is preferred for EF calculation and calculation of peak ejection and filling rates.

10. **Count density.** Studies containing approximately 20,000 counts/cm^2 (1800 counts/pixel for a 3 mm pixel) over the center of the left ventricle at rest using high resolution collimation, or about 40,000 counts/cm^2 at rest with the higher sensitivity collimators (LEAP or High Sens), as used in rest/exercise studies, are preferred. [N.B.: Corresponds to about 3-4 million counts in a 15 cm × 15 cm FOV with high resolution collimator.] This count density is measured by summing all images in the gated series together and determining the count density from a small ROI at the center of the left ventricle in the LAO projection. Total counts are not a reliable indicator, as they depend too strongly on the FOV. Nevertheless, a practical rule has been to acquire at least 200,000 counts per image frame for a 16 frame resting study using a high resolution collimator. Similarly, acquisition time will give variable results depending on collimator sensitivity. To calculate a typical acquisition time, for a particular collimator and dose, sum all frames in the study together, and using a small ROI at the center of the left ventricle, determine the time necessary to achieve the above mentioned counts/cm^2. During stress, acquisition time is often the limiting factor. When this is the case, at least 2.5 minutes acquisition at stress is recommended using the LEAP or high sensitivity collimator, as previously specified.
11. **Positioning.** To acquire the ERNA study, position the patient supine (for greatest patient comfort), or in the right lateral decubitus position (to minimize interference from diaphragm and spleen). Three views should be recorded for assessment of wall motion of the left ventricle. (a) LAO optimized to visualize the septum (best septal view—usually the 45˚ LAO, but the angle will depend on body habitus and cardiac orientation). In the LAO view, the orientation should be such that the long axis of the ventricle is approximately vertical, with the apex pointing down and left ventricle on the right side of the image. The two other preferred views are (b) anterior (ANT) - 45˚ more anterior than LAO selected, and (c) lateral (LAT) - 45˚ more lateral (with patient in right side cubitus) than LAO angle selected. Caudal tilt of the LAO view, typically 10˚ to 15˚, is helpful to separate the atria from the ventricle, and may be particularly useful in patients with vertical hearts. The degree of caudal tilt is limited by the detector yoke suspension and the necessity to keep the camera face as close as possible to the chest. As an alternative to achieve a 10˚ to 15˚ caudal tilt, a slant hole collimator may be used, if available. When using caudal tilt, depending on the imaging conditions, the LV and LA separation may not be apparent. This may result in inclusion of more LA than desired, if the atrial-ventricular border is difficult to discern, as the superior aspect of the ROI may encroach into the LA. If the atrial-ventricular border is not evident, use the standard LAO view.
12. **QC.** Assessment of the adequacy of the R-wave trigger prior to instigation of the gated acquisition should be performed. Post-acquisition QC of the ERNA study is also recommended. Visualization of the beating cine loop after acquisition allows data drop-off due to inadequate triggers, significant arrhythmias, rhythm disorders, poor tag, or poor count statistics, to be assessed. Review of the beat-length R-R interval histogram can be used to assess cardiac rhythm abnormalities or determine if significant arrhythmias were present. QC can anticipate errors associated with inadequate ERNA studies prior to the reporting of ventricular performance.

Processing Protocols

1. **LV volume curve generation.** Most parameters describing ventricular function are extracted from a complete LV volume curve (TAC). This curve can be obtained from either a single ROI drawn at ED (and modified at ES, if necessary, to include any dyskinetic regions) or preferably using multiple ROIs drawn at each time point. ROIs should be edited on an amplitude or difference image to exclude overlapping atrial counts. Manually drawn ROIs are the most consistently accurate, although time-consuming. Many automatic techniques exist for drawing ROIs. It is important that the resulting ROIs be checked visually and altered manually if necessary. Irregularities in the LV contour occasionally occur using automatic algorithms, especially for exercise studies, and for ROIs drawn near ES. These irregularities can have significant effects on parameters extracted from the LV curve. If EF only is to be determined, the preferred method (and the simplest) for LV volume curve generation is from manually drawn ROIs over ED and ES, with volume curve processed by weighted interpolation of curves from end diastolic and end systolic ROIs (weighted to ED near the beginning and end of the curve and weighted to ES at curve minimum). If ejection and filling rates are to be computed, ROIs drawn on all frames is preferred. Note: Single ROI definition at ED may underestimate EF. Optionally, automatic edge detection may be used, if each frame is reviewed, and the ROI corrected, if necessary.
2. **Background.** Background is critical for the measurement of many LV parameters. Usually an ROI 5 to 10 mm away from the end diastolic border, drawn from approximately 2 o'clock to 5 o'clock is used, although the exact location

Processing parameters

Parameter	Method		For info see paragraph
LV volume curve generation	Manual ROI at ED and ES	Preferred	1
	Manual or automatic ROIs—		1
	at ED or at each time point	Optional	1
Background	Manual at ED	Preferred	2
	Automatic at ED	Standard	2
	Automatic or manual at ES	Optional	2
LVEF	From ED and end systolic ROIs	Preferred	3a
	From Fourier-filtered curve	Optional	3b
	From single end diastolic ROI (not recommended)	Optional	3c
RVEF	Not widely accepted at equilibrium—see first-pass methods	See first-pass methods	
Wall motion	Visual assessment of cine loop	Preferred	4a
	Phase and amplitude analysis	Optional	4b
	Principle component or factor analysis	Optional	4c
	Regional EF	Optional	4d
LV emptying	Peak rate of emptying	Preferred	5a
	Average rate of emptying	Optional	5b
	Time to peak and systolic interval	Optional	5a, 5b
LV filling	Peak rate of filling	Preferred	6
	Average rate of filling	Optional	6
	Time to peak and diastolic interval	Optional	6
LV volumes	Counts based	Optional	7
	Geometric based	Optional	7
Heart/lung ratio	Counts based—LV/lung	Optional	8

used is less important than consistent placement, and ensuring that atrial counts, counts from the spleen or descending thoracic aorta, LV counts, or a gastric air bubble are excluded. With automatic routines, visual verification of the background ROI is essential. A visual examination of the TAC produced from the background ROI (it should be flat) is useful to determine if LV activity or atrial activity is spilling into the background ROI. If the background curve is flat, this indicates that the background ROI is not sitting over any periodically beating structures, and that all time points may be averaged for good statistics. An ROI adjacent to the end systolic border can be used to estimate background, but care must be taken to use only those time points which do not include LV activity. A rule-of-thumb is that the background count rate/pixel typically lie in the range of 30% to 70% of the end diastolic LV counts, although exceptions to this rule are infrequently found.

3. **LVEF.** (a) Many methods are commercially available for computation of EF. All are adequate. EF can be computed by applying the end diastolic ROI to the end diastolic image and the end systolic ROI to the end systolic image, correcting for background in the end diastolic and end systolic counts, without using the entire LV curve. In this case, care must be taken to ensure the ROIs are appropriate (especially at ES, where automatic techniques occasionally produce irregular ROIs). (b) Fitting the LV curve with two or three harmonics (called Fourier filtering), and extracting the first and the minimum points, as the end diastolic and end systolic count values, is one optionally used method. Because this method uses the entire curve, it reduces statistical fluctuations, even for very short (stress) acquisitions. If the first point of the filtered curve is used, one must ensure that the ECG gate is true, such that the first point truly corresponds to ED. If the R-wave trigger is not precisely at ED (see triggers, acquisition paragraph 7), then the maximum value of the filtered curve can be used to predict end diastolic counts. Fourier fitting fails if there is "drop off" (ie, a decrease in count rate at the end of the curve, due to heart rate variability, arrhythmias) at the end of the curve. Fourier filtering should be applied only to curves that have no drop off or that have been corrected for drop off. (c) EF can be computed from the LV counts produced from a single end diastolic ROI, applied to both the image at ED and the image at ES. In this case, the EF will be consistently lower than in 3 (a) and (b),

and the EF may be more sensitive to background correction than in 3 (a) and (b). Single ROI EF calculations should be viewed with reservations.

4. **Wall motion.** (a) Visual assessment of all three standard views is preferred. It is critical that the cine loop consist of approximately 12 to 16 frames (fewer frames may lose temporal information, greater may compromise statistics). If the acquisition is performed with more than 16 frames for improved temporal resolution, it is imperative that the frames be appropriately added/recombined or filtered before visual assessment. Spatial and temporal filtering are often employed in cine loop presentations. Spatial filtering is typically a 9-point spatial smooth and reduces the apparent quantum mottle of the images. Temporal filtering typically weights the current frame two parts and the previous and post frames one part, to re-create the 16 or more frame cine loop image. Both types of filtering tend to make the cine loop appear more visually pleasing. If rest and stress are to be compared, it is preferred to show both cine loops simultaneously. Optionally, modern application of principle components analysis (PCA) or factors can create a mathematically derived cine loop which separates various types of wall motion (atrial, ventricular) and creates a visually pleasing motion image, and reduces the appearance of noise in the cine. However, the effects of PCA analysis on the assessment of regional wall motion have not been completely evaluated. (b) Phase and amplitude images have been reported to be of use for the detection and quantification of wall motion defects. It is preferred that this method supplement, not replace, visual assessment of the cine loop. Analyses of the phase image, phase histogram, as well as visual assessment of a dynamic phase image, have both been reported to be useful in reducing the subjectivity associated with visual assessment of wall motion defects using cine loops. Also, in patients with conduction abnormalities, phase analysis has proved useful in identifying the pattern, location and/or point of origin of arrhythmic foci. (c) PCA or factors analysis create a mathematically derived set of functional images expressing significant motion components in the image. Displayed as amplitude images and associated time signatures, they may add to the assessment of regional wall motion, and can be viewed in similar fashion to phase and amplitude images, or applied to process the cine loop display (see above). This method is clearly a supplement at this point and should be used in conjunction with standard cine loop assessment of wall motion. (d) Regional EF (ie, dividing the left ventricle into 6-8 sub-regions and applying the conventional formulation for EF) has been reported to aid in the assessment of regional or segmental wall motion. It is preferred that this method supplement, not replace, visual assessment of the cine loop.
5. **LV emptying.** (a) The maximal LV emptying rate is determined by measuring the peak slope of the LV curve, expressed in units of EDV/s. The counts in the end diastolic ROI are used to represent the EDV and the counts in subsequent frames are referenced to this value to compute EDV/s. The time to peak emptying (from the end diastolic frame) may also be computed and expressed in milliseconds. Measurements of the slope of the LV volume curve greatly amplify statistical noise, so the LV curve is either first filtered, or a small region of the curve is fitted to a polynomial, or other, similar, techniques are employed to minimize noise without distorting the value of slope. Measurements of peak emptying at exercise are often considered too heart rate dependent, or statistically inadequate to be of clinical use. When computing peak or maximal emptying rate, 32 frames per cardiac cycle are preferred to ensure accurate assessment of maximal rate. (b) The slope of a line connecting the end diastolic and end systolic points can be used as a measure of the average LV emptying rate. Alternatively, methods that depend on the time it takes for the left ventricle to empty one third (or any other arbitrary fraction) of the way from ED to ES have been reported. These methods do not give maximal rates of emptying, but rather only an indicator of average filling. The emptying time (ED-ES), and time to one third emptying can be computed and expressed as fractions of a second or in milliseconds.
6. **LV filling.** The same techniques described in (5) above can be used to measure diastolic filling rates. All of the same considerations mentioned above for emptying also hold for filling. Note that the gating requirements for adequate representation of diastolic parameters are more stringent than for systolic ejection parameters, due to data drop-off at the end of the cardiac cycle.
7. **LV volumes.** Acceptable results have been reported in the literature using both counts based and (to a lesser extent) geometrically-based methods, although count-based methods are preferred. Geometric methods are based on the standard "area-length" methods and are hampered by the limited spatial resolution of ERNA. Both the counts-based and geometric methods may produce highly inaccurate results unless extraordinary attention is paid to methodological detail. These methods are not widely used. Assessment of LV volume are affected by gamma ray attenuation through the patient, Compton scatter and the like. Count-based methods include the "aortic arch" method, or methods involving blood draws and calibration of the counts-to-volume ratio. The latter method is highly influenced by photon attenuation. Calculation of absolute volumes is not recommended, except for laboratories who have the ability to independently validate their methodology.

8. **Heart/lung ratio.** Heart/lung ratio can optionally be computed. The ratio of counts in the cardiac blood pool to the counts in the lung can be useful to assess ventricular inadequacy. Pooling of blood in the lungs has been reported to be indicative of left ventricle failure.

Bibliography

1. Strauss HW, Zaret BL, Hurley PJ, et al. A scintiphotographic method for measuring left ventricular ejection fraction in man without cardiac catheterization. Am J Cardiol 1971;28:575-80.
2. Zaret BL, Strauss HW, Hurley PJ, et al. A non-invasive scintiphotographic method for detecting regional ventricular dysfunction in man. N Engl J Med 1971;284:1165-70.
3. Seals AA, Verani MS, Tadros S, et al. Comparison of left ventricular diastolic function as determined by nuclear cardiac probe, radionuclide angiography, and contrast cineangiography. J Nucl Med 1986;27:1908-15.
4. Bacharach SL, Green MV, Borer JS. Instrumentation and data processing in cardiovascular nuclear medicine: evaluation of ventricular function. Sem Nucl Med 1979;9:257-74.
5. Groch MW. Cardiac function: gated cardiac blood pool and first pass imaging. In: Henkin RE, Boles MA, Dillehay GL, et al, editors. Nuclear medicine. Volume 1. St Louis: Mosby; 1996. p. 626-43.
6. DePuey EG. Evaluation of cardiac function with radionuclides. In: Gottschalk A, Hoffer PB, Potchen EJ, editors. Diagnostic nuclear medicine. Baltimore: Williams and Wilkins; 1988. p. 355-98.
7. Garcia EV. Physics and instrumentation of radionuclide imaging. In: Marcus ML, Schelbert HR, Skorton DJ, Wolf GL, editors. Cardiac imaging: a companion to Braunwald's heart disease. Philadelphia: WB Saunders; 1991. p. 997-1005.
8. Garcia EV, Bateman TM, Berman DS, Maddahi J. Computer techniques for optimal radionuclide assessment of the heart. In: Gottshalk A, Hoffer PB, Potchen EJ, editors. Diagnostic nuclear medicine. Baltimore: Williams and Wilkins; 1988. p. 259-90.
9. Groch MW, Erwin WE, Turner DA, Domnanovich JR. A dual isotope motion correction device for exercise gated scintigraphy. J Nucl Med 1985;26:1478-84.
10. Bacharach SL, Green MV, Borer JS, Hyde JE, Farkas SP, Johnson GS. Left ventricular peak ejection rate, filling rate and ejection fraction: frame rate requirements at rest and exercise. J Nucl Med 1979;20:189-93.
11. Mancini GBJ, Slutsky RA, Norris SL, et al. Radionuclide analysis of peak filling rate, filling fraction, and time to peak filling rate: response to supine bicycle exercise in normal subjects and patients with coronary disease. Am J Cardiol 1983;51:43-51.
12. Groch MW, Erwin WD, Murphy PH, Lette J, Ali A, Qian J, et al. Validation of a knowledge-based boundary detection algorithm: a multicenter study. Eur J Nucl Med 1996;23:662-8.
13. Chang W, Henkin RE, Hale DJ, et al. Methods for detection of left ventricular edges. Semin Nucl Med 1980;10:39-53.
14. Jackson PC, Allen-Naker R, Rhys Davies E, Rees Russel J, Wilde R, Watt I. The assessment of an edge detection algorithm in determining left ventricular ejection fraction using radio-nuclide multiple gated acquisition and contrast ventriculography. Eur J Nucl Med 1982;7:62-5.
15. Cahill PT, Ornstein E, Ho SL. Edge detection algorithms in nuclear medicine. IEEE Trans Nucl Sci 1976;23:555-9.
16. Murphy PH. ECG gating: does it adequately monitor ventricular contraction? J Nucl Med 1980;21:399-401.
17. Bauch TD, Rubal BJ, Lecce MD, Smith TE, Groch MW. S2 triggered gated blood imaging for the assessment of diastole. Biomed Sci Instrum 1995;31:201-6.
18. Watson DD, Liedholdt EM, Carabello ME, et al. Gated blood pool imaging in patients with atrial fibrillation [abstract]. J Nucl Med 1981;22:P153.
19. Wagner RH, Halama JR, Henkin RE, et al. Errors in the determination of left ventricular functional parameters. J Nucl Med 1989;30:1870-74.
20. Bacharach SL, Green MV, Bonow RO, et al. Measurement of ventricular function by ECG gating during atrial fibrillation. J Nucl Med 1981;22:226-31.
21. Pavel DG, Byron E, Bianco JA, Zimmer AM. A method for increasing the accuracy of the radionuclide measurement of ejection fraction and left ventricular volume curve [abstract]. J Nucl Med 1977;18:641.
22. Miller TR, Goldman KJ, Epstein DM, et al. Improved interpretation of gated cardiac images by use of digital filters. Radiology 1984;152:795-800.
23. Maddox DE, Holman BL, Wynne J, et al. Ejection fraction image: a noninvasive index of regional left ventricular wall motion. Am J Cardiol 1978;41:1230-8.
24. Steckley RA, Kronenberg MW, Born ML, Rhea TC, Bateman JE, et al. Radionuclide ventriculography: evaluation of automated and visual methods for regional wall motion analysis. Radiology 1982;142:179-85.
25. Bonow RO, Bacharach SL, Green MV, et al. Impaired left ventricular diastolic filling in patients with coronary artery disease: assessment with radionuclide angiography. Circulation 1981;64:315-23.
26. Turner DA, Shima MA, Ruggie N, Von Behren PL, Jarosky MJ, Ali A, et al. Coronary artery disease: detection by phase analysis of rest/exercise radionuclide angiograms. Radiology 1983;148:539-45.
27. Turner DA, Von Behren PL, Ruggie NT, Hauser RG, Denes P, Ali A, et al. Non-invasive identification of initial site of abnormal ventricular activation by least-squares analysis of radionuclide cineangiograms. Circulation 1982;65:1511-8.
28. Rosenbush SW, Ruggie NT, Turner DA, Von Behren PL, Denes P, Fordham EW, et al. Sequence and timing of ventricular wall motion in bundle branch block. Circulation 1982;66:1113-9.
29. Wendt RE, Murphy PH, Treffert JD, Groch MW, Erwin WD, Schneider PM, et al. Application and interpretation of principal component analysis of gated cardiac images [abstract]. J Nucl Med 1993;34:175P.
30. Wendt RE, Murphy PA, Schneider PM, Treffert JD, Groch MW, Ford PV, et al. Lossy compression of dynamic studies using eigenimage methods [abstract]. J Nucl Med 1994;35:P178.
31. Cavailloles F, Baxin JP, Di Papla R. Factor analysis in gated cardiac studies. J Nucl Med 1984;25:1067-75.
32. Slutsky R, Karliner J, Ricci D, et al. Left ventricular volumes by gated equilibrium radionuclide angiography. Circulation 1979;60:556-65.
33. Bourgiugon MH, Schindeldecker JG, Carey GA, et al. Quantification of left ventricular volume in gated equilibrium radioventriculography. Eur J Nucl Med 1981;6:349-53.
34. Links JM, Becker LC, Shindledecker JG, Guzman P, Burow RD, Nickoloff EL, et al. Measurement of absolute left ventricular volume from gated blood pool studies. Circulation 1982;65:82-91.

SPECT

Note: At this writing, gated blood pool SPECT has only been recently applied to patient studies in more than an anecdotal fashion. Both the full merits and pitfalls of gated blood pool SPECT have yet to be determined.

Acquisition Protocols

Acquisition parameters

	SPECT		For info see paragraph
Radiopharmaceutical	Tc-99m–labeled RBCs	Preferred	1
Dose	25-30 mCi/70 kg	Preferred	1
Labeling method	In vitro or modified		
	in vivo (2-3 mg Sn-PYP)	Preferred (either)	2
	Ultra-tag kit	Optional	2
Camera	Dual-headed-90° configuration	Preferred	3
	Single head	Optional	3
Collimator	Parallel-high RES (dual head)	Preferred	4
	Parallel-LEAP (single head)	Preferred	4
Pixel size	~4-5 mm/pixel	Standard	5
Energy window	140 KeV ± 10%	Standard	6
Beat length window	± 25%-35%	Standard	7
Bad beat	Reject beat	Standard	7
	Reject beat and next beat	Preferred	7
Acquisition method	Frame mode	Standard	8
Frame rate	16 frames/cycle over full cycle	Standard	9
	16 frames/cycle over partial cycle	Optional	9
Number of views	64	Standard	10
	32	Optional	10
	32 (single head)	Standard	10
Time per view	30 s	Standard	10
	60 s	Optional	10
	60 s (single head)	Standard	10
Rotation	180°	Standard	11
	360°	Optional	11

Radiopharmaceutical

1. Inject the patient with Tc-99m–labeled red blood cells, with activity of approximately 25 to 30 mCi/70 kg-body weight (14 to 17 MBq/kg) to provide the radioisotope tag.
2. **Labeling methods:**
   a) In vitro or modified in vivo/in vitro methods (eg, using 2 to 3 mg stannous pyrophosphate 15 minutes before injection of the radiopharmaceutical).
   b) Ultra-tag kit

Camera/computer Set Up

3. **Camera.** Use of a dual-head gamma camera in the 90-degree configuration is preferred. With a dual-headed system, ERNA SPECT can be performed in half the time, about 15 minutes, of a 3-view planar ERNA series. Dual-headed cameras in the 180-degree configuration are optional, but not recommend. Single headed gamma camera with 180-degree rotation is optional, but not recommended. Acquisition time with a single-headed camera is approximately 30 minutes.
4. **Collimator.** Parallel hole high resolution collimator (resolution approximately 8 to 10 mm FWHM or better at 10 cm and sensitivity [Tc] of approximately 4000 to 5000 counts/s/mCi [108 to 135 counts/s/MBq]) is preferred when

using dual-headed gamma. An LEAP collimator (typically 12 mm FWHM at 10 cm and sensitivity of approximately 10,000 counts/s/mCi, or approximately 280 counts/s/MBq) is preferred when using a single-headed gamma camera.

5. **Pixel size.** A 64 by 64 matrix size of 16-bit word pixels is preferred with a zoom that results in a pixel size of about 4-5 mm/pixel. These acquisitions are usually performed using a zoom of 1.25 to 1.75 with large FOV cameras (1.75 for patients with small body habitus). The zoom required to meet the 4 to 5 mm/pixel criteria will depend on the FOV of the camera used. Large FOV cameras (circular–15 inch diameter) require a zoom of 1.25 to 1.35, whereas for FOV (rectangular–21 inch) cameras, a zoom of 1.5 to 1.75 is recommended. It is critical that the entire cardiac blood pool be in the FOV in all projections. Do not use a zoom so severe that a portion of the cardiac silhouette is cut-off in any projection. A test rotation and observation of the blood pool with a persistence scope is recommended.
6. **Energy window.** 140 KeV, ± 10% window.
7. **Bad beat/beat length window (arrhythmia rejection).** Preferred arrhythmia rejection mode is, on-the-fly, bad beat rejection. Typically, the standard arrhythmia rejection method terminates data acquisition if a premature beat is seen outside of the beat length window. Rejection of the short or long beat is typical, with rejection of subsequent beat preferred. The typical beat length window for SPECT is ± 25% to 35%, but will vary depending on heart rate and rhythm. This window is larger than planar ERNA, as significant arrhythmias may result in poor statistics, which will adversely effect the quality of the gated SPECT reconstruction. Beat length window may require lengthening. Poor statistics in SPECT ERNA studies result in streaking in the reconstruction image. Trigger: It is recommended that the ECG trigger point be checked to ensure that the ECG gating circuitry is gating on the peak of the ECG R wave. Checks can be performed either visually, with a dual trace oscilloscope, or checked with a commercially available dynamic phantom. Bad or delayed triggers can adversely affect volume curve, and severely lengthen acquisition time or results in poor statistics.
8. **Acquisition method.** Frame mode (forward framing) is standard.
9. **Frame rate.** 16 frames per cardiac cycle are preferred. LVEF values decrease if 8 gated frames per cycle are acquired. Statistics in SPECT acquisition typically preclude the use of higher frame rates. An alternative to higher frame rates per cycle, is to acquire 16 frames, over 1/2 or 2/3 of the cardiac cycle, if systolic ejection parameters and EF only are required. With this optional acquisition mode, diastolic function analysis may be compromised.
10. **Number of projections (views) and time per view.** 64 projections (32 per head) over a 180-degree rotation (RAO to LPO) at approximately 30 seconds per view is preferred when using a dual-headed gamma camera (total acquisition time about 16 minutes). Optionally, 32 views may be used (16 per head) at 60 seconds per view for enhanced statistics or in severely arrhythmic patients (total acquisition time about 16 minutes). When using a single-head gamma camera, 32 projections at 60 seconds per view is recommended (total acquisition time about 32 minutes).
11. **Rotation.** 180-degree rotation is preferred. 360-degree rotation is optional, but not recommended unless a triple-headed gamma camera is used.

Processing Protocols: SPECT

1. **SPECT reconstruction/filter.** Filtered backprojection is the suggested reconstruction method. Differing SPECT reconstruction filters are preferred by differing clinical sites. The suggested filter for each of the 16 gated frames is a Butterworth filter with 0.55 Nyquist frequency cut-off, and order = 7. If the study is noisy (due to significant arrhythmias, poor tag, or other technical reasons), a Butterworth filter with 0.45 Nyquist frequency cut-off, and order = 7 may improve the quality of the reconstruction. As algorithms become available, iterative reconstruction methods may be employed.
2. **Oblique reorientation.** Preferably, each of the 16 gated frames transverse reconstructions are re-oriented in short axis oblique slices, and optionally, long axis coronal and long axis sagittal slices. Typical 3-dimensional reconstructions of the SPECT ERNA data are accomplished using the short axis oblique data only. Long axis views may be useful when observing regional wall motion by cine loop display of the oblique slice data. See paragraph 7.
3. **LV volume curve generation.** Most parameters describing ventricular function are extracted from a complete LV volume curve in like manner to planar ERNA studies. This curve can be obtained from either a single ROI drawn at ED (and modified at ES, if necessary,) or using multiple ROIs drawn at each time point over the summed short axis slices which include the entire left ventricle, but exclude the LA. Automatic techniques exist for defining 2-dimensional (2D) or 3-dimensional (3D) regions encompassing the entire left ventricle. Although automatic methods often require less effort than manually drawn ROI methods, it is important that the automatic results be checked visually and modified as necessary. Irregularities in the LV contour occasionally occur using automatic algorithms. These irregularities can have significant effects on parameters extracted from the LV curve.

Processing parameters

Parameter	Method		For info see paragraph
SPECT reconstruction:	Filtered backprojection	Standard	1
Reconstruction filter	Butterworth 0.55 Nyquist cut-off		
	Order = 7	Standard	1
	Butterworth 0.45 Nyquist cut-off	Optional	1
Oblique reorientation	Short axis oblique	Standard	2
	Long axis coronal	Optional	2
	Long axis sagittal	Optional	2
LV volume curve generation	Automatic ROIs—at ED or at each time point	Preferred	3
	Manual ROI at ED	Standard	3
Background	None	Standard	4
LVEF	Counts-based 2D/3D method	Preferred	5
	Geometrically based method	Optional	5
	Automated method	Optional	5
	From singled end diastolic ROI	Optional	5
RVEF	Not validated at this point		6
See LVEF			
Wall motion	3D visual assessment of movie loop	Preferred	7a
	Slice-based visual assessment of movie loop	Optional	7b
	Regional EF	Optional	7c
LV emptying	Peak/average rate of emptying	Optional	8
LV filling	Peak/average rate of filling	Optional	9
LV volumes	Counts based	Standard	10
	Pixel based	Optional	10

4. **Background.** Background subtraction is not required in SPECT imaging. The process of acquisition and reconstruction in SPECT imaging obviates the need for background correction.
5. **LVEF.** Unlike planar ERNA, there are not many commercially available methods for computation of EF, but some do exist. EF can be computed by applying an end diastolic ROI to the end diastolic images (and end systolic ROI to end systolic images) of slices summed to include the entire left ventricle (and excluding other cardiac chambers), or use of an automatic program which includes the left ventricle by using 2D short axis slices or considers the left ventricle as a 3D data set. LV volume curves can be generated, and LVEF can be computed in like fashion to planar ERNA, with a counts-based method preferred. Optionally a geometric based method may be used to compute LVEF from end diastolic and end systolic volumes. LVEF obtained from SPECT ERNA is likely to be higher than LVEF values determined from planar ERNA method due to the complete removal of all activity from the left atrium. Preliminary results indicate that SPECT ERNA LVEF is approximately 7% to 10% higher, in EF units, than planar studies. Fitting the LV curve with two or three harmonics and extracting the first and the minimum points as the end diastolic and end systolic count values is one optionally used method. If the original TAC is produced from a single end diastolic ROI, the EFs will be consistently lower than if the TAC is produced from multiple ROIs. In this case, SPECT ERNA LVEF magnitudes may be comparable or slightly less than multi-region planar ERNA. *Care must be used when applying SPECT ERNA LVEF values to the evaluation of chemotherapy patients where standards have been established using planar methods.* An understanding of the LVEF normal values between SPECT and planar studies is required.
6. **RVEF.** Unlike planar ERNA studies, accurate computation of RVEF may be possible with SPECT ERNA due to the removal of chamber overlap and the 3D nature of SPECT. Methods to date have not been validated. The same techniques described in (5) above can be used to measure RVEF. All of the same considerations mentioned above also hold, but since the RV chamber is more tortuous than the left ventricle, final results may vary.

7. **Wall motion.** Regional wall motion in SPECT ERNA may be determined from 3D display of the cardiac chambers in cine-loop fashion (preferred). The 3D display maybe surface shaded (preferred) or optionally volume rendered, and preferably, displayed in multiple cardinal views or rotated at user command. Optionally, the short and/or long axis reconstructed slices separately, or summed, may be view in cine loop fashion. The latter method is available on most commercial computer systems as part of a gated SPECT package. Wall motion by SPECT ERNA may be the most useful application of this technique, and can be performed on most commercial systems. Optionally, regional EF can be computed from 2D and 3D segments over the left ventricle. Segmental SPECT EF has been shown to be helpful in identifying wall motion defects in patients with CAD.
8. **LV emptying.** LV emptying, average and maximum, may be computed in similar fashion to planar ERNA methods, as can the systolic ejection period.
9. **LV filling.** LV filling, average and maximum, may be computed in similar fashion to planar ERNA methods, as can the diastolic filling period(s).
10. **LV volumes.** LV volumes can, potentially, be accurately computed using SPECT ERNA techniques. A count based or geometrically based (pixel/voxel) method for computation of LV volumes is unhampered by chamber overlap. Moreover, the spatial distribution of the left ventricle is more clearly delineated. The simplest approach for LV volume determination is to sum pixels contained within the left ventricle, but excluding all other structures. By simple calibration of pixel (voxel) size, LV volume in ED and ES can be computed. As a caution, LV volumes have not been validated extensively, but recent studies have compared LV volumes to those derived from cardiac MRI.

Bibliography

1. Moore ML, Murphy PH, Burdine JA. ECG gated emission computed tomographs of the cardiac blood pools. Radiology 1980;134:233-5.
2. Corbett JR, Jansen DE, Lewis SE, et al. Tomographic gated blood pool radionuclide ventriculography analysis of wall motion and left ventricular volumes in patients with coronary artery disease. J Am Coll Cardiol 1985;6:349-58.
3. Gill JB, Moore RH, Tamaki N, et al. Multigated blood-pool tomography: new method for the assessment of left ventricular function. J Nucl Med 1986;27:1916-24.
4. Fischman AJ, Moore RH, Gill JB, Strauss HW. Gated blood pool tomography: a technology whose time has come. Semin Nucl Med 1989;19:13-21.
5. Bartlett ML, Srinivassan G, Baker WC, Kitsiou AN, Dilsizian V, Bacharach SL. Left ventricular ejection fraction. Comparison of results from planar and SPECT gated blood pool studies. J Nucl Med 1996;37:1795-99.
6. Groch MW, Leidholdt EM, Marshall RA, et al. Gated blood pool SPECT imaging: sources of artifacts [abstract]. Clin Nucl Med 1991;16:717.
7. Faber TL, Stokely EM, Templeton GH, et al. Quantification of three-dimensional left ventricular segmental wall motion and volumes from gated tomographic radionuclide ventriculograms. J Nucl Med 1989;30:638-49.
8. Groch MW, Marshall RC, Erwin WD, Schippers DJ, Barnett CA, Leidholdt EM. Quantitative gated blood pool SPECT for the assessment of coronary artery disease at rest. J Nucl Cardiol 1998;5:567-73.
9. Chin BB, Bloomgarden DC, Xia W, et al. Right and left ventricular volume and ejection fraction by tomographic gated blood-pool scintigraphy. J Nucl Med 1997;38:942-8.
10. Groch MW, Erwin WD, Bieszk JA. Single photon computed tomography. In: Treves S, editor. Pediatric nuclear medicine. New York: Springer-Verlag; 1994. p. 33-87.
11. Groch MW. Cardiac function: gated cardiac blood pool and first pass imaging. In: Henkin RE, Boles MA, Dillehay GL, et al, editors. Nuclear medicine. Volume 1. St Louis: Mosby; 1996. p. 626-43.
12. Groch MW, Schippers DJ, Marshall RC, Barnett C. A quantitative program for gated blood pool SPECT imaging [abstract] . Clin Nucl Med 1991;16:713.
13. Schippers DJ, Groch MW, Marshall RC, Leidholdt EM, Ali A. Three dimensional analysis of gated blood pool SPECT [abstract]. J Nucl Med 1995;36:12P.
14. Groch MW, Marshall RC, Erwin WD, Schippers DJ. Quantitative gated blood pool SPECT imaging: enhanced sensitivity for non-invasive assessment of coronary artery disease [abstract]. J Nucl Med 1993;34:35P.
15. Smith WH, Kastner RJ, Calnon DA, et al. Quantitative gated single photon emission computed tomography imaging: a count-based method for display and measurement of regional and global systolic ventricular function. J Nucl Cardiol 1997;4:451-63.
16. Calnon DA, Kastner RJ, Smith WH, et al. Validation of a new counts-based gated single photon emission computed tomography method for quantifying left ventricular systolic function: comparison with equilibrium radionuclide angiography. J Nucl Cardiol 1997;4:464-71.

MYOCARDIAL PERFUSION PLANAR IMAGING PROTOCOLS

Although SPECT is preferable for myocardial perfusion scintigraphy, in certain circumstances, planar imaging may be useful or may be the only modality available.

Purpose. To evaluate regional myocardial perfusion and function. Planar imaging is an acceptable method for myocardial perfusion imaging. The anatomy of the heart is sufficiently simple that the imaging specialist can comprehend the location and extent of defects from multiple projections without need of computer reconstruction. Although SPECT imaging is presently considered state-of-the-art for myocardial perfusion imaging, planar imaging still has a role in the daily routine of a laboratory. Imaging at the bedside of acutely ill patients, or instrumented patients, can only be performed using planar imaging technique and portable gamma cameras. Planar views can be quickly repeated if the patient moves during acquisition. Planar imaging may be the only way to acquire images in very obese patients, who are too heavy for the imaging table of a SPECT camera.

ECG gated planar images can be obtained using standard software for ERNA studies. Finally, planar imaging is the basis for good SPECT imaging. The ability to obtain high-quality planar images is an essential skill, even for those who routinely use SPECT imaging.

Procedure

Exercise. Adequate exercise is most important if the aim of the study is to detect CAD. In patients with mild and moderate CAD, myocardial blood flow may become abnormal only at high heart rates or at high double products. At lower heart rates, myocardial blood flow may be normal and perfusion images will be correspondingly normal. In patients with known CAD who are being evaluated for extent and severity of inducible myocardial ischemia, submaximal exercise can provide clinically relevant information.

Positioning. The most important part of positioning is the ability to reproduce the same position on initial and delayed (or rest) images. Even slight differences in angulation of the camera, positioning of breasts, or the pressure of the camera on the chest wall can produce artifacts and inaccuracies in comparing rest and stress images.

The standard imaging positions are supine ANT, supine 45° LAO, and a right side decubitus 90° left lateral (LL). The 90° LL decubitus view provides optimal visualization of the inferior wall and reduces subdiaphragmatic and breast attenuation artifacts. Admittedly the right side decubitus position is less stable than the supine position, making it somewhat more difficult to obtain identical repositioning. An alternate left lateral view is the shallow 70° LAO position. The latter position is suboptimal at times due to frequent occurrence of artifacts: subdiaphragmatic attenuation of the inferior wall and breast attenuation of the anterior wall.

The LAO view should be chosen in such a way that the right ventricle and left ventricle are well separated by a vertically visualized septum (ie, "best septal" view). One should be aware that in individual patients the heart may not always be in the same position. Hearts may be rotated clockwise or counterclockwise so that a "straight" 45° LAO will not always display the desired image. It is preferred to search for the "best septal" view instead of a straight 45° LAO. The angulation of the detector head for acquisition of anterior, and left lateral views should then be correspondingly modified. The advantage of this option is that it provides greater standardization of the imaged left ventricle, which will simplify quantitative analysis. The disadvantage of this option is the increased complexity and carries the potential for nonreproducible positioning.

Female patients should be imaged consistently with bra off and without camera pressure, which might produce variable tissue displacement.

Positioning

View	Patient position	Detector position	Alternative
Shallow LAO	Supine	45°	"best septal"
Anterior	Supine	0°	"best septal" minus 45°
Steep LAO	Supine	70°	"best septal" plus 25°
Left lateral	Right decubitus	0°	N/A

Positions of cameras and patient must be exactly reproduced for rest and stress imaging.

Image Acquisition

Gamma camera positions are as shown in the previous table. Using either Tl-201 or Tc-99m–labeled agents one may optionally use ECG-synchronized gating and acquire in 16-frame, multiple-gated acquisition (ERNA) mode. No beat rejection should be used. In patients with atrial fibrillation ECG-gating should not be performed. ECG-gated acquisition allows for cine review of wall thickening and motion. The multiple frames of the ECG-gated myocardial perfusion images can be summed to produce a single static planar image for conventional visual and quantitative analysis.

Static planar images should be acquired for a total of 1 million counts per view. The total imaging time for static planar Tl-201 imaging should be 8-10 minutes, whereas the total imaging time for static planar Tc-99m–labeled agents time can be reduced to 5 minutes. When ECG-gating is used, imaging time per view using Tc-99m agents should be extended to 8 to 10 minutes. For ECG-gated image acquisition with Tl-201 image acquisition time per view should be at least 10 minutes. Planar images acquired with a 10-inch diameter gamma camera should have at least 600,000 counts (1 million counts preferred) in the FOV. Alternatively, optimal count density can be defined as at least 100 counts in the pixel with maximal counts in the left ventricle.

In female patients an optional l-minute image of a line source marker that delineates the contour of the breast can be acquired to aid in identifying breast attenuation artifacts.

Cardiac shields or other masking devices should not be used. The extracardiac background cannot be determined correctly unless both the cardiac and extracardiac activity have been recorded in the raw data.

Acquisition

	Tc-99m	Tl-201
Collimator	High resolution	Low energy, medium resolution
FOV	Full 10-inch field of small camera or 1.2-1.5 zoom with LFOV camera	Same
Matrix	128 × 128	128 × 128
Window	140 keV 20% centered	78 keV, 30% centered
Gating	Optional 16 frames/cardiac cycle	Same
Imaging time (per view)	5 min (10 min ECG-gated)	8-10 min (10 min ECG-gated)
Imaging counts	At least 1 million	At least 1 million

Thallium Stress-delayed Imaging Protocol. Inject 2.5 to 3.0 mCi at peak exercise. Attempt to continue exercise for at least 1 to 2 minutes after injection. Begin imaging at 5 to 10 minutes after injection. Delayed imaging can be performed from 2 to 5 hours after injection. Preferred delayed imaging time is 3 hours.

Thallium Rest-redistribution Imaging Protocol. Inject 3.0 mCi at rest and start imaging within 15 minutes. Wait at least 3 hours to perform delayed rest-redistribution images. With rest injections, additional delayed imaging at 24 hours after injection may be helpful to establish more completely redistribution in myocardial regions, which appear to have significant tracer uptake but no redistribution by 4 hours.

Thallium Reinjection. Protocols for rest reinjection vary with regard to the timing of thallium reinjection and the timing of the reinjection-to-imaging interval. After stress injections, further injection of 1.5 mCi at rest may enhance the amount of uptake in an initially severe defect, which shows no redistribution on delayed imaging.

Repeat imaging at 24 hours after rest reinjection may further enhance the detection of redistribution in severe defects.

Imaging protocols for Tl-201

Protocol	Inject	Initial image	Delayed image	Optional reinject	Late image
Standard stress-delay	2.5-3.0 mCi at peak stress	Within 5-10 min	2-4 h preferred 3 h	1.5 mCi	1-4 h after reinject
Injection at rest	2.5-3.0 mCi at rest	Within 10-15 min	At least 3 h	Do not reinject	24 h

Tc-99m Two-day Stress-rest Imaging Protocol. Inject 15 to 30 mCi at peak exercise. Imaging starts 15 to 30 minutes after injection during exercise. On day 2 the same dose is given at rest. Imaging begins at 45 to 60 minutes after the injection at rest.

Tc-99m One-day Rest-stress Imaging Protocol. A same-day imaging protocol using a low-dose rest study followed by a high-dose stress study allows Tc-99m sestamibi or Tc-99m tetrofosmin imaging to be completed within a few hours on the same day. The higher dose given for the stress study preferably 3× higher than the lower resting dose, yielding an adequate stress image without the need for subtracting the residual activity from the low-dose rest image. Suggested doses are 8 to 10 mCi for the resting and 24 to 30 mCi for the exercise study. The rest-stress sequence allows the higher dose to be given during exercise. This gives optimum imaging of stress-induced defects and may improve detection of defect reversibility compared with the alternative stress-rest sequence. A same day stress/rest protocol has also been used successfully with an initial stress injection of 10 to 15 mCi and a rest injection of 30 to 45 mCi given with an interval of 2 to 4 hours.

Imaging protocols for Tc-99m sestamibi and tetrofosmin

Protocol	Inject	Initial image	Next image	Inject	Image
2-day stress test	20-30 mCi at peak stress	15-30 min after injection	Next day	20-30 mCi at rest	45-60 min after injection
1-day stress test	0-9 mCi at rest	45-60 min after injection	2-4 h interval	24-27 mCi at peak stress	15-30 min after injection
1-day stress test	10-15 mCi at peak stress	15-30 min after injection	2-4 h interval	30-45 mCi at rest	45-60 min after injection

Quantitative Processing of Planar Images

Quantitative processing includes using the computer to produce standardized raw images for visual evaluation. The gray scale should be fully utilized to display the heart normalized to maximal LV count density, and not scaled to visceral activity. Background subtraction is performed. The background subtracted images are useful for visual evaluation and are used for measurements of myocardial activity. These measurements provide quantitative determination of a suspected defect so that consistent standards can be set for defect detection. The measurements are especially useful in comparing defects in stress and rest images and to detect subtle defect reversibility. Registration of the stress and rest images also can be performed to ensure that the same myocardial region is being sampled. A normal database also may be incorporated in the quantitative program so that segmental tracer activity can be compared with the average obtained from the normal database.

There is no single "generic" description for what all good computer programs should offer. There are common features among several successful programs. In the following we review these features and comment on acceptable variations.

Regions of Interest. The first step in quantification is to locate the heart by placing reference regions of interest around the heart. Regions can be rectangular or elliptical. Elliptical regions fit the heart better. Rectangular regions are best used by having the operator set the boundaries by touching the apparent "edge" of the heart and then move the region outwards approximately 4 pixels. This operation is highly reproducible. The reference boundaries are used to separate the region containing myocardial activity from background activity.

Background Subtraction. Background subtraction is the removal of the background, or more precisely the "tissue crosstalk," from the raw image. For each image, a background image is generated from the smoothed image using the above mentioned reference background region. The background is then subtracted from the unsmoothed raw image, leaving behind the myocardial activity.

Background subtraction is essential to planar imaging both for valid quantitation and to restore defect contrast adequate for visual assessment. Background correction is in fact more critical for planar imaging with Tc-99m–labeled agents than for imaging with Tl-201. The relative tissue distribution of Tc-99m–labeled agents at rest and after exercise may be markedly different compared to that of Tl-201.

A modified version of the conventional interpolative background algorithm has worked well for both Tl-201 and Tc-99m sestamibi planar images. The modification allows the background defining regions to cross regions of intense extracardiac activity without causing significant background error in the background-subtracted cardiac image.

Rescaling the Image Gray Scale. When Tl-201 is used as the imaging agent, the heart is usually the organ with the most intense activity. When using myocardial tracers labeled with Tc-99m, activity in the abdominal viscera often exceeds that of the heart. This normally causes the computer to scale image intensities to the extra-cardiac activity, which will cause erratic and suboptimal visualization of the heart. Any computer program for quantitative image processing should have a convenient mechanism to suppress activity outside the heart if it becomes greater than the activity in the heart. When comparing initial and delayed images or images obtained after reinjection, each image should be individually scaled to the area of most intense cardiac activity. If the images were scaled to different maxima, the appearance of defect reversibility would be distorted.

Image Registration. Comparison of rest and exercise images to detect redistribution or reversibility can be accurate only if the same myocardial segments are being compared. Image registration so that stress and rest images are precisely aligned facilitates accurate comparisons. There are several ways of doing this. Maximizing the cross-correlation coefficient between the two images is a robust method that can be performed by the computer without operator intervention.

Profile Generation. After subtraction of the reference (background) plane to compensate for tissue crosstalk and registration of the images to allow precise comparisons, quantification becomes the relatively simple matter of finding a convenient way of indicating image count density. Again, there are several ways of doing this. One basic way is to display count profiles across the heart. Four profiles will sample the myocardial count distribution adequately within the limitations of image resolution (each profile represents an average of about a 1 cm wide slice across the heart) and produce an intelligible display. A more commonly used alternative for graphic display of myocardial activity is the circumferential count distribution profile. The circumferential profile method provides a more compact and dense single-curve display of counts sampled around the myocardial "rim" and allows the simple plot of a second profile indicating normal limits. Either method, transverse count profiles or circumferential count profiles, will provide an adequate and ultimately equivalent quantitative representation of myocardial activity. Either method facilitates standardization and reproducibility of image interpretation.

A more fundamental choice is what parameter to use to quantify myocardial activity. Many programs, including most methods used to generate bulls' eye maps for SPECT imaging, perform a search across the myocardium for the maximum pixel count in a transmural myocardial sample. The other choice is to take an average of counts in the transmural sample. The advantage of the latter method is that it reduces statistical noise because it is an average, and it is intuitively more representative in regions of subendocardial scar or ischemia. The disadvantage is that the transmural average is quite sensitive to the accurate definition of endocardium and epicardium. Variability in locating the epicardial and endocardial limits probably nullifies the gain in precision from the averaging of more pixels. The use of maximum counts provides a quantitative parameter that is less sensitive to edge location. This parameter has been used extensively and has been reasonably robust in practice. Either method is usable. Normal standards and normal limits will be quite different for those using the transmural average. They are not comparable with values based on transmural maximum.

Normal Database. Data from "normal" subjects may be incorporated into the computer program and indicated in the output as normal limits. Because of variations in equipment and positioning, the normal database should not be used until it has been validated in-house using standardized imaging protocols.

Along with the average values obtained from the normal database, the standard deviations also need to be obtained. Different myocardial segments will have different degrees of normal variability, which should be accounted for in deciding if a segment is outside normal limits. Individual segments may be flagged using limits of 2.0 to 2.5 standard deviations. The computer may also flag reversible segments, but this is a more complex operation. The database must have standard deviations comparing stress and rest segments. If a segment has a significant stress defect, reversibility may be indicated if that defect changes toward normal by more than 1 standard deviation. Additional "expert logic" may also be incorporated to scan for secondary segments with nonsignificantly reduced initial uptake and significant reversibility.

Flashback Display. If the computer program performs image registration, then flashback display can be added. This display flashes between the stress and rest images. Since the images are in registration, there will be little change except in regions of reversibility. This is a powerful tool to visually highlight areas of redistribution or reversibility.

Limitations. Well-trained readers consistently outperform readings even from relatively sophisticated computer programs. The programs are valuable in standardizing the images and image processing and in maintaining consistent interpretive standards. However, the judgment of a well-trained reader should override the computer logic. Computer programs that dogmatically indicate normal and abnormal scans or scan segments can be intimidating and misleading. Readers must be prepared to disagree and overrule the computer. Otherwise, the readers will be no better than the computer.

Bibliography

1. Garcia E, Maddahi J, Berman D, et al. Space/time quantitation of thallium-201 myocardial scintigraphy. J Nucl Med 1981;22:309-17.
2. Watson DD, Campbell NP, Beller GA, et al. Spatial and temporal quantification of plane thallium myocardial images. J Nucl Med 1981;22:577-84.
3. Koster K, Wackers F, Mattera JA, Fetterman RC. Quantitative analysis of planar technetium-99m isonitrile myocardial perfusion images using modified background subtraction. J Nucl Med 1990;31:1400-8.
4. Watson DD, Smith WH. Sestamibi and the issue of tissue crosstalk [editorial]. J Nucl Med 1990;31:1409-11.
5. Smith WH, Watson DD. Technical aspects of myocardial planar imaging with Tc-99m sestamibi. Am J Cardiol 1990;66:16E-22E.
6. Watson DD, Smith WH, Beller GA. Planar imaging with Tc-99m sestamibi. In: DePuey EG, editor. Myocardial imaging with Cardiolite workbook. 2nd ed. Wilmington (DE): DuPont Pharma; 1994.
7. Sinusas AJ, Beller GA, Smith WH, Vinson EL, Brookeman V, Watson DD. Quantitative planar imaging with technetium-99m methoxyisobutyl isonitrile: comparison of uptake patterns with thallium-201. J Nucl Med 1989;30:1456-63.
8. Maddahi J, Rodrigues E, Kiat H, Van Train K, Berman DS. Detection and evaluation of coronary artery disease by thallium 201 myocardial perfusion scintigraphy. In: DePuey EG, Berman DS, Garcia EV, editors. Cardiac SPECT imaging. New York: Raven Press; 1994. p. 103-20.
9. Gutman J, Berman DS, Freeman M, et al. Time to completed redistribution of thallium-201 in exercise myocardial scintigraphy: relationship to the degree of coronary artery stenosis. Am Heart J 1983;106:989-95.

MYOCARDIAL PERFUSION AND FUNCTION SPECT PROTOCOLS

Purpose. To evaluate regional myocardial perfusion and function.

Acquisition Protocols

Protocols for the various nuclear cardiology SPECT acquisition studies are presented in the following pages. For each of the protocols the acquisition parameters are listed along with their corresponding value for exercise and rest. Implementation of these protocol acquisition parameters will provide acceptable images of good quality for routine clinical interpretation and quantitation. However, protocol parameters other than those listed may be preferred at other institutions and ongoing research into corrections for attenuation, scatter and camera response depth-dependence may result in new optimal parameters in the future. Therefore these protocols should be viewed as the current suggested list of acquisition parameters. A description for each of the acquisition parameters is listed below.

1. **Dose.** The doses for each of the protocols represent standard doses commonly used clinically. The standard doses described are given for an average 70 kg patient. Doses are adjusted for heavier patients by 0.04 mCi/kg for Tl-201 and by 0.31 mCi/kg for Tc-99m. Similar Tl-201 doses are used for ungated and gated studies. Increased imaging times or use of multidetector systems may be needed for some patients to acquire adequate gated Tl-201 counts. Gated Tl-201 imaging times can be adjusted based on the counts acquired for a preliminary 4-minute planar study in order to ensure acquiring at least 0.5 million background-subtracted myocardial counts.
2. **Position.** Supine position routinely is used for SPECT imaging in all protocols. Prone imaging is associated with less patient motion and less inferior wall attenuation than supine imaging. The combination of supine and prone images is also helpful in identifying breast attenuation and attenuation due to excessive lateral chest-wall fat, due to the shift in position of the attenuating structures that occur in the prone position. In some laboratories the advantages of prone imaging in clarifying artifactual defects has lead to a routine use of the combination of supine followed by prone acquisitions. When being used in this fashion, gating is generally not performed (unless the supine gated images were deemed uninterpretable for patient motion), and the acquisition time for the secondary (prone) image set is reduced by 20% to 40%. Using a dual-detector camera with a 25 to 30 mCi Tc-99m dose, supine acquisitions are performed for 25 seconds per stop and prone acquisitions 15 seconds per stop, with 32 stops per detector being obtained per acquisition. With Tl-201, imaging must be performed very close to the stress testing, and if soft tissue attenuation or patient motion compromises a study, the benefit of repeating the acquisition is questionable. In contrast, Tc-99m sestamibi or tetrofosmin permit stress testing and tracer injection to take place at a location remote from the imaging laboratory and image acquisition can simply be repeated when patient motion, soft tissue attenuation or other artifact is considered to be responsible for the production of a perfusion defect. However, since the prone position frequently causes an artifactual anteroseptal defect secondary to increased sternal attenuation in this position, prone imaging is used as an adjunct to, not a replacement for, supine imaging.
3. **Delay time.** These times are listed as ranges; specific values are optional. The main precautions to be observed are to delay imaging following exercise stress testing sufficiently to preclude "upward creep" phenomena, and to delay resting Tc-99m sestamibi and Tc-99m tetrofosmin sufficiently to minimize overlap of hepatobiliary with myocardial activity. Provided that imaging times fall within the specified ranges, clinically useful SPECT images should result.
4. **Energy windows.** Energy window size and position are optional. The values shown are the most prevalently used, and have been found to be acceptable for most cameras. On systems offering improved energy resolution, the window size could be reduced, resulting in decreased scatter and improved image resolution, so long as imaging times are extended to acquire the same clinically useful number of counts. The same energy windows used in performing patient studies should be used for routine daily QC.
5. **Collimator.** Parallel hole collimators primarily are employed for cardiac SPECT acquisitions. They fall into two categories: LEAP, used mostly for Tl-201 studies, and low-energy high-resolution (LEHR), used for Tc-99m studies. Compared with LEAP collimators, LEHR collimators have longer bores, thinner septa, and smaller holes, which provide better resolution at the expense of reduced sensitivity. Therefore, to use LEHR collimators, imaging agents providing high count rates are required (ie, Tc-99m agents). Generally, LEAP collimators are used for 3 mCi Tl-201 studies, including gated SPECT acquisitions. Converging collimators now are available on multiple systems, but remain investigative and are not yet employed clinically routinely.
6. **Orbit.** For single detector systems, 180˚ orbits continue to be preferred over 360˚ orbits, (45˚ RAO to 45˚ LPO)

because of resultant higher contrast resolution. Avoiding posterior projections lessens noise contamination due to significant attenuation and decreased image resolution due to the further distance of the heart to the detector. This is particularly true for acquiring the relatively low-energy 70 keV Tl-201 photons. For multiple detectors, only 45° RAO to 45° LPO data are used commonly. It is possible that in the future either 180° or 360° orbits will yield the same image quality once scatter, attenuation, and variable resolution effects are corrected.

7. **Orbit type.** The main orbit options in SPECT myocardial perfusion imaging are circular versus noncircular (elliptical or body-contoured) orbits. Noncircular orbits follow the contour of the patient, bringing the camera closer to the patient, optimizing spatial resolution. Circular orbits maintain a fixed radius of rotation, and on average result in the detector being farther from the patient. In general, there is reduced spatial resolution with circular orbits since the detector-to-source distance is greater with this technique. Imaging artifacts have been observed when noncircular orbits are used, due to increased variation of source-to-detector distance, thereby involving increased variation of spatial resolution. Circular acquisitions continue to be the most frequently used option, but some manufacturers do provide convenient noncircular orbit capability.
8. **Pixel size.** The SPECT protocols listed here specify a 6.4 ± 0.2 mm pixel size for a 64 × 64 image matrix. This size offers adequate image resolution for interpretation and quantitation of both Tl-201 and Tc-99m tomograms.
9. **Acquisition type.** The most widespread mode of tomographic acquisition is the "step-and-shoot" method. In this approach, the detector stops at pre-selected angles, typically 32 to 64 projection/180° orbits or 64 to 128 projections/360° orbits. The detector acquires gamma rays while stationary for a pre-determined time, after which the detector moves to the next angular position. No events are recorded as the detector moves. This process is repeated until the total number of pre-selected projections is acquired. A second acquisition mode is "continuous" acquisition, for which the camera moves continuously while collecting data. Although there is some minimal spatial resolution loss associated with "continuous" acquisition, more total counts are collected during the same total time. A third mode of acquisition is "continuous step-and-shoot," involving continued acquisition during detector movement from one angle to the next in the "step-and-shoot" mode. This results in increased counting statistics as compared to the standard "step-and-shoot" acquisition mode while reducing most of the (minimal) blurring associated with continuous acquisition. Both "continuous step-and-shoot" and "continuous" modes are preferred to "step-and-shoot" because of improved counting statistics and reduced imaging time.
10. **Number of projections.** The optimal number of projections for emission studies depends on matching the number of projections to the resolution of the system. A thallium SPECT acquisition with a LEAP collimator is a relatively low-resolution study, for which 32 projections over 180° are sufficient. A higher resolution study using Tc-99m agents should be collected with a high-resolution collimator; this requires at least 64 projections over 180° to prevent loss of resolution. Larger numbers of projections are not warranted at this time, but could become necessary if technical innovations result in improved overall system resolution.
11. **Matrix.** The standard matrix size for emission SPECT is 64 × 64 pixels. While a 128 × 128 matrix may offer slight improvement in contrast, the increase in disk storage space and processing time for the larger matrix make it a difficult implementation to justify presently.
12. **Time/projection.** The emission acquisition times listed have been found to produce images of acceptable and comparable quality for rest and stress studies.
13. **Total time.** For single detector systems, the total time for an emission acquisition ultimately is based on how long a patient can tolerate the procedure without moving, balanced by the need to acquire sufficient counts. The maximum practical time is on the order of 30 minutes. For biplane systems, this time can be halved, and many laboratories obtain gated perfusion SPECT studies in only 12 to 15 minutes using biplane cameras. Some studies have shown it is advisable to use myocardial counts acquired in a preliminary 1 minute planar Tl-201 image to adjust the subsequent time per projection of tomographic data acquisition, in order to guarantee uniformity of count density from one patient to another.
14. **Gated SPECT.** Gating greatly improves study specificity by revealing areas of reduced perfusion to be diminished artifactually due to anterior wall breast attenuation or inferior wall diaphragmatic attenuation. Assessment of regional wall motion and/or thickening can be valuable tools for detecting viability within a stress-induced perfusion defect. LVEFs and volumes, and regional wall motion and thickening, now are computed routinely from gated SPECT data. The majority of stress myocardial perfusion radionuclide studies currently are acquired as gated SPECT data. However, there is mounting evidence that the information content of the post-stress acquisition may be different from that of the resting data. Providing that there is adequate count density, particularly with regard to the lower dose acquisitions, both stress and rest SPECT perfusion studies should be acquired as gated data sets. Optimizing protocols for which both stress and rest data are acquired gated remains an area of investigation.

15. **Multidetector systems.** It is recommended for multidetector systems that total imaging time be adjusted to obtain greater than the minimum counts listed in Section I (subsection Clinical QC for Each Patient Protocol), but less than a maximum total imaging time of 30 minutes.

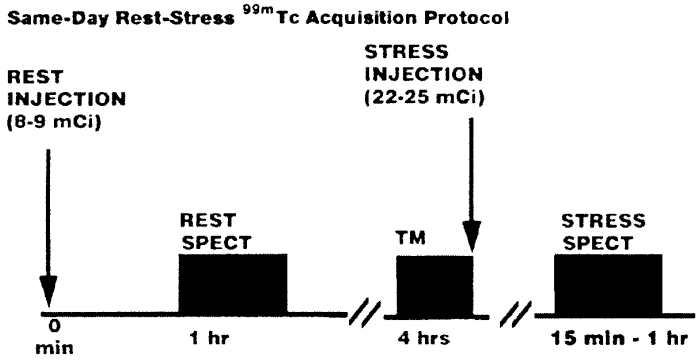

Note: Times displayed are optional (see below); TM, treadmill.

Patient protocol

	Rest study	Exercise study		For info see paragraph
Dose	8-9 mCi	22-25 mCi	Standard	1
Position	Supine	Supine	Standard	2
	Prone	Prone	Optional	2
Delay time (intervals)				
Injection → imaging	1-2 h	15 min-1 h	Optional	3
Rest → stress		1-4 h	Optional	3
Acquisition protocol				
Energy window	20% symmetric	Same	Optional	4
Collimator	Low-energy, high-resolution	Same	Preferred	5
Orbit	180° (45° RAQ-45° LPO)	Same	Preferred	6
Orbit type	Circular	Same	Standard	7
	Non-circular	Same	Optional	7
Pixel size	6.4 ± 0.2 mm	Same	Standard	8
Acquisition type	Continuous	Same	Preferred	9
	Step-and-shoot	Same	Standard	9
No. of projections	64	Same	Standard	10
Matrix	64 × 64	Same	Standard	11
Time/projection	25 s	20 s	Standard	12
Total time	30 min	25 min	Standard	13
ECG gated	No	Yes	Optional	14
Frames/cycle	N/A	8	Optional	14
R-to-R window	100%	100%	Optional	14
Multidetector systems			Optional	15

Processing Protocols

1. **Filtering.** Reconstruction filter selection continues to be a critical aspect of SPECT data processing, whether the reconstruction algorithm is filtered backprojection or iterative restoration. The primary goal of filtering is to find the optimal balance for suppressing image noise (achieving image "smoothness") while preserving image spatial resolution (or myocardial wall "sharpness"). Over-smoothing can obscure genuine perfusion defects, while under-smoothing can complicate the interpretation of normally perfused territories. A filter with a sufficiently high "cut-off" frequency, or "critical" frequency, known as a high-pass filter, preserves spatial resolution, but at the expense

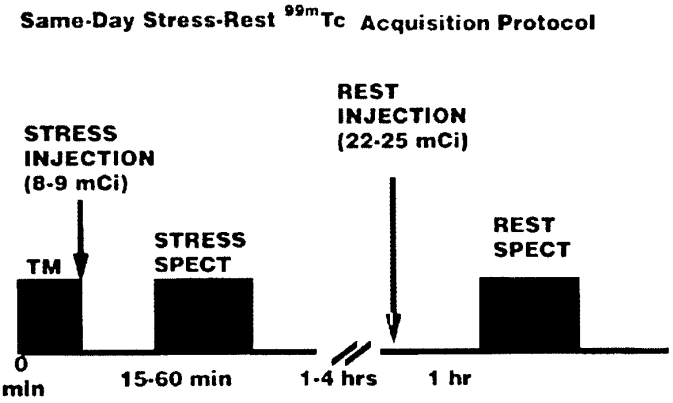

Note: Times displayed are optional (see below); TM, treadmill.

Patient protocol

	Exercise study	Rest study		For info see paragraph
Dose	8-9 mCi	22-25 mCi	Standard	1
Position	Supine	Supine	Standard	2
	Prone	Prone	Optional	2
Delay time (intervals)				
Injection → imaging	15 min–1 h	1-2 h	Optional	3
Stress → rest		1-4 h	Optional	3
Acquisition protocol				
Energy window	20% symmetric	Same	Optional	4
Collimator	Low-energy, high-resolution	Same	Preferred	5
Orbit	180° (45° RAQ-45° LPO)	Same	Preferred	6
Orbit type	Circular	Same	Standard	7
	Non-circular	Same	Optional	7
Pixel size	6.4 ± 0.2 mm	Same	Standard	8
Acquisition type	Continuous	Same	Preferred	9
	Step-and-shoot	Same	Standard	9
No. of projections	64	Same	Standard	10
Matrix	64 × 64	Same	Standard	11
Time/projection	25 s	20 s	Standard	12
Total time	30 min	25 min	Standard	13
ECG gated	No	Yes	Optional	14
Frames/cycle	N/A	8	Optional	14
R-to-R window	100%	100%	Optional	14
Multidetector systems			Optional	15

of allowing noise to remain in the image. Low-pass frequency filters remove noise, but at the expense of blurring potentially important structures, thereby diminishing contrast.

Multicenter trials have been executed to determine which filters optimize study accuracy. These evaluations have been performed both using realistic input phantom data of known radioisotope distribution, and using routine clinical studies for which other correlative data was available, such as x-ray contrast angiography. Both algorithmic accuracy and visual accuracy have been evaluated, and it should be noted that filters which optimize visual accuracy might not necessarily optimize quantitative accuracy. Likewise, filters which are best for summed images (or non-gated tomograms) may differ from those which are best for gated cines. Furthermore, optimal filters for stress studies may differ from those for rest studies, since these types of data sets differ from one another as to count density. Manufacturers generally follow the recommendations of multicenter research studies in setting the default val-

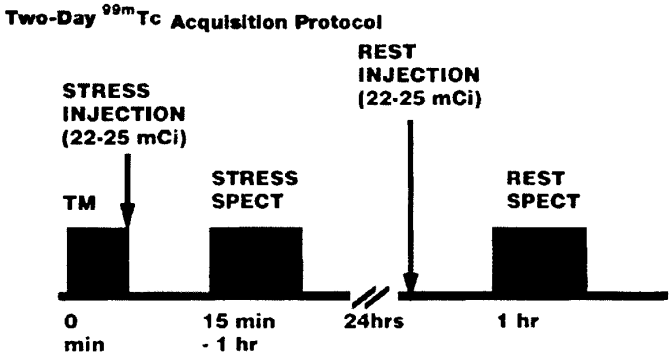

Note: Times displayed are optional (see below); TM, treadmill.

Patient protocol

	Exercise study	Rest study		For info see paragraph
Dose	22-25 mCi	22-25 mCi	Standard	1
Position	Supine	Supine	Standard	2
	Prone	Prone	Optional	2
Delay time (intervals)				
Injection → imaging	15 min–1 h	1-2 h	Optional	3
Acquisition protocol				
Energy window	20% symmetric	Same	Optional	4
Collimator	Low-energy, high-resolution	Same	Preferred	5
Orbit	180° (45° RAQ-45° LPO)	Same	Preferred	6
Orbit type	Circular	Same	Standard	7
	Non-circular	Same	Optional	7
Pixel size	6.4 ± 0.2 mm	Same	Standard	8
Acquisition type	Continuous	Same	Preferred	9
	Step-and-shoot	Same	Standard	9
No. of projections	64	Same	Standard	10
Matrix	64 × 64	Same	Standard	11
Time/projection	20 s	20 s	Standard	12
Total time	25 min	25 min	Standard	13
ECG gated	Yes	Yes	Optional	14
Frames/cycle	8	8	Optional	14
R-to-R window	100%	100%	Optional	14
Multidetector systems			Optional	15

ues of their recommended filters. It should be noted that units describing parameters such as cutoff and critical frequencies vary among manufacturers.

On a case-by-case basis it may be tempting to alter the default filter values, such as for an isolated case of injection infiltration. Unfortunately, sufficient adjustments in filter values can be made until any desired image result is obtained, thereby incurring the danger of accidentally inducing false positives or false negatives. Therefore, it is recommended that standardized filters be used for all patients undergoing the same imaging protocol. Without a thorough experimental analysis of a new filter, such as by means of phantom data, it can be difficult to appreciate the extent to which an unusual filter will alter clinical interpretations. Before selecting a new filter, scientific publications and computer vendor's clinical operations manuals should be reviewed to determine the recommended filters for a particular imaging protocol.

Filters are classified as "conventional," which are independent of image counts, and "adaptive," which vary from one image to another and require as input individual image counts and known system resolution. The most common

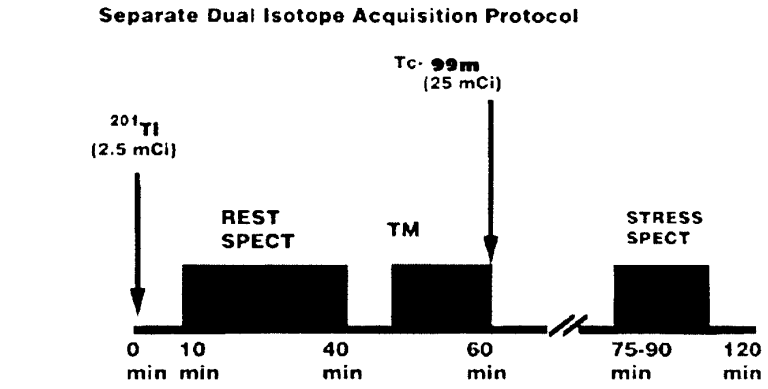

Note: Times displayed are optional (see below); TM, treadmill.

Patient protocol

	Rest study	Exercise study		For info see paragraph
Dose	2.5 mCi Tl-201	22-25 mCi Tc-99m	Standard	1
Position	Supine	Supine	Standard	2
	Prone	Prone	Optional	
Delay time (intervals)				
Injection → imaging	10-15 min	15 min-1 h	Optional	3
Rest → stress		No delay	Optional	3
Acquisition protocol				
Energy window	30% symmetric 70 keV	15% symmetric 140 keV	Optional	4
	20% symmetric 167 keV			
Collimator	Low-energy, high-resolution	Same	Preferred	5
Orbit	180° (45° RAQ-45° LPO)	Same	Preferred	6
Orbit type	Circular	Same	Standard	7
	Non-circular	Same	Optional	7
Pixel size	6.4 ± 0.2 mm	Same	Standard	8
Acquisition type	Continuous	Same	Preferred	9
	Step-and-shoot	Same	Standard	9
No. of projections	64	Same	Standard	10
Matrix	64 × 64	Same	Standard	11
Time/projection	25 s	20 s	Standard	12
Total time	30 min	25 min	Standard	13
ECG gated	No	Yes	Optional	14
Frames/cycle	N/A	8	Optional	14
R-to-R window	100%	100%	Optional	14
Multidetector systems			Optional	15

conventional filters are Butterworth, Hanning, Hamming, and Parzen filters. The most common adaptive filters are Wiener and Metz filters. The latter often are referred to as "restoration" filters and have the added feature of enhancing image contrast by selectively boosting the contrast of structures of a pre-determined size. Butterworth and Hanning filters are the most commonly used and are available on all manufacturers' systems.

The preferred processing sequence continues to be applying a frequency filter to the original projection images prior to reconstruction, followed by applying only a ramp filter during filtered backprojection. Optional approaches include applying a frequency filter during backprojection, but usually an additional filter must then be applied to filter images in the "z" dimension across transaxial planes. The use of filters in conjunction with iterative restoration techniques, such as maximum likelihood approach, varies widely at the present time.

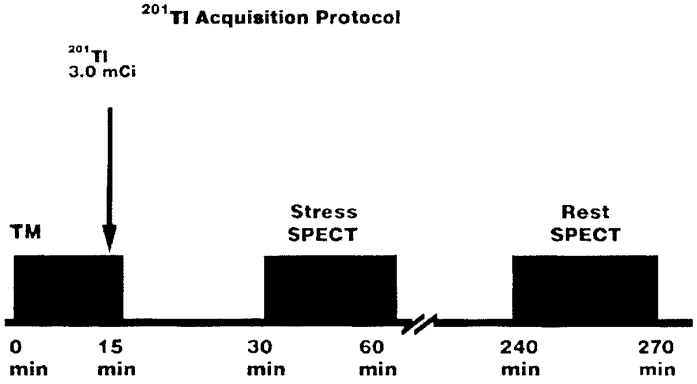

Note: Times displayed are optional (see below); TM, treadmill.

Patient protocol

	Stress study	Redistribution rest study		For info see paragraph
Dose	3 mCi	N/A	Standard	1
Position	Supine	Supine	Standard	2
	Prone	Prone	Optional	
Delay time (intervals)				
Injection → imaging	10-15 min*	N/A	Optional	3
Stress → rest		4 h	Optional	3
Acquisition protocol				
Energy window	30% symmetric 70 keV	Same	Optional	4
	20% symmetric 167 keV			
Collimator	Low-energy, all-purpose	Same	Preferred	5
Orbit	180° (45° RAQ-45° LPO)	Same	Preferred	6
Orbit type	Circular	Same	Standard	7
	Non-circular	Same	Optional	7
Pixel size	6.4 ± 0.2 mm	Same	Standard	8
Acquisition type	Continuous	Same	Preferred	9
	Step-and-shoot	Same	Standard	9
No. of projections	32	Same	Standard	10
Matrix	64 × 64	Same	Standard	11
Time/projection	40 s	40 s	Standard	12
Total time	22 min	22 min	Standard	13
Multidetector systems			Optional	15

*An anterior planar image may be acquired during this interval to evaluate Tl-201 lung uptake.

2. **Reconstruction.** The two main reconstruction methods are classified as "analytic" or "iterative." Analytic methods are based on an exact mathematical solution to image reconstruction, whereas iterative methods estimate the distribution through successive approximations. The most common analytic method, offered by all manufacturers, is filtered backprojection, which remains the primary reconstruction method.

   There is considerable evidence that iterative methods, such as OSEM, provide a more accurate approximation of the actual count distribution. The most thorough and realistic of this class of reconstruction techniques still may be too time-consuming for routine clinical use. However, sufficient improvements in computer hardware and software have made clinical implementation of some iterative reconstruction methods feasible, and some manufacturers do supply these as an option. A major reason this class of algorithms is being pursued vigorously is that they permit the incorporation of attenuation, scatter and detector resolution depth dependence corrections.

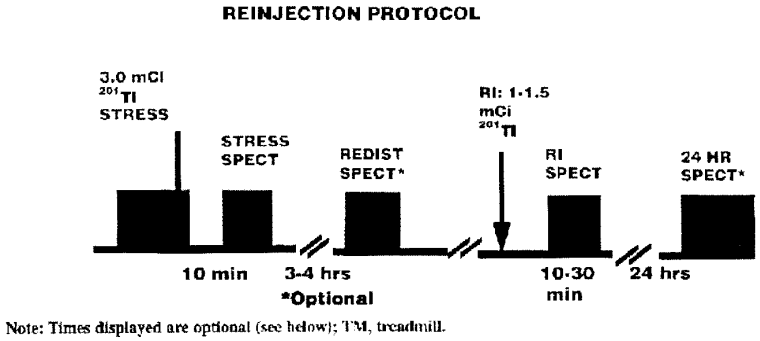

Note: Times displayed are optional (see below); TM, treadmill.

Patient protocol

	Stress study	Reinjection	(Redistribution) rest study		For info see paragraph
Dose	3 mCi	1.5 mCi	N/A	Standard	1
Position	Supine		Supine	Standard	2
	Prone		Prone	Optional	2
Delay time (intervals)					
Injection → imaging	10-15 min		N/A	Standard	3
Stress → redistribution			3-4 h	Optional	3
Reinjection → imaging (MI)		10-30 min		Optional	3
Acquisition protocol					
Energy window	30% symmetric 70 keV		Same	Optional	4
	20% symmetric 167 keV				
Collimator	Low-energy, all-purpose		Same	Preferred	5
Orbit	180° (45° RAQ-45° LPO)		Same	Preferred	6
Orbit type	Circular		Same	Standard	7
	Non-circular		Same	Optional	7
Pixel size	6.4 ± 0.2 mm		Same	Standard	8
Acquisition type	Continuous		Same	Preferred	9
	Step-and-shoot		Same	Standard	9
No. of projections	32		Same	Standard	10
Matrix	64 × 64		Same	Standard	11
Time/projection	40 s		40 s	Standard	12
Total time	22 min		22 min	Standard	13
Multidetector systems				Optional	15

3. **Reorientation.** A critical phase of myocardial processing is reorientation of tomographic data into the natural approximate symmetry axes of an individual patient's heart. This is performed either by an observer or automatically, and results in sectioning the data into vertical long axis, horizontal long axis, and short axis planes. Long axis orientation lines should be parallel to long axis walls of the myocardium and should be consistent between rest and stress studies. Inappropriate plane selections can result in misaligned myocardial walls between rest and stress data sets, potentially resulting in clinical misinterpretations. It is crucial that all axis choices be available as QC screens, and that these are reviewed by the technologist and the physician who reads each study to verify that axes were selected properly.
4. **Display—cine review.** The most important post-acquisition QC procedure is to view the original projection data in cine mode. This presentation offers a sensitive method for detecting patient and/or heart motion, "upward creep," breast shadow due to attenuation, diaphragmatic attenuation, and superimposed abdominal visceral activity, all of which can create artifacts in the reconstructed images. Review of cined images is performed twice: once by the technologist immediately after the acquisition, and again by the physician during image interpretation. For gated stud-

Processing protocol

			For info see paragraph
Filtering		Mandatory	1
Methods	Prereconstruction	Standard	
	With reconstruction	Optional	
Types	Adaptive	Optional	1
	Conventional	Standard	1
Reconstruction			
Transverse	Analytical	Standard	2
	Iterative	Optional	
Oblique angle	Manual	Standard	3
	Automatic	Optional	
Display			
Cine review		Mandatory	4
Study review	Screen	Preferred	5
	Hard copy	Optional	

ies, usually it is only the sum of all gated tomograms that is reviewed in this manor; this will alert the observer to most types of gating errors due to arrhythmias as a "flickering" of image counts. However, for the detection of gating errors due to some types of transient arrhythmias, a full display of all count-versus-projection curve data is required. Cine reviews also offer the opportunity to discover other unusual features of potential clinical relevance, including the detection of neoplasms, particularly of the lungs and lymph nodes. Abnormal findings of this nature should be reported and pursued further.

5. **Display—study review.** It is recommended that physicians use the active computer screen for reviewing images, and use film and paper hard copies only for record-keeping purposes. Images produced by formatters onto hard-copies are produced by exposing x-ray film to varying contrast and intensity output. These outputs can fluctuate over time and may require frequent calibration, making consistent film exposures problematic. Computer screen outputs are relatively more stable, and always have readily available monochromatic contrast bars or color code bars to the side of the images, enabling consistent viewing conditions. In addition, computer screens offer rapid sequential and/or cinematic displays of vast quantities of image data. For all of these reasons, screen interpretation is recommended over relying on interpretations from hard copies.

Perfusion Quantitation

1. **Data sampling.** The initial process required for quantification of regional relative myocardial perfusion is data sampling. Most techniques to accomplish this perform circumferential profile sampling using a hybrid coordinate system, which is spherical near the apex and cylindrical toward the base. The count values between endocardial and epicardial surfaces along rays extending out from the center of the LV cavity are then tabulated at each spatial location. The values subsequently processed can either be a single maximum count per ray, an average of several pixels along a ray, or the result of Gaussian fitting of count profiles. Currently, the maximum count technique is the most widely used of these options.
2. **Normalization.** Circumferential count profiles must be normalized before subjecting them to defect analysis, and there are several techniques used for this normalization. Usually this is accomplished by normalizing counts per pixel to the highest myocardial count, generally assumed to be the "most normal" part of the heart. In reformatting circumferential profiles into polar plots, these profiles can be scaled according to the distance from apex to base ("distance weighted") for equal ring thickness, or alternatively "volume weighted" to account for the likely different thickness of the myocardium at each level from apex to base.
3. **Analysis.** To determine if an individual patient's study is normal or abnormal, the patient's sampled values must be compared to a set of profiles that are taken to be normal. Popular techniques for this involve comparisons to normal databases, which consist of mean relative percent of myocardial activity and standard deviations about these means for each of several (often 20) vascular territories. The determination of what constitutes the cutoff threshold value

often is determined based on a set of correlative visual readings by panels of experts. Thus, this approach is oriented towards incorporating the knowledge of experts in reading groups of patients defined as being normal based on Bayesian analysis for having a low likelihood of CAD. This approach also increases the likelihood that algorithmic pronouncements of abnormality will agree with visual assessments. The resulting algorithms for detecting the presence of perfusion abnormalities then are tested against prospective groups of patients known to be normal or abnormal on the basis of other clinical findings. Traditionally, separate databases have been used for male and female patients. With the advent of different data sampling approaches and attenuation corrections, new normal databases are being tested and are proliferating presently. Some commercially available systems enable the observer to construct normal databases unique to the patient population of each individual institution.

4. **Variables.** The standard variables extracted for myocardial perfusion are "extent," "severity," and "reversibility." All of these variables are derived after comparison of the patient's profiles to normal limits. "Extent" represents the number of pixels that fall below the normal limit and indicates a lesion's size. "Severity" is computed from the curve area below the normal limit. "Reversibility" indicates the difference between rest and stress profiles. Areas of resting perfusion significantly above stress perfusion are considered reversible and indicate reversible ischemia. Other variables that can be derived from myocardial perfusion are washout for Tl-201, which indicates to what degree the initial Tl-201 has cleared from the myocardium over a set time interval, usually 4 hours. A measure indicating the difference in size between the myocardium at stress versus rest is referred to as transient ischemic dilatation or TID. This value is derived by measuring the circumference of the heart and computing a ratio of stress size to rest size, and some commercially available algorithms report this result. Lung washout indicates how much activity has cleared from the lungs between stress and rest imaging. The TID and lung washout variables can indicate the presence of severe and extensive CAD if they fall beyond normal ranges.
5. **Display.** The traditional method for displaying patient's circumferential profiles is to incorporate them into a single 2D display referred to as a polar map. Relative counts, defect extent, severity, and reversibility maps all can be generated. Often, areas below normal limits are set to zero (black) on perfusion maps to form a "defect map," while areas seen to be significantly reversible are set at the highest brightness level or color intensity to form a "reversibility map." Most commercial systems also display 3D representations of perfusion maps, with representations of defect and reversibility zones, freely reorientable by the observer using a computer "mouse" or trackball. The potential advantages of 3D display formats are to provide the observer with a visual appreciation of the magnitude and orientation of areas of myocardial scar or ischemia specific to the actual shape of each patient's left ventricle.

Functional Quantitation From Gated SPECT Data

1. **Data sampling.** Originally, the simplest methods used only paired mid-ventricular VLA and HLA slices, reminiscent of echocardiographic and angiographic processing, but most computer systems now include software which samples gated myocardial perfusion SPECT data fully 3-dimensionally. All approaches assume the myocardial center to correspond to the location of the brightest mid-myocardial count, and some approaches determine this by Gaussian count profile fitting. Initial probable candidate points identified in this fashion are tested against expected spatial distributions of myocardial locations, and refined using various criteria until the most probable distribution of mid-myocardial locations eventually are determined. The different approaches vary somewhat in their ventricular modeling assumptions as to the means by which endocardial locations are offset from mid-myocardial points.
2. **Automation.** Fully automated versions of these different approaches are now widely available. Depending on the approach, various quality assurance screens are provided during or following automated location of LV centers, mid-myocardial and/or endocardial locations, and valve planes. The observer must review these suggested locations and adjust them as necessary if for any reason any part of the automated choices were judged to have failed. Unless some territories are severely hypoperfused, these automated approaches have been observed to work quite well in general, and very high degrees of data processing reproducibility have been reported. The most common circumstances defeating automated myocardial localization algorithms are intense hepatobiliary activity adjacent to hypoperfused inferior myocardial walls, and unusually high RV activity in conjunction with hypoperfused septa.
3. **Analysis.** From the final user-accepted endocardial points are computed LV volumes, at least for ED and ES, and preferably for each frame of the cardiac cycle. From these volumes the EF is computed. Some software packages also compute regional EF, regional wall motion changes in units of millimeters, and wall thickening changes in terms of relative percents. The latter primarily are based on observed changes of mid-myocardial maximum counts from diastole to systole, and assume a linear relationship for the well-known "partial volume" effect.

4. **Variables.** Of the variables computed, EF has been the most extensively tested for all gated SPECT approaches against all of the other available cardiac imaging modalities, and agreement with these has consistently been shown to be quite high, particularly when compared to other radionuclide (equilibrium and first pass) EF methods. Reproducibility of values has been found to be quite high. Overall, absolute volume measurements correlate well with those from more established imaging modalities. Evidence is growing that volumes vary somewhat among the various gated SPECT approaches, and may underestimate or overestimate echo and angiographic values, depending on the approach. The most consistent finding to date has been that gated SPECT volumes tend to be genuinely too low for the smallest hearts.
5. **Display.** In addition to the QC screens described above, summary screens are available showing the results of computations along with moving sections through the mid-left ventricle along with computed endocardial borders. Studies have shown that regional wall motion read from such cine displays agree quite well with independent readings, such as from echocardiography. Also, most new systems now include moving 3D displays of surface-shaded representations of "beating" endocardial and epicardial surfaces, with or without superimposed wire cage end diastolic reference surfaces. These generally show ventricular shapes, the appearance of which differ from one patient to another, and are freely reorientable by the user.

Bibliography

1. Juni JE, Van Train K. Atlas of artifacts in Tl-201 SPECT cardiac perfusion imaging. In: Van Nostrand D, editor. Selected atlases of cardiovascular nuclear medicine. New York: Springer-Verlag; 1993. p. 29-50.
2. Segall GM, Davis MJ. Prone versus supine thallium myocardial SPECT. A method to decrease artifactual inferior wall defects. J Nucl Med 1989;30:548-55.
3. Kiat H, Van Train KF, Friedman JD, et al. Quantitative stress-redistribution thallium-201 SPECT using prone imaging: methodologic development and validation. J Nucl Med 1992;33:1509-15.
4. Galt JR, Germano G. Advances in instrumentation for cardiac SPECT. In: DePuey EG, Berman DS, Garcia EV, editors. Cardiac SPECT imaging. New York: Raven Press; 1994. p. 91-102.
5. Maniawski PJ, Morgan HT, Wackers FJ, et al. Orbit-related variation in spatial resolution as a source of artifactual defects in thallium-201 SPECT. J Nucl Med 1991;32:871-5.
6. Faber T, Akers MS, Peshock RM, et al. Three dimensional motion and perfusion quantification in gated single photon emission computed tomograms. J Nucl Med 1991;32:2311-7.
7. Germano G, Kavanaugh PB, Hsiao-Te, et al. Automatic reorientation of three-dimensional, transaxial mid-myocardial perfusion SPECT images. J Nucl Med 1995;36:1107-19.
8. Greer KL, Jaszczak RJ, Coleman RE. An overview of a camera-based SPECT system. Med Phys 1982;9:455-63.
9. Nowak DJ, Gullberg GT, Eisner RL, et al. An investigation to determine uniformity requirements for rotating gamma camera tomography. J Nucl Med 1982;23:52-3.
10. Rogers WL, Gullberg GT, Eisner RL, et al. Field-flood requirements for emission tomography with an Anger camera. J Nucl Med 1982;23:162-8.
11. Friedman J, Berman DS, Van Train KF, et al. Patient motion in thallium-201 myocardial SPECT imaging: an easily identified frequent source of artifactual defect. Clin Nucl Med 1988;13:321-4.
12. Friedman J, Van Train KF, Maddahi J, et al. "Upward creep" of the heart: a frequent source of false positive perfusion defects on thallium-201 stress-redistribution SPECT. J Nucl Med 1989;30:1718-22.
13. Cooper JA, Neuman PH, McCandless BK, et al. Effect of patient motion on tomographic myocardial perfusion imaging. J Nucl Med 1992;13:1566-71.
14. Eisner RL, Churchwell A, Noever T, et al. Quantitative analysis of the tomographic thallium-201 myocardial bullseye display: critical role of correcting for patient motion. J Nucl Med 1988;29:91-7.
15. Galt JR, Hise HL, Garcia EV, et al. Filtering in frequency space. J Nucl Med Technol 1986;14:153-60.
16. King MA, Glick SJ, Penney BC, et al. Interactive visual optimization of SPECT prereconstruction filtering. J Nucl Med 1987;28:1192-8.
17. King MA, Schwinger RB, Doherty PW, et al. Two-dimensional filtering of SPECT images using the Metz and Weiner filters. J Nucl Med 1984;25:1234-40.
18. Brooks RA, DiChiro G. Principles of computer assisted tomography (CAT) in radiographic and radioisotopic imaging. Phys Med Biol 1976;21:689-732.
19. Burow RD, Pond M, Schaffer AW, et al. Circumferential profiles: a new method for computer analysis of thallium-201 myocardial perfusion images. J Nucl Med 1979;20:771-7.
20. DePasquale E, Nody A, DePuey EG, et al. Quantitative rotational thallium-201 tomography for identifying and localizing coronary artery disease. Circulation 1988;77:316-27.
21. Garcia EV, Van Train K, Maddahi J. Quantification of rotational thallium-201 myocardial tomography. J Nucl Med 1985;26:17-26.
22. Mahmarian JJ, Boyce TM, Goldberg RK, et al. Quantitative exercise thallium-201 single photon emission computed tomography for the enhanced diagnosis of ischemic heart disease. J Am Coll Cardiol 1990;15:318-29.
23. Gibbons RJ, Verani MS, Behrenbeck T, et al. Feasibility of tomographic Tc-99m-hexakis-2-methoxy-2-methylpropyl-isonitrile imaging for the assessment of myocardial area at risk and the effect of acute treatment in myocardial infarction. Circulation 1989;80:1277-86.
24. Nuyts J, Mortelmans L, Suetens P, et al. Model-based quantification of myocardial perfusion images from SPECT. J Nucl Med 1989;30:1992-2001.
25. Garcia EV, Cooke CD, Van Train KF, et al. Technical aspects of myocardial SPECT imaging with Tc-99m sestamibi. Am J Cardiol 1990;66:23E-31E.
26. Caldwell J, Williams DL, Harp GD, et al. Quantitation of size of relative myocardial perfusion defect by single-photon emission computed tomography. Circulation 1984;70:1048-56.

27. Maddahi J, Garcia EV, Berman DS, et al. Improved non-invasive assessment of CAD by myocardial distribution and washout of thallium-201. Circulation 1981;64:924-35.
28. Van Train K, Areeda J, Garcia EV, et al. Quantitative same-day rest stress technetium-99m-Sestamibi SPECT: definition and validation of stress normal limits and criteria for abnormality. J Nucl Med 1993;34:1494-502.
29. Van Train K, Maddahi J, Berman DS, et al. Quantitative analysis of tomographic stress thallium-201 myocardial scintigrams: a multicenter trial. J Nucl Med 1990;31:1168-79.
30. Van Train K, Garcia EV, Maddahi J, et al. Multicenter trial validation for quantitative analysis of same-day rest-stress technetium-99m-sestamibi myocardial tomograms. J Nucl Med 1994;35:609-18.
31. Klein JL, Garcia EV, DePuey EG, et al. Reversibility bullseye: a new polar bull's-eye map to quantify reversibility of stress induced SPECT-Tl-201 myocardial perfusion defects. J Nucl Med 1990;31:1240-6.
32. Chouraqui P, Rodrigues E, Berman DS, et al. Significance of dipyridamole induced transient dilation of the left ventricle during thallium-201 scintigraphy in suspected coronary artery disease. Am J Cardiol 1990;66:689-94.
33. Levy R, Rozanski A, Berman DS, Garcia EV, et al. Analysis of the degree of pulmonary thallium washout after exercise in patients with coronary artery disease. J Am Coll Cardiol 1983;2:719-28.
34. Berman DS, Kiat H, Wang FP, et al. Separate acquisition rest thallium-201/stress, technetium-99m sestamibi dual isotope myocardial perfusion SPECT: a clinical validation study. J Am Coll Cardiol 1993;22:1455-64.
35. Berman DS, Kiat H, Van Train K, et al. Tc-sestamibi imaging in the assessment of chronic coronary artery disease. Semin Nucl Med 1991;21:190-212.
36. Dilsizian V, Perrone-Firaldi P, Arrighl JA, et al. Concordance and discordance between stress-redistribution-reinjection and rest-redistribution thallium imaging for assessing viable myocardium. Circulation 1993;88:941-52.
37. Kiat H, Berman DS, Maddahi J, et al. Late reversibility of tomographic myocardial thallium-201 defects: an accurate marker of myocardial viability. J Am Coll Cardiol 1988;12:1456-63.
38. DePuey EG, Nichols K, Dobrinsky C, et al. Left ventricular ejection fraction assessed from gated technetium-99m-sestamibi SPECT. J Nucl Med 1993;34:1871-6.
39. Germano G, Kiat H, Kavanagh PB, et al. Automatic quantification of ejection fraction from gated myocardial perfusion SPECT. J Nucl Med 1995;36:2138-47.
40. Nichols K, DePuey EG, Rozanski A. Automation of gated tomographic left ventricular ejection fraction. J Nucl Cardiol 1996;3:475-82.
41. Faber TL, Cooke DC, Folks RD, et al. Left ventricular function from gated SPECT perfusion images: an integrated method. J Nucl Med 1999;40:650-9.
42. Mochizuki T, Murase K, Tanake H, et al. Assessment of left ventricular volumes using ECG-gated SPECT with technetium-99m-MIBI and technetium-99m-tetrofosmin. J Nucl Med 1997;38:53-7.
43. Nichols K, Tamis J, DePuey EG, et al. Relationship of gated SPECT ventricular functional parameters to angiographic measurements. J Nucl Cardiol 1998;5:295-303.
44. Iskandrian A, Germano G, VanDecker W, et al. Validation of left ventricular volume measurements by gated SPECT Tc-99m sestamibi imaging. J Nucl Cardiol 1998;5:574-8.
45. Case JA, Cullom SJ, Bateman TM, et al. Count density and filter requirements for accurate LVEF measurements from gated Tl-201 SPECT: a gated MCAT study [abstract]. J Nucl Med 1997;38:27P.
46. Case JA, Bateman TM, Cullom SJ, et al. Obtaining optimum and consistent SPECT myocardial counts using and anterior planar view to determine SPECT acquisition times [abstract]. J Am Coll Cardiol 1998;31:84A.
47. Case J, Bateman T, Cullom SJ, O'Keefe, et al. Improved accuracy of SPECT LVEF using numerical modeling of ventricular image blurring for patients with small hearts [abstract]. J Am Coll Cardiol 1999;33(2;A):436A.
48. Nichols K, Lefkowitz D, Faber T, et al. Ventricular volumes compared among three gated SPECT methods and echocardiography [abstract]. J Am Coll Cardiol 1999;33:409A.
49. Chua T, Kiat H, Germano G, et al. Gated technetium-99m sestamibi for simultaneous assessment of stress myocardial perfusion, post exercise regional ventricular function and myocardial viability. J Am Coll Cardiol 1994;23:1107-14.
50. Germano G, Erel J, Lewin H, et al. Automatic quantitation of regional myocardial wall motion and thickening from gated technetium-99m sestamibi myocardial perfusion single-photon emission computed tomography. J Am Coll Cardiol 1997;30:1360-7.
51. Nichols K, DePuey EG, Krasnow N, et al. Reliability of enhanced gated perfusion SPECT in assessing wall motion of severely hypoperfused myocardia: an echocardiographic validation. J Nucl Cardiol 1998;5:387-94.
52. Johnson L, Verdesca S, Aude W, et al. Postischemic stunning can affect left ventricular ejection fraction and regional wall motion on post-stress gated sestamibi tomograms. J Am Coll Cardiol 1997;30:1641-8.
53. Germano G, Erel J, Kiat H, et al. Quantitative LVEF and qualitative regional function from gated thallium-201 perfusion SPECT. J Nucl Med 1997;38:749-54.
54. DePuey EG, Parmett S, Ghesani M, et al. Comparison of Tc-99m sestamibi and thallium-201 gated perfusion SPECT. J Nucl Cardiol 1999;6:278-85.
55. Cullom SJ, Case JA, Bateman TM. Electrocardiographically gated myocardial perfusion SPECT: technical principles and quality control considerations. J Nucl Cardiol 1998;5:418-25.
56. Nichols K, Dorbala S, DePuey EG, et al. Influence of arrhythmias on gated SPECT myocardial perfusion and function quantification. J Nucl Med 1999;40:924-34.
57. Wintergreen panel summaries. J Nucl Cardiol 1999;6(Part 1):93-155.
58. Case J, Bateman T, Cullom S, et al. Obtaining optimum and consistent SPEW myocardial counts using an anterior planar view to determine SPECT acquisition times [abstract]. J Am Coll Cardiol 1998;31:82A.
59. Bateman TM, Berman DS, Heller GV, et al. ASNC position statement on ECG-gating of myocardial perfusion SPECT scintigrams. J Nucl Cardiol 1999;6 470-1.
60. Esquerre JP, Coca FJ, Martinez SL, et al. Prone decubitus: a solution to inferior wall attenuation in thallium-201 myocardial tomography. J Nucl Med 1989;30:398-401.

IMAGING GUIDELINES FOR TRANSMISSION-EMISSION TOMOGRAPHIC SYSTEMS TO BE USED FOR ATTENUATION CORRECTION

Introduction

Transmission-emission tomographic (TCT-ECT) systems are commercially available options for correcting SPECT data for photon attenuation. At this time, attenuation correction of myocardial perfusion SPECT is in a phase of rapid development and evaluation. There are considerable differences in hardware and software implemented by the various camera manufacturers as each vendor strives to provide the "best of class" attenuation correction system. The diversity in imaging hardware and software and the relative infancy of attenuation correction technology makes it very difficult to provide "cookbook" guidelines as provided by the other sections of the imaging guidelines. Given this difficulty, the structure of the attenuation correction guidelines will differ slightly from the rest of the imaging guidelines. This section will attempt to outline potential areas of concern, provide specific guidelines where applicable and provide generic comments on imaging parameters that cannot be made specific due to vendor differences. In short, the attenuation correction guidelines outlined in this section will serve as a template on which future guidelines can be written as the technology matures to the level of the other sections in the guidelines.

This section contains two sub-sections. The first section expands on the guidelines for SPECT QC of TCT-ECT systems. This section will describe the TCT-ECT systems that were commercially available when these guidelines were written and some quality assurance protocols that can be performed in the clinic to ensure the quality of the TCT-ECT system. The second section, myocardial perfusion imaging, will expand on the myocardial perfusion SPECT guidelines when incorporating TCT-ECT imaging.

A. Quality Control

A.1 Equipment

The following TCT system geometries are commercially available.

1. Scanning line source systems
2. Multiple line source arrays
3. Scanning point source system
4. X-ray transmission source

The scanning line source TCT systems are the most prevalent because of their implementation on dual detector systems in the 90° configuration with parallel hole collimation. This system uses Gd-153 transmission lines sources that translate axially across the body. By incorporating an electronic mask coupled to the transmission source position, this system is capable of measuring bi-directional crosstalk between the transmission and emission energy windows. Removal of the "crosstalk" between the emission and transmission windows is essential processing before reconstructing the projection data. The multiple line source geometry uses an array of Gd-153 line sources opposite detectors with parallel hole collimation. Since the sources are distributed across the imaging FOV, this system tends to give a higher transmission signal-to-crosstalk ratio (TCR) compared to the scanning line source geometry. Crosstalk from this system is measured using a split energy window about the Gd-153 photopeak. The last geometry, the scanning point source system, detects the 356 keV photons from a Ba-133 point source. Any low energy collimator typically used for cardiac imaging can be used with this system as the 356 keV photons will penetrate the lead septa of these collimators. For this system, the crosstalk in the transmission data is measured in the same manner as described for the scanning line source system.

Each of these systems in conjunction with processing software was considered by the committee in constructing the following attenuation correction imaging guidelines. Due to the very recent introduction of the x-ray TCT system and its significant differences from the other transmission source based geometries, there was insufficient information acquired from this unique geometry for it to be included in the guidelines.

A.2 QC Procedures

The SPECT parameters outlined in the QC Section of these imaging guidelines should be used to ensure the quality of the emission tomographic data. In addition to those parameters, QC guidelines need to be followed to ensure that the transmission system is operating as designed. These tests are tabulated in the following table.

QC procedures for TCT-ECT systems

Test	Frequency	For info see paragraph
Energy peaking	Daily	1
Transmission source mechanics	Daily	2
Source strength	Monthly	3

1. **Energy peaking.** This test is performed to verify that the camera is counting photons in the proper energy windows. Using a pulse height energy (z) analyzer, which is available on all acquisition stations, the operator should verify that the emission, transmission, and scatter (if applicable) windows are properly set and that photons are being counted in each window. For some systems, this may necessitate manually opening the shutter to the transmission source. If this is not possible, a quick "blank" scan (see next paragraph) can be acquired to verify that transmission photons are being properly counted.
   NOTE: Consult the vendor's recommendation for energy peaking. Some vendors do not permit or require the peaking of all windows simultaneously.
2. **Transmission source mechanics.** When patients are not being imaged, the transmission source is shielded and, on systems where the source translates across the FOV, it is in the "parked" position. When a patient is imaged, the shutter used to shield the source is opened allowing transmission photons to be directed toward the patient. For translating sources, the source will then translate axially along the axis of the body for each projection. To verify the operation of the source shutter and translating mechanics, a reference "blank" transmission scan should be acquired. This scan is required for all TCT protocols and is likely recommended to be acquired weekly and possibly daily prior to the first use of the system for that day. The frequency will depend on the half life of the isotope of the transmission source and the stability of the TCT system. Follow the recommended acquisition protocol for acquiring a transmission blank scan. When complete, visually inspect planar images and check for artifacts (ie, focal cold spots, bands of missing data, axial discontinuities). A common misconception is that the blank scan should be uniform, similar to uniformity floods. Stringent uniformity indices of ± 10% are not reasonable for the blank scan. Rather the blank scan should be inspected to ensure that there are no gross non-uniformity artifacts (ie, holes or bands of pixels with no counts). For scanning source systems, the blank scans should not show discontinuities or abrupt changes in pixel intensity in the axial direction of the scanning source. The presence of these artifacts is consistent with improper scanning-detection alignment and should be checked by a service engineer.
3. **Source strength.** For systems using a Gd-153 transmission source, photons collected in the transmission window consist of primary transmission photons and scattered photons (crosstalk) from the emission isotope. The ratio of these components, transmission and crosstalk, we will refer to as the TCR. This value depends on the transmission source strength, the injected radiopharmaceutical, the injected activity, and the body habitus. Transmission source decay, higher injected activities, and larger body sizes all tend to decrease the TCR value. Lower TCR values result in reconstructed attenuation maps with increased bias and noise. Since the TCR value will decrease as the source decays, its behavior should be trended over the life of the source which can guide the user as to when the sources should be replaced. This QC protocol should be performed at least monthly with the baseline scan being performed when the TCT-ECT system is installed or the transmission sources have been replaced. If the user suspects problems with the TCT-ECT system, a test should be done immediately prior to using the system for patient imaging. Two protocols are provided, one using a cylinder phantom, the other using an anthropomorphic chest phantom. The chest phantom provides the more comprehensive check of the TCT-ECT system for cardiac imaging compared to the cylinder for obvious reasons. For those sites that may not have access to a chest phantom, the cylinder protocol is provided which is quite capable of identifying potential problems with a TCT-ECT system.

Protocol #1 Cylinder Phantom

Required Equipment

- 18 to 20 cm in diameter fillable cylinder
- 111 to 185 MBq (3-5 mCi) of Tc-99m or 37 MBq (1 mCi) Tl-201

Acquisition Protocols

1. Position cylinder with the long axis of the cylinder collinear to the table bed. Since processing will involve summing slices, minimize any tilt in the cylinder as seen by the detector.

2. Use vendor recommended TCT-ECT acquisition protocol. ***NOTE:*** *The total acquisition time should not be less than 12 minutes.*

Processing Protocols

1. Remove emission crosstalk from transmission data (for most systems, this is done automatically and does not need to be initiated by the user).
2. Reconstruct attenuation maps from the transmission projection data. If a filter is applied to the reconstructed image data, use the vendor recommended filter.
3. Add map slices from the center of the cylinder to provide a single 5-cm thick slice.
4. With an ROI tool, draw a circular ROI centered in the cylinder image that is approximately 90% of the diameter of the cylinder.
5. Record the mean attenuation coefficient (μ) value in the ROI. Consult the following chart for the expected range of values for the transmission isotope energy of your system.
6. Reconstruct uncorrected (NC) and attenuation corrected (AC) emission data. Add slices from the center of the cylinder to provide a 5-cm thick slice. Visually inspect the NC and AC images together. The AC image should be more uniform than the uncorrected image. Due to the low activity levels injected into the phantom, it is difficult to provide an acceptable quantitative range for an ROI.

Isotope	Energy (keV)	Expected range
Gd-153	100	0.160/cm-0.176/cm
Co-122	122	0.152/cm–0.168/cm
Tc-99m	140	0.145/cm–0.161/cm
Ba-133	360	0.106/cm–0.117/cm

Troubleshooting

If the ROI value from step (5) falls outside of the accepted range, your system can potentially yield erroneous data. Possible sources of error are as follows:

1. Transmission sources are too weak. Repeat the acquisition with a longer scan duration (ie, double the scan time). Repeat the processing steps and record a new ROI value for the attenuation map. If the value improves, then your sources are weak, and it is recommended that you either increase the imaging times for your protocols or replace your transmission sources.
2. Crosstalk correction is incorrect. While this correction is typically done automatically without user interaction, it does have the potential for failure. To investigate if improper crosstalk correction is the source of error, repeat the measurement with no activity injected in the cylinder. This will necessitate refilling the tank with water (no activity) and repeating the protocol. If the new ROI value for attenuation map without activity is within the tabulated range, you should call your service representative to have your TCT-ECT system checked. The crosstalk estimate used to correct the transmission data is likely the problem as the uncontaminated data are within the acceptable range and the crosstalk "compensated" values are not.
3. Bad blank scan. Acquire a new blank scan and re-acquire the cylinder phantom filled only with water (no activity injected into cylinder). If the new ROI value is not within the tabulated range and your sources have not expired, call your service representative. In this case, there is likely a serious inconsistency problem between the transmission and blank scan data. If the new ROI value is within the acceptable range, inject activity into the phantom and re-acquire the phantom.

Protocol #2 Chest Phantom

Required Equipment

An anthropomorphic chest phantom with a heart insert (no defects in heart).

Injected activity concentrations—a simulated 1110 MBq (30 mCi) sestamibi stress study

Heart:	250 kBq/mL	(6.8 uCi/mL)
Tissue:	25 kBq/mL	(0.7 uCi/mL)
Liver:	150 kBq/mL	(4.0 uCi/mL)
Lungs:	0 kBq/mL	(0.0 uCi/mL)

Acquisition Protocols

1. Position phantom on imaging bed.
2. Use vendor recommended TCT-ECT cardiac acquisition protocol. **NOTE:** The total acquisition time should not be less than 12 minutes.

Processing Protocols

1. Remove emission crosstalk from transmission data (for most systems, this is done automatically and does not need to be initiated by the user).
2. Reconstruct attenuation maps from the transmission projection data.
3. Visually inspect the transmission maps. Identify possible artifacts and their sources. Obvious artifacts include image truncation (ring artifact on periphery of imaging FOV) and crosstalk correction errors (depressed pixel intensities in region of heart or liver). If the truncation artifact involves a significant area of the imaging FOV, reposition the phantom and reacquire the data. If crosstalk errors are present, see the troubleshooting section below.
4. With an ROI tool, draw two small circular ROI in the region of the heart and the liver.
5. Record the mean values for the heart and liver ROIs. Consult the following chart for the expected range of values for the transmission isotope energy of your system.

Isotope	Energy (keV)	Expected range
Gd-153	100	0.160/cm-0.176/cm
Co-122	122	0.152/cm–0.168/cm
Tc-99m	140	0.145/cm–0.161/cm
Ba-133	360	0.106/cm–0.117/cm

6. Reconstruct NC and AC emission data. Construct NC and AC polarmaps from the image data.
7. View the NC and AC short axis, horizontal and vertical long axis images in a comparative display. Visually, the AC images should be more uniform than the NC images. No region of the heart should be noticeably hotter than the rest. The apex of some phantom hearts may be cooler than the rest of the phantom as the wall thickness of some phantom hearts does vary and can fall below the imaging resolution. In this case, the partial volume effect can be attributed to the lower activity values.
8. Using the ROI tool with either the polar maps or a mid-short axis image, record the AC intensity values in the anterior, lateral, posterior and septal regions. The anterior-posterior and septal-lateral ratios should be 1.0 ± 10%.

Troubleshooting

If the ROI value from step (5) falls outside of the accepted range, your system can potentially yield erroneous data. Possible sources of error are as follows

1. Transmission sources are too weak. Repeat the acquisition with a longer scan duration (ie, double the scan time). Repeat the processing steps and record a new ROI value for the attenuation map. If the value improves, then your sources are weak, and it is recommended that you either increase the imaging times for your protocols or purchase new transmission sources.
2. Crosstalk correction is incorrect. While this correction is typically done automatically without user interaction, it does have the potential for failure. To investigate if improper crosstalk correction is the source of error, repeat the measurement with no activity. This will necessitate refilling the tank with water (no activity) and repeating the protocol. You could also opt to perform the cylinder protocol as this protocol is ideally suited to determine crosstalk of blank scan problems. See troubleshooting comments (2) and (3) for the cylinder protocol.

If the ROI ratio values from step (7) fall outside of the accepted range, your system can potentially yield erroneous data. Possible sources of error are as follows

1. Transmission sources are too weak. Repeat the acquisition with a longer scan duration (ie, double the scan time). Repeat the processing steps and record a new ROI value for the attenuation map. If the value improves, then your sources are weak, and it is recommended that you either increase the imaging times for your protocols or purchase new transmission sources.
2. Crosstalk correction is incorrect. While this correction is typically done automatically without user interaction, it does have the potential for failure. To investigate if improper crosstalk correction is the source of error, repeat the measurement with no activity. This will necessitate refilling the tank with water (no activity) and repeating the pro-

tocol. If the new ROI value for attenuation map without activity is within the tabulated range, you should call your service representative to have your TCT-ECT system checked. If the new value is not within the tabulated range and your sources have not expired, call your service representative. If the sources are near their expiration date, replace your sources.

A.3 Clinical QC for Patient Procedures

In addition to the bulleted items for emission tomographic data under "Instrumentation Quality Assurance and Performance—Clinical QC for Each Patient Procedure," QC should be implemented for the patient specific transmission data. As stated above, the TCR parameter is sensitive to the patient size and injected dose, and its value can have a significant effect on the accuracy of the reconstructed AC data. Unfortunately, not all of the available TCT-ECT systems provide a measurement of this parameter or an equivalent. If the TCR parameter can be measured for each patient prior to initiating the TCT-ECT acquisition (ie, single planar projection), then the user could make the decision to increase the acquisition time (ie, $0.8 < TCR < 4$) or not to perform the TCT study at all ($TCR < 0.8$). This capability would provide a measure of confidence for the AC images on a patient specific basis.

In the absence of quantitative tools for the QC of the acquired TCT patient data, the reconstruction attenuation maps should be visually inspected for the following artifacts

1. Truncation – bright ring artifacts at the periphery of the body.
2. Crosstalk – decreased intensity in regions of heart or liver.
3. Low count study – high noise content in reconstructed maps.

B. AC Myocardial Perfusion SPECT Imaging

This section should be used in conjunction with the Imaging Guidelines for Myocardial Perfusion SPECT. Parameters that are affected by performing attenuation corrected myocardial perfusion imaging with TCT-ECT imaging systems are outlined.

B.1 Acquisition Parameters

Energy Windows

Nearly all of the transmission-emission systems that are commercially available use a Gd-153 sealed source to produce the transmission photons to measure anatomical density information. The photons of interest from Gd-153 are 97 keV (28% yield) and 103 keV (20% yield). To capture both of these photons, a 20% energy window should be centered at 100 keV.

For systems performing scatter correction based on energy spectral methods, it is advised to use the window settings recommended by the vendor as the performance and accuracy of the scatter correction algorithm has likely been optimized for these settings.

NOTE: Consult the vendor's recommendation for energy peaking. Some vendors do not permit or require the peaking of all windows simultaneously.

Collimators

For transmission systems using a converging source-collimator system (ie, fan beams), one should use the collimator recommended by the vendor. For transmission systems using parallel hole collimators, the choice between LEAP and LEHR should be based on the radiopharmaceutical being imaged as the resolution of the transmission data for myocardial perfusion SPECT is not as critical as the resolution and contrast of the reconstructed emission data. It should be noted that separate transmission blank scans are required for each different collimator used to collect transmission data.

Acquisition Orbit and Projections

Some of the 90° configurable systems with attenuation correction permit only 180° orbits. Nearly all transmission systems permit the use of circular and non-circular acquisition orbits.

The number of projections recommended in the Myocardial Perfusion Imaging Guidelines also applies to the TCT-ECT imaging.

Acquisition Mode

TCT-ECT systems can acquire the TCT and ECT data (1) simultaneously, (2) sequentially, and (3) interleaved sequential. In simultaneous mode, photons are collected in the transmission and emission windows simultaneously. Both projection sets are acquired for the same time duration and are perfectly aligned in time and space. In sequential mode, the system collects TCT data with the source open and then closes the source and collects the emission data. The sequence can also be reversed, ECT and then TCT. In this mode, there is no contamination to the emission data from the transmission source and the crosstalk in the transmission window from the emission photons can be measured directly during the ECT study with the transmission source closed. The disadvantage of this acquisition mode is that the acquisition time is increased by performing two separate scans and patient and/or heart motion between the TCT and ECT scans has the increased potential for alignment artifacts in the attenuation corrected emission images due to misalignment errors between the TCT and ECT data. The third mode, interleaved sequential, is performed by the scanning source systems. In this mode, transmission data is collected in a spatial window of defined width centered about the current transmission source position. Emission and emission-to-transmission crosstalk data is collected over the entire camera face outside of the transmission spatial window. For the interleaved sequential mode, transmission data is collected for a fraction of the time of the emission data. While the acquisition time for the interleaved sequential mode is equivalent to the sequential mode, alignment errors are minimized for this mode compared to the sequential mode, as the time separation between the TCT and ACT data is decreased.

Matrix and Pixel Size

Because the resolution of the reconstructed attenuation map does not significantly affect the reconstructed emission data, there are no constraints on the matrix or pixel size for the transmission data. Magnification of the transmission data is strongly discouraged if it results in truncation of the measured data as truncation can produce significant artifacts in the reconstructed attenuation maps (especially if filtered backprojection reconstruction is used to reconstruct the transmission data) and subsequently the reconstructed attenuation corrected emission data.

Most vendors support a 64×64 matrix with a 6.4 ± 0.2 mm pixel size, as recommended in the Myocardial Perfusion Imaging Guidelines section.

Acquisition Time per Projection

Since the measured transmission counts in most cases exceed the measured emission counts, the time spent per projection is dictated by the desired emission statistics. However, transmission counting statistics are influenced by patient size and source age. Large patients will absorb and scatter more transmission photons thereby decreasing the number of detected transmission photons. Decreased projection counts translate into noisy attenuation maps and subsequently noisy AC emission data. As most transmission computed tomographic systems (TCT) systems use Gd-153 transmission sources with a half life of 281 days, the number of emitted and subsequently detected photons will decrease with source age resulting in an increase in image noise as the source ages. Since the transmission counting statistics for each of the commercial transmission systems are unique, each of the vendors should provide guidelines for acquisition times as a function of patient size and source age. It should also be noted that the TCR decreases with source age and patient size. Thus, there is a point in the source's life where increasing the time for the transmission scan will not be sufficient and the sources will need to be replaced.

Total acquisition time is also based on patient comfort.

Patient Positioning

Patient positioning is important in TCT imaging. For parallel hole collimated systems, try to position the patient in the center of the imaging FOV and the acquisition orbit. Positioning the patient off-center can result in truncation artifacts in the transmission data which can result in artifacts in the reconstructed attenuation maps and the attenuation corrected emission images.

For the converging collimation systems, the problem is more complex. If both transmission and emission data is collected by converging collimators, it is more important to center the heart in all projections. This will minimize truncation artifacts in the emission data. If only the transmission data is collected with converging collimators, position patients

in the center of the FOV as suggested for parallel collimated systems. For these systems, sophisticated reconstruction software will be provided for handling the truncated transmission data.

ECG Gating

The TCT system should not affect or be affected by ECG gating. However, for TCT systems that do not irradiate the entire FOV (ie, scanning point or line source systems), the user should inquire from the vendor whether bad beat rejection or acceptance windows less than 100% can be used during transmission-emission tomography.

B.2 Image Reconstruction and Processing

For all current TCT-ECT imaging systems, the following steps are required to produce attenuation corrected emission images

- Correct transmission projection data for emission crosstalk.
- Reconstruct attenuation maps from the transmission projection data.
- Reconstruct attenuation corrected emission images using the attenuation maps reconstructed from the transmission projection data.
- Post filter the attenuation corrected emission images.

Crosstalk Correction

The correction methodology for removing scattered emission photons from the transmission data is vendor specific as it depends on the TCT imaging geometry, the acquisition type (ie, sequential or simultaneous imaging), and the photopeak windows used to collect transmission photons from the transmission source and the emission photons from the injected radiopharmaceutical. The crosstalk correction is not user configurable. If this process is suspected to be in error, then the QC procedure outlined in section A.2 should be performed.

Reconstruction

The class of reconstruction algorithm can have a profound affect on the noise and distribution of activity in the reconstructed images. With attenuation correction systems, reconstruction algorithms incorporating attenuation, scatter and resolution recovery have been made available. Since there are many classes of algorithms and the implementation can be significantly different between vendors, the user should review the literature, scientific publications and computer vendor's clinical operation manuals to determine the optimal reconstruction parameters for each imaging protocol. Since most attenuation correction systems use an iterative algorithm, the number of the reconstruction iterations should be specified in addition to how the recommended number of iterations is affected by patient size, source age, and any other variable that can affect image quality due to the number of reconstruction iterations performed.

Image Filtering

While some reconstruction software programs recommend filtering the projection data prior to reconstruction with filtered backprojection, it is not appropriate to filter the projection data if a statistical reconstruction algorithm (ie, EM-ML OS-ML, WLS) is used to reconstruct the data. Whether the raw detected data is modeled as Poisson or Gaussian, filtering the raw data invalidates the model. For statistical reconstruction algorithms, filtering should be performed in 3D post reconstruction.

Before selection of a filter you should review the literature, scientific publications and computer vendor's clinical operation manuals to determine the recommended filter for the particular imaging and processing protocol you are using.

B.3 Image Review

In the absence of a thorough characterization of the AC system as outlined by the Wintergreen Instrumentation Panel, the interpreting physician is encouraged to read the non-AC images and use the AC results to support the reading.

This approach will provide the comfort of using non-AC images with their well-understood artifacts while the physician learns the characteristics of the AC imaging system.

B.4 Quantification

Defect threshold limits for attenuation corrected images may be different compared to uncorrected images. Also, since there are unique differences between each of the commercial TCT-ECT systems, the normal distribution of activity in the myocardium may be different for each system. As a result, defect thresholds may be specific for each TCT-ECT system. The user should consult the vendor's protocol manual for the optimal defect thresholds.

Bibliography

1. Celler A, Sitek A, Stoub E, Hawman P, Harrop R, Lyster D. Multiple line source array for SPECT transmission scans: simulation, phantom and patient studies. J Nucl Med 1998;39:2183-9.
2. Corbett JR, Ficaro EP. Clinical review of attenuation-corrected cardiac SPECT. J Nucl Cardiol 1999;6:54-68.
3. Frey EC, Tsui BM, Perry JR. Simultaneous acquisition of emission and transmission data for improved Tl-201 cardiac SPECT imaging using a Tc-99m transmission source. J Nucl Med 1992;33: 2238-45.
4. Hudson HM, Larkin RS. Accelerated image reconstruction using ordered subsets projection data. IEEE Trans Med Imaging 1994;13:601-9.
5. Fessler JA. Penalized weighted least squares image reconstruction for positron emission tomography. IEEE Trans Med Imaging 1994;13:290-300.
6. King MA, Tsui BMW, Pan T. Attenuation compensation for cardiac single-photon emission computed tomographic imaging: part 2. Attenuation compensation algorithms. J Nucl Cardiol 1996;3:55-63.
7. King MA, Tsui BMW, Pan T, Glick SJ, Soares EJ. Attenuation compensation for cardiac single-photon emission computed tomographic imaging: part 1. Impact of attenuation maps and methods of estimating attenuation maps. J Nucl Cardiol 1995;2:513-24.
8. Lange K, Carson R. EM reconstruction algorithms for emission and transmission tomography. J Comput Assist Tomogr 1984;8:306-16.
9. Tan P, Bailey DL, Meikle SR, Eberl S, Fulton RR, Hutton BF. A scanning line source for simultaneous emission and transmission measurements in SPECT. J Nucl Med 1993;34:1752-60.
10. Tsui BMW, Frey EC, LaCroix KJ, et al. Quantitative myocardial perfusion SPECT. J Nucl Cardiol 1998;5:507-22.
11. Tung C-H, Gullberg GL, Zeng GL, Christian PE, Datz FL, Morgan HT. Non-uniform attenuation correction using simultaneous transmission and emission converging tomography. IEEE Trans Nucl Sci 1992;39:1134-43.
12. National Electrical Manufacturers Association. NEMA standards publication NU I-1994. Performance measurements of scintillation cameras. Rosslyn (VA): National Electrical Manufacturers Association; 1994.
13. Wintergreen Panel Summaries. J Nucl Cardiol 1999;6(Part 1):93-155.